

UNIVERSITY OF CAPE COAST

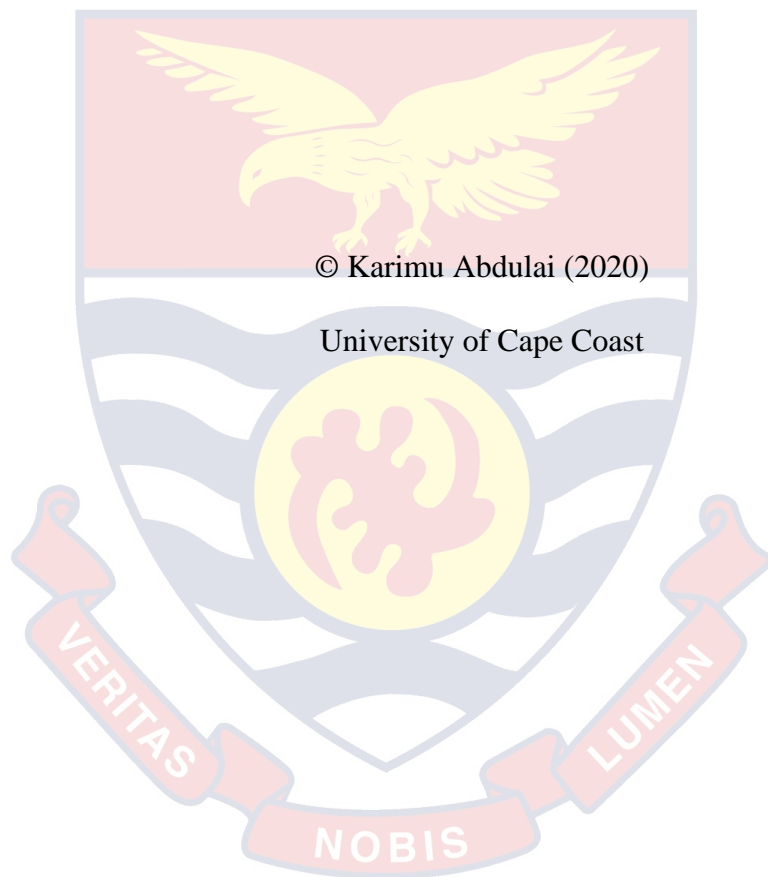
DEVELOPMENT AND EVALUATION OF A SEMI-AUTOMATIC

PEPPER SEEDLING TRANSPLANTER



KARIMU ABDULAI

2020

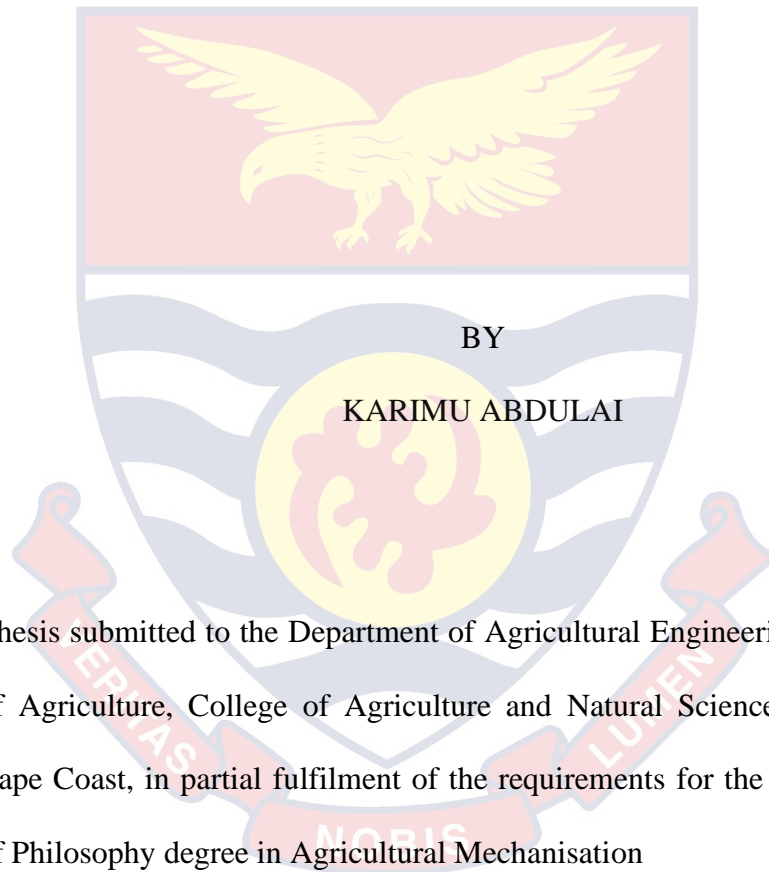


© Karimu Abdulai (2020)

University of Cape Coast

UNIVERSITY OF CAPE COAST

DEVELOPMENT AND EVALUATION OF A SEMI-AUTOMATIC
PEPPER SEEDLING TRANSPLANTER



This thesis is submitted to the Department of Agricultural Engineering of the School of Agriculture, College of Agriculture and Natural Sciences, University of Cape Coast, in partial fulfilment of the requirements for the award of Master of Philosophy degree in Agricultural Mechanisation

OCTOBER 2020

DECLARATION

Candidate's Declaration

I hereby declare that this thesis is the result of the author's research and that, to the best of my knowledge, it contains neither material previously published by another person nor material which has been presented for another degree in this university or elsewhere, except where due acknowledgement has been made in the text.

Candidate's Signature: Date:

Name:

Supervisors' Declaration

We hereby declare that the preparation and presentation of the thesis were supervised in accordance with the guidelines on supervision of thesis laid down by the University of Cape Coast.

Principal Supervisor's Signature: Date:

Name:

Co-Supervisor's Signature: Date:

Name:

ABSTRACT

Vegetable producers in Ghana are mostly small or medium scale farmers who are unable to afford expensive and sophisticated transplanters used in the developed countries. Hence there is the need for a relatively affordable transplanter for local small scale farmers. The aim of this research was to develop and evaluate the performance of a semi-automatic pepper seedling transplanter. A single row power tiller-pulled semi-automatic pepper transplanter was developed for plug seedlings, and evaluated in the field with pepper seedlings. A factorial arrangement in randomized complete block design (RCBD) with three replications was used for the evaluation. Two methods – transplanter machine and manual – were used. The treatments were 4 cm, 6 cm, and 8 cm planting depths for each method. The transplanter and manual method were each carried by two people. Transplanting time, field capacity, survival of transplanted seedlings, and cost of use of the machine were compared with the traditional manual transplanting method. Generally, the transplanter performed better than doing so manually. The maximum performance parameters were obtained under 8 cm depth while that of 4 cm depth recorded the lowest. At the 8 cm depth, the machine's transplanting success was found to be 84.45 % with 0.04 ha/h field capacity and 72.3 % field efficiency at a speed of 0.9 km/h and inter plant-spacing of 0.6 m. A mean maximum wheel slip of 13.75 % was recorded for machine under field conditions. Compared to the 90.8 man-h/ha of the manual method, the transplanter saved 67 % of the time required by the manual method. There was no significant difference in the percentages of the survived seedlings for both methods. The cost of the machine transplanting (GH¢1,720.51 per hectare) was found to be cheaper than that of the manual method (GH¢1,816.20 per hectare). With the transplanter, the operators were seated on the machine instead of walking throughout the transplanting field. There was also no manual handling of trays and no acute bending to manually make holes or plant seedlings during the transplanting process.

KEY WORDS

Design

Evaluation

Pepper

Seedlings

Simulation

Transplanter



ACKNOWLEDGMENTS

I would like to express my profound gratitude to the Almighty God for sustaining and guiding me throughout this programme. Indeed, with God all things are possible.

My next appreciation goes to my main supervisor (Dr. R. S. Amoah) and my co-supervisor (Dr. Francis Kumi) for their patience, encouragements, and support throughout the period of the research work. I owe the successful completion of this study to their prolific suggestions and guidance.

My heartfelt gratitude goes to Ghana National Petroleum Corporation (GNPC) Foundation, for the scholarship awarded me during my programme.

I also want to show my appreciation to the Regional Manager of GRATIS Foundation - Central Region (Mr. Benjamin Bannerman) and the technicians, for making their workshop available to me for the manufacture of the vegetable transplanter after the design and simulation.

My sincere gratitude goes to Professor Ernest Ekow Abano, for among other things, recommending me to GNPC foundation, which resulted in the scholarship award I got from the foundation. I cannot leave out the lecturers in the College of Agriculture and Natural Sciences of University of Cape Coast, who impacted on me in one way or the other.

I am indebted to the workers at the A.G. Carson Technology Village of University of Cape Coast, especially Mr. Stephen Aidoo, for his immense support during the field evaluation of the developed vegetable transplanting machine.

DEDICATION

To my father (Dungu Naa Karimu Mahame), my late mother (Memunatu Dawuda) and my lovely wife (Zakaria Rukaya).



TABLE OF CONTENTS

	Page
DECLARATION	ii
ABSTRACT	iii
KEY WORDS	iv
ACKNOWLEDGMENTS	v
DEDICATION	vi
TABLE OF CONTENTS	vii
LIST OF TABLES	xi
LIST OF FIGURES	xii
LIST OF ACRONYMS	xv
CHAPTER ONE: INTRODUCTION	
Background to the Study	1
Statement of the Problem	3
Aim and Specific Objectives	3
Hypotheses	4
Significance of the Study	4
Delimitations	5
Limitations	5
CHAPTER TWO: LITERATURE REVIEW	
Introduction	6
The Pepper Crop	6
The Traditional Manual Transplanting Practice	7
Manual transplanting procedure	7
Merits of traditional manual transplanting	8

Demerits of traditional manual transplanting	9
Development and Classification of Vegetable Transplanters	9
Hand operated vegetable transplanter	10
Semi-automatic vegetable transplanters	11
Fully automatic vegetable transplanters	19
Design Simulation	26
Performance Evaluation of Vegetable Transplanters Compared to the Traditional Practice	27
CHAPTER THREE: MATERIALS AND METHODS	
Introduction	30
Experimental Site Description	30
Materials and Tools	31
Design Concepts	33
Mechanism for forward movement and up-and-down motion of the planting arm	33
Design mechanism for the opening-and-closing of the furrow opener	34
Concept Evaluation	37
Design of functional components of the vegetable transplanter	41
Design of the seedling handling system	60
Simulation Procedure of the Designed Semi-Automatic Vegetable Transplanter	61
Setting up the model environment	61
Setting up the geometry	61
Definition of boundaries	61
Specification of material properties	62

Definition of physics	62
Creation of mesh and running of the simulation	62
Post-processing of the results	62
Manufacture of the Pepper Transplanter	63
The structure sub-assembly	63
Steering system sub-assembly	65
The mechanism sub-assembly	66
The furrow opener sub-assembly	67
Actuator sub-assembly	68
The compacting wheels' sub-assembly	69
Evaluation of the Manufactured Vegetable Transplanter	70
Experimental design and field layout	70
The theoretical field capacity (C_{th}) of the transplanter	70
Operating speed (V)	71
Field efficiency	71
The effective field capacity of the transplanter	71
Field capacity of the manual transplanting	72
Percentage transplanting success	72
Wheel slip (S)	72
Force prediction of the furrow opener in the soil	73
Cost analysis	75
Statistical analyses	78
CHAPTER FOUR: RESULTS AND DISCUSSION	
Introduction	79
Design and Construction of the Semi-Automatic Pepper Transplanter	79

Design Simulation	81
Material properties and meshing of the geometry	81
Stress concentrated areas	82
Joint Forces at the crank-coupler joint	83
Joint forces at the rocker-coupler joint	84
The trajectory of the furrow opener tip	85
Performance Evaluation of the Transplanter Under Local Field Condition	86
Preliminary testing and machine modifications	86
Field experiment	87
Field capacities	88
Field efficiency	89
Comparison of Machine Transplanting to the Manual Method	93
Transplanting time	93
Transplanting cost estimation	95
CHAPTER FIVE: CONCLUSIONS AND RECOMMENDATIONS	
Conclusions	99
Semi-automatic pepper seedling transplanter design, simulation and manufacture	99
Field performance of semi-automatic pepper seedling transplanter	99
Comparison of time requirement and cost of the transplanter and manual methods	99
Recommendations	100
REFERENCES	101
APPENDICES	110

LIST OF TABLES

Table		Page
1	Cost of Transplanting Vegetable by Manual and by Transplanter Methods	28
2	Effect of Transplanting Methods on Plant Height, Number of Branches & Leaf Area Index in Brinjal	29
3	Selected Soil Properties at the Experimental Site	31
4	Evaluation Criteria	39
5	Decision Matrix	40
6	Assumed Values for the Crank-Rocker Chain Sprockets	43
7	Assumed Figures for the Crank-Rocker Chain Length	46
8	Narrow Tine Force Calculations	75
9	Assumptions for ownership cost calculation	76
10	Assumptions for Operating Cost Calculation	77
11	Results of Ownership Cost Estimation	95
12	Results of operating cost calculation	96
13	Assumptions for Manual Transplanting Cost Calculation	97

LIST OF FIGURES

Figure		Page
1	Manually operated single row vegetable transplanter (a) CAD drawing (b) Field testing	10
2	Orthographic drawing of the single-row manual vegetable transplanter	11
3	Cam-driven Roller Follower Dibbling Transplanter	12
4	Full assembly of the power tiller operated vegetable transplanter	14
5	Tractor operated three row plug type vegetable transplanter	15
6	Two row vegetable transplanter with revolving magazine metering mechanism, (a) top view (b) front view	16
7	The two-row hand-fed vegetable transplanter drawn by hand tractor	18
8	Single row Bullock-drawn Vegetable Transplanter	19
9	Modified transplanter with horizontal trays and robotic arm	20
10	The 3 models of Fully automatic riding-type vegetable transplanters	22
11	The Automatic vegetable transplanter for the gantry system	23
12	The walk behind tractor operated 2-row array type vegetable transplanter	24
13	The fully automatic single-row vegetable transplanter	25
14	The single-row automatic transplanting device for potted vegetable seedlings	26
15	Crank-Rocker Mechanism (A 4-bar linkage)	33
16	Cam-lever mechanism design	35

17	Chain-cam mechanism design	36
18	Hydraulic plunger design	37
19	The 3-Dimensional drawing of the transplanter	41
20	Parts of the Crank-Rocker Mechanism (a) Frame, (b) Crank, (c) Coupler (d) driven link, follower, or rocker.	42
21	Chain drive system for the Crank-Rocker mechanism	45
22	Actuator chain drive system	47
23	(a) Crank Shaft attachments (b) free body diagram	49
24	Free body diagram of the crank	50
25	Free body diagram of the crank-rocker mechanism chain drive	51
26	Free body diagram of the actuator chain drive	52
27	Vertical loading of the crank shaft	53
28	(a) Shearing force diagram (b) Bending moment diagram for the YZ plane	54
29	Horizontal loading of the crank shaft	55
30	(a) Shearing force diagram (b) Bending moment diagram for XZ plane	56
31	Structure sub-assembly	64
32	Steering system sub-assembly	65
33	Mechanism Sub-Assembly	67
34	Furrow opener sub-assembly	68
35	The actuator sub-assembly	69
36	The compacting wheel sub-assembly	70
37	Two dimensional views of the transplanter (a) Side view (b) Top view	80

38	(a) The manufactured vegetable Transplanter (b) the furrow opener section	81
39	Tetrahedral meshing of the planting arm geometry under study.	82
40	Multibody dynamics displacement results indicating stress concentrations	83
41	Forces at the crank-coupler joint	84
42	Forces at the rocker-coupler joint	85
43	Trajectory of the furrow opener tip	86
44	(a) Dummy seedlings, (b) preliminary testing with dummy seedling	87
45	(a) Actual field testing, (b) pepper seedling with well-developed root system	88
46	Effect of transplanting depth on the field capacity	89
47	Effect of transplanting depth on field efficiency	90
48	Effect of transplanting depth on transplanting success.	91
49	Effect of transplanting depth on wheel slip	92
50	Effect of transplanting depth on seedling survival	93
51	Effect of depth and method on actual transplanting time	94

LIST OF ACRONYMS

AISI	American Iron and Steel Institute
ANOVA	Analysis of Variance
ASABE	American Society of Agricultural and Biological Engineers
CAD	Computer Aided Design
CIAE	Central Institute of Agricultural Engineering
DC	Direct Current
FAOSAT	Food and Agriculture Organization of United Nations Statistics
FEA	Finite Element Anal
GNPC	Ghana National Petroleum Corporation
IRRI	International Rice Research Institute
NSK	Nippon Seiko Kabushiki-gaisha
PLC	Programmable Logic Control
PAU	Punjab Agricultural University
RPM	Revolutions Per Minute
RCBD	Randomized Complete Block Design
USA	United States of America
WHO	World Health Organization

CHAPTER ONE

INTRODUCTION

Background to the Study

The level of agricultural mechanisation in Ghana is still low with only 16 % of the agricultural land being cultivated with machines and 11 % of the arable land being irrigated (Panel, 2018). Comparing this to mechanisation percentages in other countries – 45 % of Indian agriculture, 75 % of Brazilian agriculture, 90 % of Australian agriculture, 91 % of Chinese agriculture, 95 % of US agriculture, 97 % of South Korean agriculture and 99 % of Japanese agriculture (Khetigaadi, 2016); the country really lags behind in terms of vegetable production than other crops like cereals, resulting in a very low level of vegetable production compared to cereals.

Vegetables are parts of plants that can be eaten either raw or cooked by humans or animals as food. Being the main source of many vital nutrients such as vitamin A and C, potassium, folic acid and dietary fiber, vegetables play a very important role in human nutrition, and have been part of the human diet since time immemorial. Eating a diet rich in fruits and vegetables helps in preventing a number of chronic diseases, including heart disease, type 2 diabetes, some cancers, and obesity according to the Piercy and Troiano (2018). It is advised that individuals consume at least two servings of fruit and three servings of vegetables daily as part of a balanced diet in order to meet the World Health Organization (WHO) recommended daily intake of 400 g or more per capita (Nishida, Uauy, Kumanyika, and Shetty, 2004).

The global production of fresh vegetables in 2017 was 1094.34 million metric tons according to Statista (2019). Out of this figure, Africa was able to

produce only 79.14 million metric tons, representing about 7.23 % of the global production. Asia was the leading producer with a production of 834.2 million metric tons, representing 73.23 % of the global production. Europe came second with a production level of 96.26 million metric tons representing about 8.8 %. The high agricultural production in these regions clearly demonstrates the undisputable link between the use of mechanisation and higher crop outputs (Khetigaadi, 2016). The main vegetable crops grown in Ghana are tomatoes, pepper, onions, eggplants and okra (Lei, Ur, and Obeng, 2014). According to the Food and Agriculture Organization of the United Nations Statistics (FAOSTAT, 2017), the area dedicated to the production of these vegetables was 79,149 hectares with a total annual production of 753,616 tons.

Vegetable production and consumption have the potential to create employment and generate income in developing countries (Chagomoka, Drescher, Glaser, Marschner, Schlesinger, 2015). The domestic market is growing at a rate of over 10 % per year and the potential value for export vegetables is estimated at US\$250 million (Rijk & Beatrixlaan, 2014). Among the reasons attributed to this growth are; the suitability of Ghana's local conditions for the production of tropical fruits and vegetables, and Ghana's close proximity to many European Countries (Gonzalez et al., 2014). In vegetable production, the most labour-intensive operations are transplanting, weeding and harvesting. If these operations are successfully mechanized, the production figures recorded above could be significantly increased. Transplanting is a very important activity in vegetable production. It allows for only healthy seedlings to be selected for propagation, better

penetration of roots in the soil, and promotes better development of the plant shoot system. Apart from okra which is propagated by sowing its seed directly in the main field, most of the main vegetables grown in Ghana usually have their seeds nursed in either a nursery or a seedbed prepared separately in a greenhouse or part of the field, and then transplanted unto the main field after they grow into matured seedlings.

Statement of the Problem

In Ghana, vegetable production (especially pepper) is dominated by small scale farmers who are incapable of acquiring capital-intensive machinery to boost their production. As a result, the majority of vegetable seedlings, are transplanted manually. However, manual transplanting is costly, time consuming and, requires a lot of labour. Even as timely transplanting of crops is essential for good yield, delayed transplanting operations result in poor yield (Kumar and Tripathi, 2016). Manual transplanting of bare root seedlings requires 185–260 man-h/ha if seedlings are planted on raised beds, and 320 man-h/ha if seedlings are planted on flat beds and ridges (Kumar and Raheman, 2008). Consequently, considering the numerous nutritional benefits and ready market for vegetables both locally and internationally, this study sought to develop and evaluate the performance of a semi-automatic vegetable transplanter to reduce the drudgery involved in seedling transplanting and consequently boost vegetable production in Ghana.

Aim and Specific Objectives

The aim of the research was to develop and evaluate the performance of a semi-automatic pepper seedling transplanter for small and medium scale farmers.

The specific objectives were to:

1. design, simulate and manufacture a semi-automatic pepper seedling transplanter
2. evaluate the field performance of the semi-automatic pepper seedling transplanter under varying transplanting depths
3. determine the total time required and cost of using the semi-automatic pepper seedling transplanter in comparison to manual transplanting

Hypotheses

1. The use of a semi-automatic pepper seedling transplanter is more efficient than transplanting manually.
2. The use of a semi-automatic pepper seedling transplanter is timelier than transplanting manually.

Significance of the Study

Mechanized transplanting machines are more efficient than manual transplanting. Mechanized transplanting machines have capacities of up to 16.08 h/ha equivalent to work rate of 0.08 ha/h. Compared to manual transplanting, mechanization of the process reduces labour input up to 97.8 % (Mkomwa et al., 2008).

Research for the development of a vegetable transplanter began several years ago. Qiang and Zhang (2005) designed an automatic transplanter for lettuce in China Agricultural University. Tian et al. (2010) developed automatic transplanter for plug seedlings using Gantry-gate type arm and conveyor system. Kumar and Tripathi (2016) evaluated the performance of a tractor operated two-row vegetable transplanter. Dihingia, Kumar, Sarma and Neog (2017) developed Hand-Fed Vegetable Transplanter for use with a Walk-

Behind-Type Hand Tractor using a metering conveyor system. However, literature search indicates very little or no report on the development of such machinery in Ghana and other sub-Saharan countries.

The purpose of the present study was to develop a simple and efficient semi-automatic transplanter for vegetable seedlings, powered by a power tiller which is affordable to the small scale farmer in Ghana. The transplanter was to be designed to use crank-rocker mechanism to achieve the up and down movement of the furrow opener.

Delimitations

The study was carried out in Cape Coast but the findings will be applicable to all parts of Ghana and all sub Saharan countries with climatic conditions similar to that found in the study area. The study covered the design and simulation of the transplanter with computer software (AutoCAD and Comsol multiphysics), fabrication of the transplanter, nursing of pepper seedlings, preparation of the field, transplanting of the seedlings and monitoring of the seedlings to the germination stage, and costing.

Limitations

Though the transplanter was designed for more than one vegetable crop, due to scarcity of time the evaluation was conducted using pepper seedlings only. The performance of the machine recorded may not be the same if other crops like tomato or egg plants are being transplanted with the machine. Also, the study does not cover up to the fruiting and harvesting stage, it ends at the establishment stage. However, it is possible that important trends could have been observed on the yield.

CHAPTER TWO

LITERATURE REVIEW

Introduction

Transplanting is one of the tedious operations in vegetable production. This study is on the development and evaluation of a semi-automatic pepper seedling transplanter to help eliminate the difficulty vegetable farmers go through when transplanting vegetables manually. Several researches have already been done on the mechanization of the transplanting process (Yujie and Jun, 2016). This chapter therefore presents a brief review of these research works. It covers the pepper crop, the traditional manual transplanting practice; development and classification of vegetable transplanters; design simulation, and performance evaluation of vegetable transplanters compared to the traditional practice.

The Pepper Crop

Pepper (*Capsicum* spp) is an age-long flowering plant grown as a main vegetable or spice crop, which originates from the Americas (Tripodi & Kumar, 2019). The genus *Capsicum* belonging to the large family of Solanaceae, has about 20 wild species and 5 species (*C. annuum*, *C. frutescens*, *C. chinense*, *C. baccatum*, and *C. pubescens*) domesticated (Eshbaugh, 1983). Among the five domesticated species, *C. annuum* which is categorised into hot pepper and sweet pepper, is the most widely cultivated species (Lin et al., 2013).

In developing countries like Ethiopia, Nigeria, Ghana, China, India, Pakistan, and Thailand, pepper production is a very lucrative business for smallholder farmers (Lin et al., 2013). The global production of pepper has

increased from more than 12 million tonnes in 1993 to over 31 million in 2013, covering a land area of about 1.93 million ha of crop growing surface area (Penella & Calatayud, 2018). China produced 16 million tonnes out of the global figure, making it the leading producer, Mexico came second with 2.3 million tonnes followed by Turkey with 2.2 million tonnes, and then Indonesia with 1.8 million tonnes. Between the years 2000 and 2007, Ghana was able to pull about 1 % of the global chilli production figure, placing it on the 11th position. Ghanaian chilli exports for that period ranged between 26,000 and 41,000 metric tonnes (DIA, 2014).

The Traditional Manual Transplanting Practice

Manual transplanting procedure

In Ghana, vegetable production is characterised by a lot of manual transplanting, resulting in low production level of this category of crops. Manual transplanting is done either at random or in straight-rows. In the random method, no definite spacing is given between plants, whereas in the straight-row method, a uniform spacing between plants is given. The straight line method is done with the help of planting guides which may be in the form of rope, wire or wood, with knots or marks (IRRI, 2007).

Ferminger (1953) stated in his description of the manual transplanting method, as cited by Kumar and Raheman (2008), that on the average in India, small-scale gardeners manually dig holes 60 mm in diameter and 30 mm deep, at desired spacing in the field. The soil is mixed with farmyard manure, bone meal, and wood ashes. The hole is then filled to a depth of 15–20 mm and packed. With a seedling placed in the middle of the hole, topsoil is filled

around the seedling, compacted, and water applied immediately. With this method no field operation is required.

Raised bed transplanting is a manual transplanting method practiced by medium scale farmers in India. A well-pulverized seed bed is prepared and raised beds, 90–120 cm wide and 30 cm high, are built manually or with tractor-drawn implements and bare root seedlings transplanted manually on them using a spade to compact soil around the seedlings (Punjab Agricultural University [PAU], 2004). There are also instances where seedlings are transplanted before ridges are built as the plants grow. This method is called flat planting and requires about 320 man-hours/ha for transplanting tomato at 60 cm row-to-row spacing and 45 cm plant-to-plant spacing (Central Institute of Agricultural Engineering [CIAE], 2004)

Rotty (1960) reported, as cited by Kumar and Raheman (2012) that in North America, transplanting of vegetable crops used to be done by hand or with a transplant board. The transplant board consists of a board of wood, aluminium, or other metals that are not heavy. It has channel or angle bar cross section to which seedlings are attached. A trench is made in the field, the transplant board transported to the trench and the seedlings are released. Soil is then put around the seedling and compacted with the aid of a spade.

Merits of traditional manual transplanting

IRRI (2003) recounted some merits of manual transplanting. He stated that manual transplanting can be done with basic tools and does not require capital-intensive machines. In addition, it is suitable for labour-surplus areas where the cost of labour is relatively cheaper. He stated that the method is the most suitable one for small scale farming. He also indicated that manual

transplanting is possible in fields with uneven surface levelling and with varying water levels.

Demerits of traditional manual transplanting

Available literature has recorded some weaknesses of the manual transplanting practice. According to Kumar and Raheman (2012), manual transplanting of seedlings is very labour-demanding and has labour requirement, especially in India, of about 240 to 320 man-h /ha.

Tsuga (2000) reported that the time required in Japan for manual seeding and transplanting of vegetables accounted for about 40% of the total time required for cultivation of pepper. When manual transplanting of vegetables is practiced on a large commercial farm, it is found to be labour intensive and time consuming compared to mechanical transplanting. Also, the varying transplanting depths which occurs in manual transplanting usually results in non-uniform growth of plants in the field (Orzolek, 1996).

Development and Classification of Vegetable Transplanters

Vegetable transplanters can basically be categorised into three main groups namely; hand operated transplanters, semi-automatic transplanters and fully automated transplanters. With the hand operated transplanter, the power source for operating the transplanter is the user and seedlings are also hand-fed by the user. In a semi-automatic transplanter, there is a power source (not from the user) that drives the transplanter, however seedlings are hand-fed into the transplanter by the user. In fully automated transplanters, there is a power source that drives the transplanter and a mechanism for picking and feeding seedlings into the transplanter as well as picking and transplanting seedlings directly into the ground without human intervention.

Hand operated vegetable transplanter

Nandede et al. (2017) developed a manually operated single row vegetable transplanter for plug and pot type vegetable seedlings in India. Its main components were jaw assembly, delivery tube, lever, handle, spacing marker and frame. The transplanter is raised by one foot and allowed to drop into the soil by gravity. A seedling is dropped into the delivery tube, the lever is pressed upward to open the jaw and the seedling drops into the opened furrow by gravity. The transplanter is then raised with the opened jaw to a height of about 300 mm and then closed before dropping it again. The transplanter was tested on both ridges and on plastic mulch beds. Figure 1 shows the computer aided design (CAD) drawing and field testing of the transplanter.

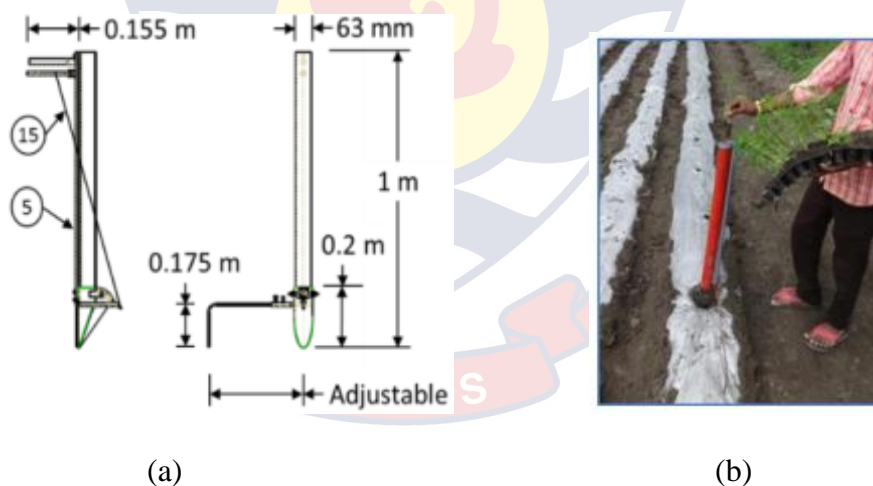


Figure 1: Manually operated single row vegetable transplanter (a) CAD drawing (b) Field testing (Nandede et al. (2017))

Kumar and Dixit (2018) developed a single row manual vegetable transplanter for eggplant, chilli and tomato. In this design a hopper was added to the top of the delivery tube to make dropping of seedlings into the tube

much easier. While holding the handle with both hands, a little force is applied to drive the jaw of the transplanter into the soil. A seedling is dropped into the delivery tube through the hopper, and the jaw opened with a lever. The transplanter is then lifted with the opened jaw, closed before driving it into the soil again. Figure 2 shows the top and front views of the single row manual vegetable transplanter.

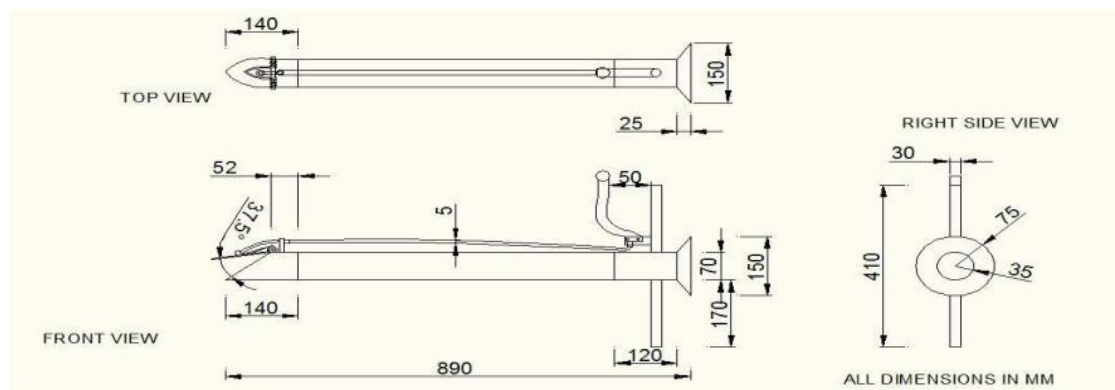
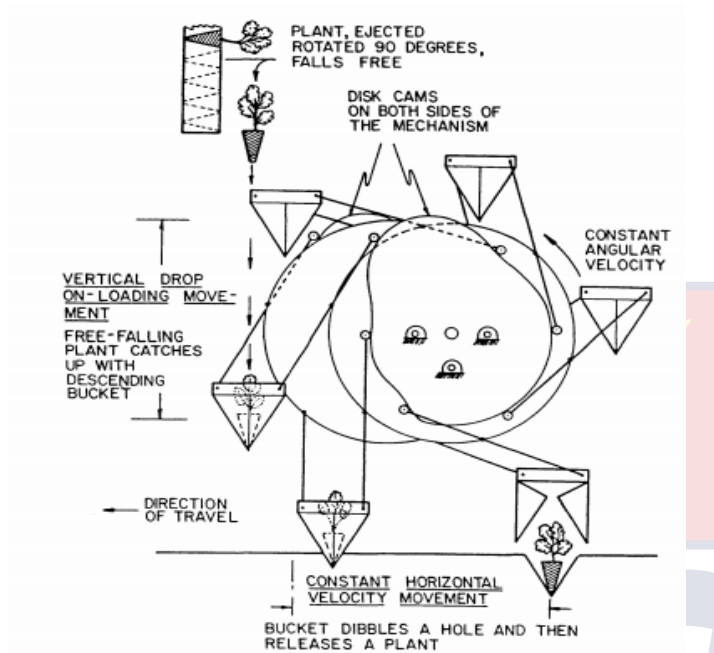


Figure 2: Orthographic drawing of the single-row manual vegetable transplanter (Kumar and Dixit, 2018)

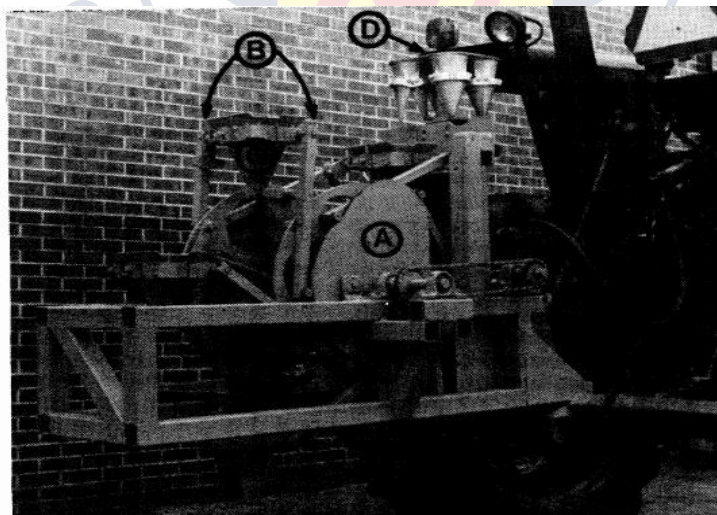
Semi-automatic vegetable transplanters

Semi-automatic vegetable transplanters are mechanical transplanters that may be self-propelled, tractor mounted, or drawn by tractor, power tiller, or bullock. They can also be classified into continuous furrow type or dibbling type. Manilla & Shaw (1987) designed and tested a tractor-mounted transplanter using a cam-driven roller follower movement mechanism that transplants seedlings extracted directly from a commercial growing flat. The major components of the transplanter were the cam, planting wheels, parallel follower arms, dibble-buckets and feeder (Figure 3). The transplanter was tested at a forward speed of 3.62 km/h, using four-week old tomato seedlings. During the field tests, though synchronizing the transplanter's revolution to the

tractor's forward speed, and maintaining the targeted feeding rate of 130 plants/min were challenges, planting success rate of 93% (seedlings in well-formed holes and with less than 30° inclination) was achieved.



(a) Kinematic representation of the transplanter



(b) The major parts of the transplanter (A) cam, (B) parallel follower arms, (C) dibble-bucket, (D) feeder

Figure 3: Cam-driven Roller Follower Dibbling Transplanter (Manilla and Shaw, 1987)

Mahapatra (2006) designed and developed a vegetable transplanter operated by a power tiller. It had two attachments, one is the transplanter with compacting wheels attached for planting on flat bed and the other is the transplanter with moldboard and truncated conical ridge shaper attachment to simultaneously make ridges as the transplanting goes on. The main components of the flat bed transplanting attachment are multipurpose tool bar, side trail wheels, furrow opener and furrow covering-emu-press wheels. The main components of the simultaneous ridging attachment are mould boards for furrow covering and soil gathering, and then ridge shapers. The machine also has seedling feeding and metering mechanism, and funnel shaped chute for seedling dropping (Figure 4). The speed range for optimum performance of the transplanter was 1.0-1.2 km/h and the ideal suitable soil moisture content for its optimum operation was 10-14 % (d.b). The transplanter had effective field capacities of 0.057, 0.058, 0.073, 0.046 and 0.074 ha/h for transplanting cabbage, chilli, tomato, knolkhol and brinjal, respectively. Two people are required for the use of the transplanter and the optimum height of all crops ranged between 150 mm and 300 mm.

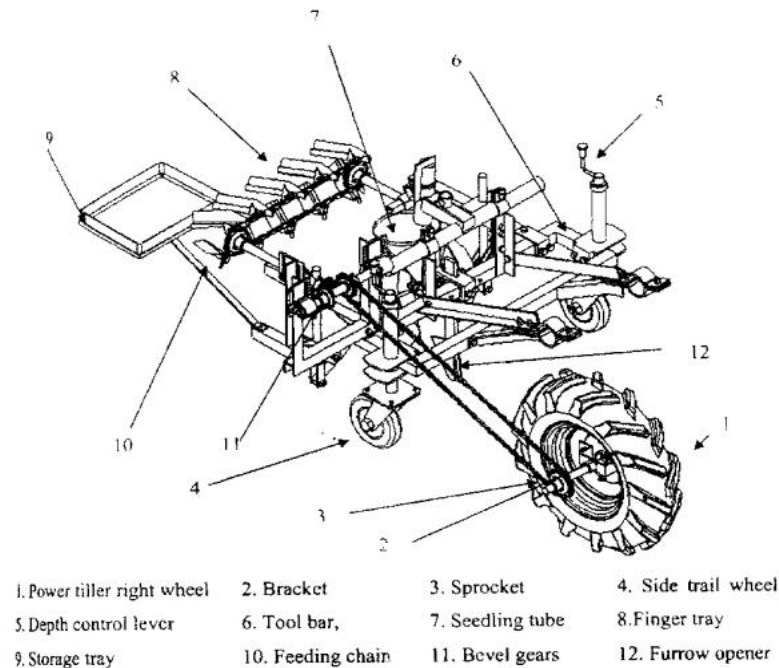


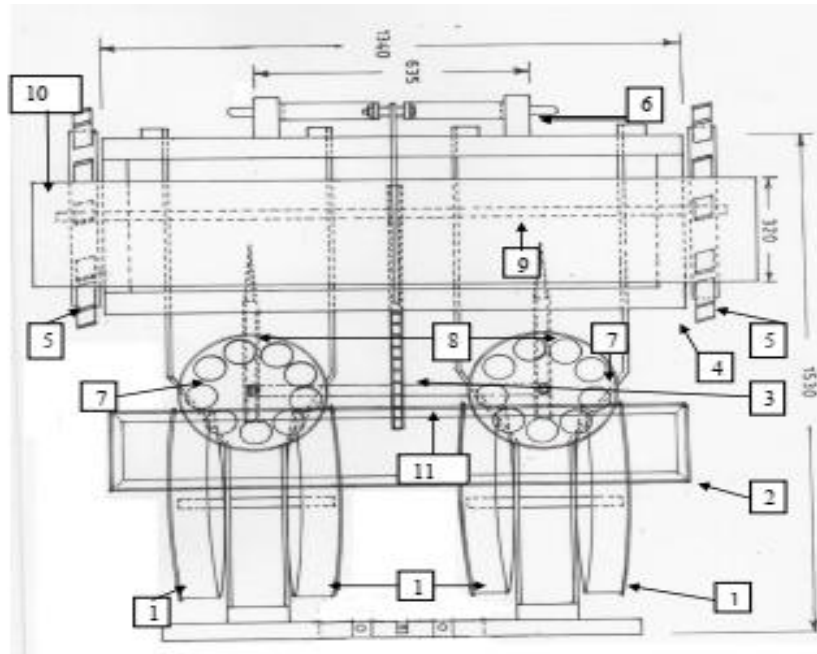
Figure 4: Full assembly of the power tiller operated vegetable transplanter
(Mahapatra, 2006)

Kavitha and Karunanithi (2008) designed and developed a tractor-operated three row (plug type) vegetable transplanter. It comprised of a main frame with hitching system, ground wheel, shoe type furrow openers, compaction wheels inclined at 15° to the vertical plane, operator's seats, two depth control wheels and plug type metering mechanism. The transplanting mechanism is driven by power from 750 mm diameter ground wheels through gearbox and chain and sprockets. And then belt drive systems are used to transmit power to the discs. The transplanter had field capacity of 0.14 ha/h and field efficiency 75 %. The ideal soil moisture content for its optimum operation was found to be 12-13 % (d.b). Figure 5 shows the tractor-operated three row plug type vegetable transplanter,



Figure 5: Tractor operated three row plug type vegetable transplanter (Kavitha and Karunanithi, 2008)

Subsequently, Narang (2011) developed a two row vegetable transplanter with a revolving magazine type metering mechanism and a three-point hitch system for mounting it on a tractor. Its field performance was evaluated using brinjal and tomato crops at average speeds of 1.1 km/h and 1.05 km/h, respectively. The transplanter had average field capacity of 0.122 ha/h for brinjal and 0.1115 ha/h for tomato crops, with field efficiency of 80.4 % for brinjal and 81.6 % for tomato. The percentage of missing plants varied from 2.22- 4.44 % for brinjal and tomato crops. The maximum plants that were upright (transplants with 0 to 30 degree planting angle) was 85-90 %, and plant mortality after 20 days was 5 %. Figure 6 shows views of the two row vegetable transplanter with revolving magazine type metering mechanism and its main components.



(a)

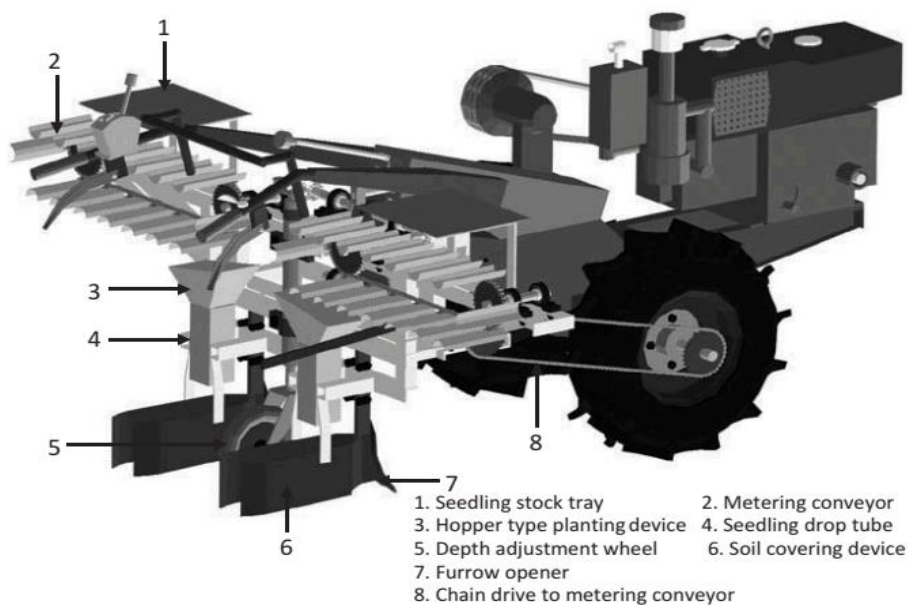
1. Press wheel 2. Seedling tray 3.Chain drive 4. Main frame
5. Ground wheel 6. Three-point hitch system 7. Revolving magazine type
metering mechanism 8. Furrow opener 9. ground wheel shaft 10.
Operator seat 11. Main shaft



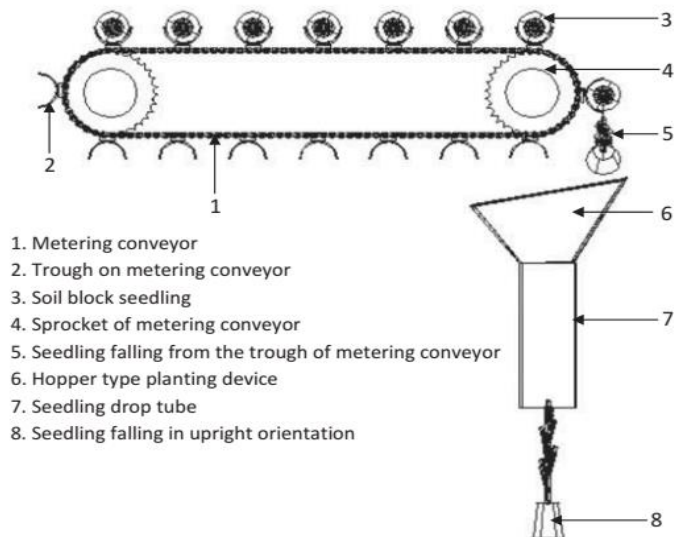
(b)

Figure 6: Two row vegetable transplanter with revolving magazine metering mechanism, (a) top view (b) front view (Narang, 2011)

Dihingia et al. (2017) developed a two-row hand-fed vegetable transplanter drawn by a walk-behind type hand tractor (power tiller) for transplanting soil block seedlings. Soil block seedlings are picked from a tray and placed on a metering conveyor of the transplanter by two labourers who also control the hand tractor. The seedlings are conveyed to a hopper-type planting device that delivers them through a drop tube into a furrow in an upright orientation. Other major components of the transplanter are furrow openers, soil covering devices, depth adjustment wheel, row marker and a hitching system (Figure 7). The transplanter had planting rate of 31 plants/min, field capacity of 0.045 ha/h for transplanting tomato (*Solanum lycopersicum* L.) and chilli pepper (*Capsicum annuum* L.) and 0.06 ha/h for transplanting eggplant (*S. melongena* L.).



(a) Three-dimensional solid model connected to the hand tractor



(b) Conceptual working of the hand-fed vegetable transplanter

Figure 7: The two-row hand-fed vegetable transplanter drawn by hand tractor (Dihingia et al., 2017)

Sahoo et al. (2018) developed and evaluated the performance of a single row semi-automatic bullock drawn vegetable transplanter in India. It had a tray type seedling metering mechanism driven by the ground wheels which maintained plant to plant spacing of 525 mm (Figure 8). Bare root seedlings of brinjal and chilli at 10-12 % moisture content were used to evaluate the field performance of the transplanter. After 21 days of transplanting, 70.78-72.76 % of the plants survived and mortality rate of 21.66-25.66 % recorded. The transplanter developed draught of 21kgf, had field capacity of 0.052 ha/h and field efficiency of 72.20 %.

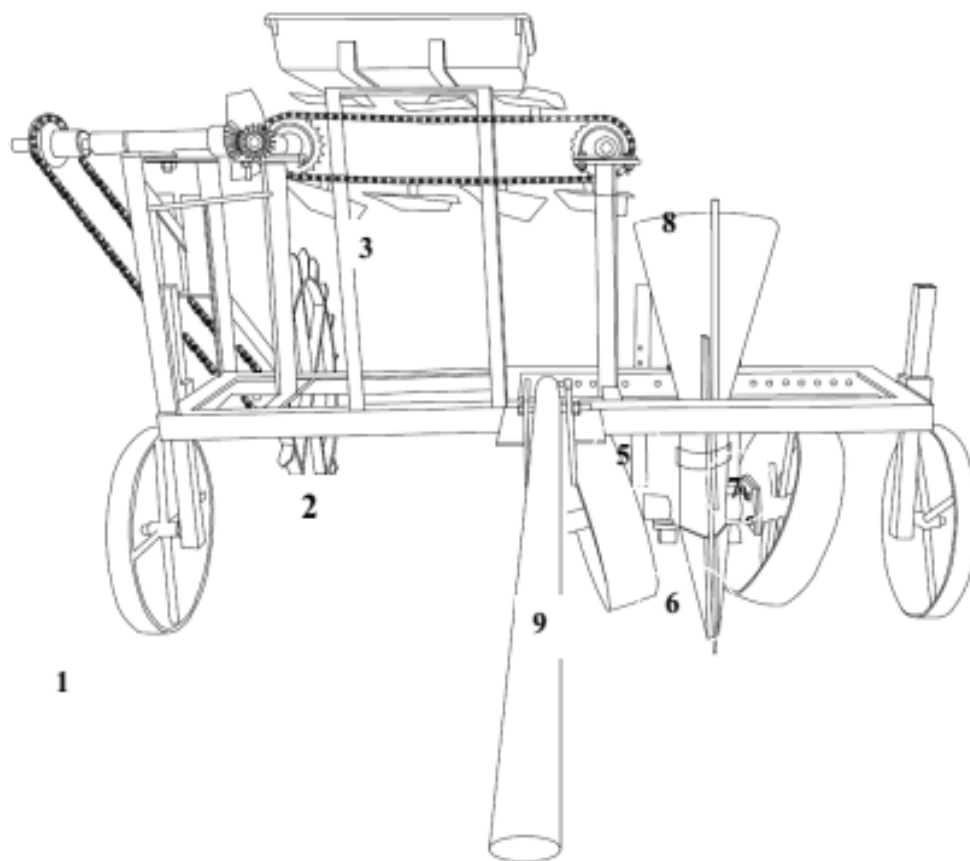


Figure 8: Single row Bullock-drawn Vegetable Transplanter (et al., 2018)

Fully automatic vegetable transplanters

Automatic vegetable transplanters are mechanical transplanters that may be self-propelled or drawn by a tractor. They may also be continuous furrow type or dibbling type and are able to transplant vegetable seedlings with little or no human involvement (Kumar & Raheman, 2008).

Hwang and Sistler (1986) developed a robotic arm comprising of a manipulator and a gripper, mounted on a commercial pot-plant mechanical transplanter which was modified to suit the manipulator, for transplanting of pepper seedlings. Seedlings are picked from a plant box and placed in a carousel, a mechanical metering mechanism driven by the press wheels synchronizes the opening and closing of the carousel cups with the operation

of a plant kicker (Figure 9). The plant drops through a guide hole into the opener shoe, it is then kicked out and held upright by the kicker for the press wheels to cover its root with soil. The robotic arm was controlled by an 8-bit microcomputer. One-month old pepper plants (Jalapeno, Pepperone, and Bell peppers) grown in a greenhouse, were used to test the transplanter at a speed of 0.16 km/h, planting rate of a little over 6 plants per minute, and an average of one plant missing per tray.

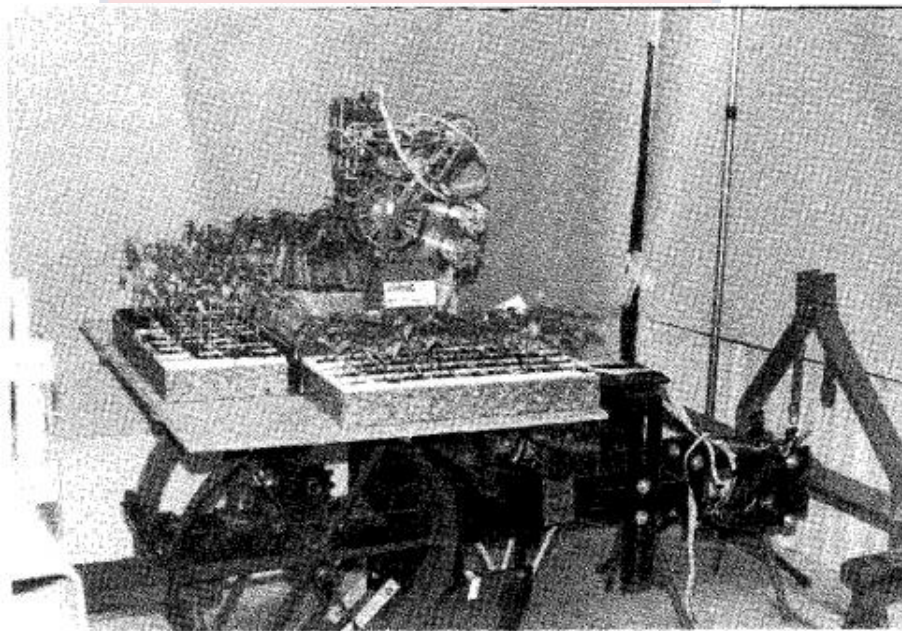
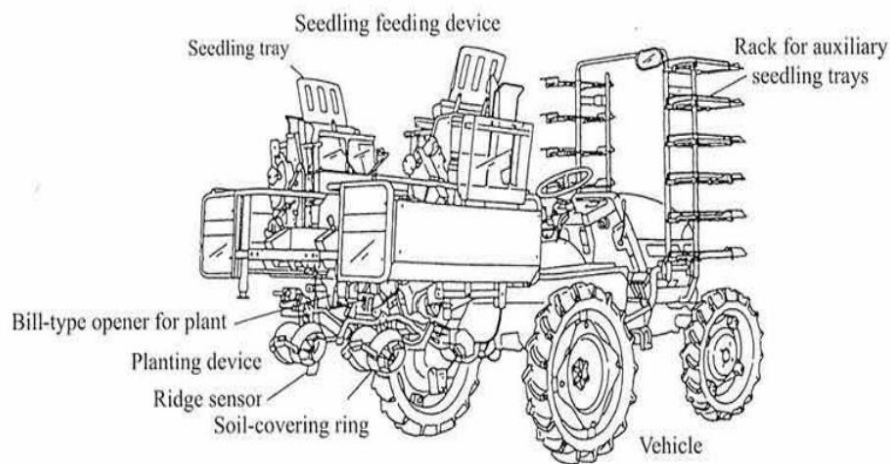


Figure 9: Modified transplanter with horizontal trays and robotic arm (Hwang and Sistler, 1986)

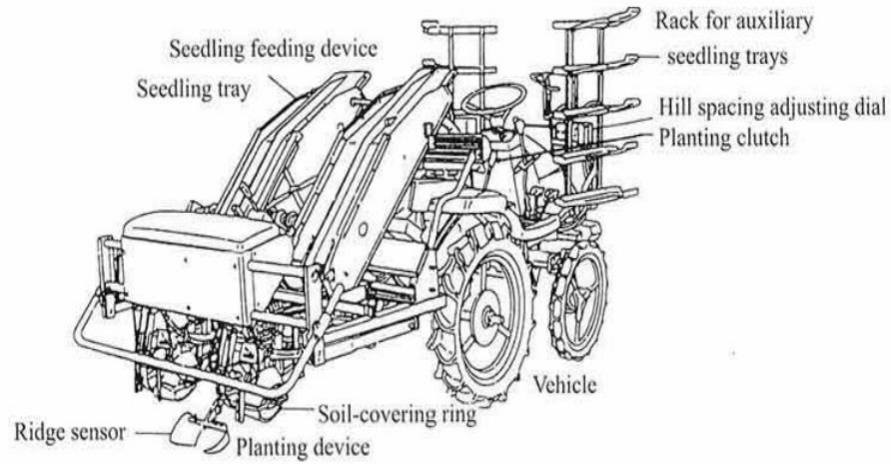
Shaw (1998) developed a fully automatic cup type vegetable seedling transplanter which can transplant through plastic mulch as well as bare ground. The transplanting rate for the machine was about 7000 seedlings per hour per row unit of Florida tomatoes. The major parts of the transplanter are plant removal mechanism and plant setting mechanism. The plant removal mechanism extracts seedlings from the trays and deliver them to the plant setting mechanism. The pointed end of each cup is able to piece holes through

plastic mulch. This or an attached hole burner and the plant setting mechanisms are synchronized to ensure seedlings are precisely planted in the mulch holes. The machine was designed for 180-200 mm high seedlings and is able to transplant over 98 % good quality seedlings on regular basis.

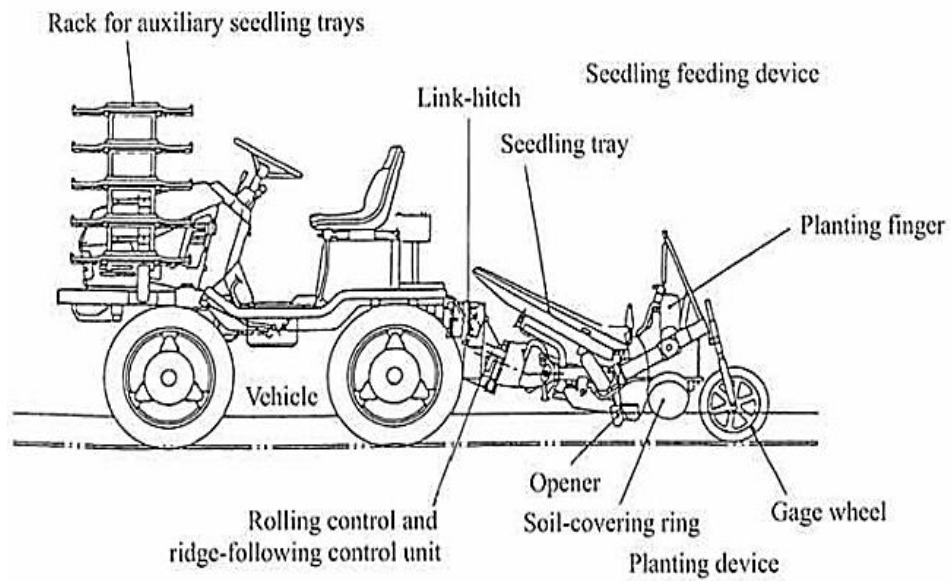
Tsuga (2000) in Japan, developed 3 models of fully automatic riding-type 2-row vegetable transplanters for cell mould and pulp mould cell pot seedlings like cabbage, Chinese cabbage, and lettuce (Figure 10). Seedlings are pulled out from the trays one after the other with the aid of seedling take-out claws and deposited into a bill-type opener. The opener then transplants the seedling into the tamped surface of the ridge. The transplanter had planting rate of 60 cells/row/min with about 3 % or less miss-planted hills. An annual coverage area of the machine for transplanting cabbage was estimated to be 53 ha/year and the minimum economically suitable area for its use was 8.2 ha.



(a) Model PR2 for cell mold seedlings (Tsuga 2000)



(b) Model SKP20 for cell mold seedlings (Source: Tsuga 2000)

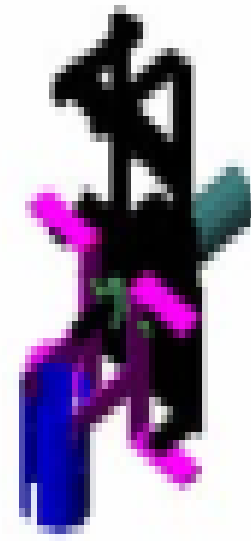


(c) Model PVP200 for pulp mold cell seedlings

Figure 10: The 3 models of Fully automatic riding-type vegetable transplanter (Tsuga, 2000)

Ishak, Awal, & Elango (2008) designed and developed an automatic vegetable transplanter for use with the main gantry system in a greenhouse. The transplanter movement system operated in a 3-axis format and based on a Cartesian configuration. It consisted of a 3-point hitch system, an X-axis model, Z-axis model, an auger, pot tray, a gripper and a watering unit (Figure 11). The auger used 12V DC motor to drill 80mm deep holes. The gripper

(Figure 11b) grabs the potted seedling, moved to the pot hole by the X-axis arm linkage and releases it in the hole. The watering unit used 12V pump to spray 100mL of water in 10sec. A graphical user interface developed by Visual Basic (VB) 6.0 and Programmable Logic Control (PLC) were used to operate the transplanter automatically. It took the transplanter an average of 2 min 35.5sec to transplant one potted eggplant seedling.



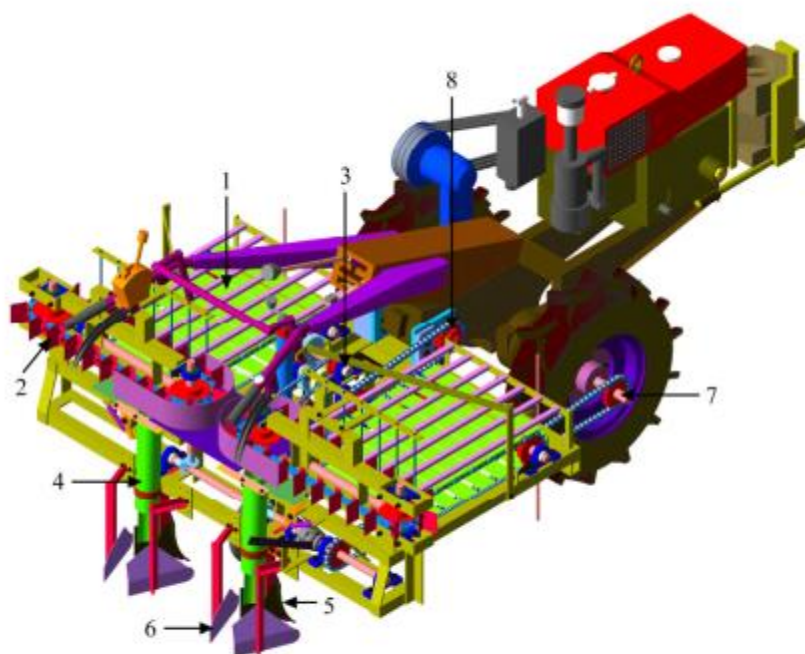
(a) The structure of the transplanter

(b) The gripper

Figure 11: The Automatic vegetable transplanter for the gantry system
(Ishak et al., 2008)

Kumar and Raheman (2012) in India, developed an automatic feeding system for vegetable transplanter. It comprised of a timing shaft, an actuating device and a clutch for automatically feeding paper pot seedlings from a slat type chain conveyor to a pusher type chain conveyor of a vegetable transplanter in upright orientation (Figure 12). The pusher type chain conveyor delivers the seedlings to a seedling drop tube. The mechanism was tested in a sandy clay loam soil of 1.32 g/cm^3 bulk density and about 9 % moisture

content (d.b) with 25-day old tomato seedlings. The transplanter was operated by a walk behind tractor at a speed of 0.9 km/h and about 98 % to 99 % percent of the seedlings were accurately separated and fed to the conveyor of the transplanter for transplanting.



1. Feeding conveyor 2. Metering conveyor 3. Automatic feeding mechanism
4. Seedling drop tube 5. Furrow opener 6. Soil covering device 7. Ground wheel shaft 8. Drive shaft of rotavator of hand tractor

Figure 12: The walk behind tractor operated 2-row array type vegetable transplanter (Kumar and Raheman, 2012).

Zamani (2014) in Iran, designed and constructed a fully automatic single-row vegetable transplanter. A step mechanism guides the seedling trays to the left, right and down, a furrower opens a furrow, a pick-up arm lifts the seedling from the cell, moves and releases it through a crash tube into the furrow (Figure 13). The machine was tested in a sandy loam soil with bulk density of 1.25 gcm^{-3} and a moisture content of 12 % (d.b) with tomato seedlings at the four leaf stage. The results showed that forward speed and transplanting depth had significant effect on the seedling damage and angle of

inclination. Physical damage to seedling leaves was 10 %; damage to seedling stem was 20 % and damage to seedling root was 30 %. The transplanter was controlled by Programmable Logic Controllers (PLC) and had field capacity of 0.06 ha/h.



Figure 13: The fully automatic single-row vegetable transplanter (Zamani, 2014)

Jin et al. (2018) in China, developed a single-row automatic transplanting device for potted vegetable seedlings. The transplanter was tested with 40 days old tomato seedlings at 50 % moisture content and room temperature of 25 °C. A clamping claw picks up the seedling and moves to drop it in the planting hole of the planting mechanism when it ascends to its highest point. The planting mechanism then moves down to plant the seedling while the clamping claw goes back to pick the next seedling (Figure 14). The kinematic parameters of the automatic seeding mechanism were optimised and analysed using kinematics orthogonality solution combined with the dynamic sequence solution method. During the testing, at a transplanting rate of 60

plants/min, success was 92.59 % and leakage was 23.13 %., when the transplanting rate was increased to 120 plants/min, transplanting success dropped to 77.78 % and leakage increased to 38.75 %.

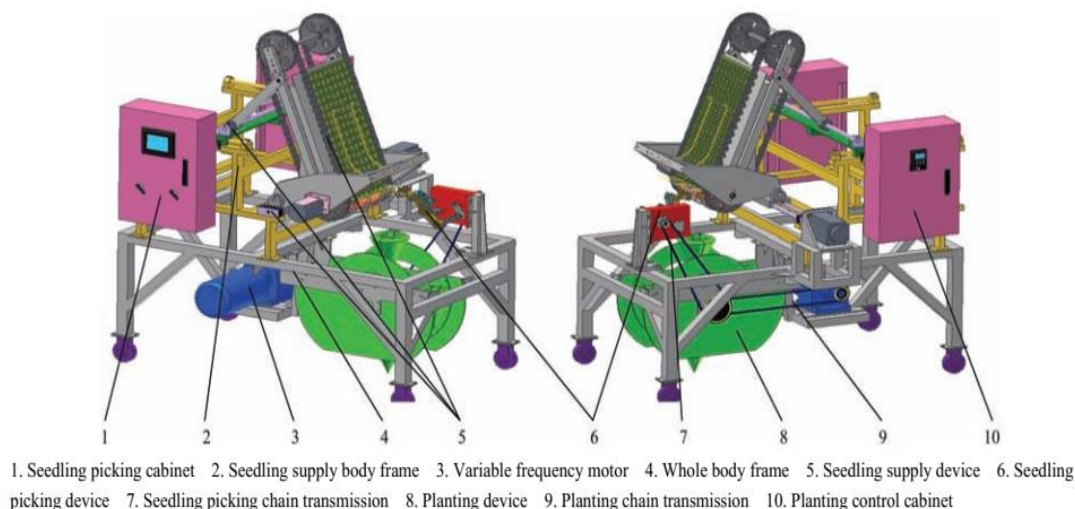


Figure .14: The single-row automatic transplanting device for potted vegetable seedlings (Jin et al. 2018)

Design Simulation

After the design process, simulation is very necessary before manufacturing is carried out. This enables the designer to clearly understand the performance of the transplanting mechanism, movement of vegetable seedlings (path/trajectory), and the forces acting on various parts of the transplanter. Yujie & Jun (2016) carried out simulation and parametric analysis of vegetable seedling transplanting mechanism using Pro/E and Adams software. They deduced the equation of displacement and velocity of vegetable seedlings. Also, they developed a nutrient soil bowl model and real size model of seedlings. Zhao et al. (2014) used Automatic Dynamic Analysis of Mechanical Systems (ADAMS) to simulate an inverted vegetable pot seedling transplanting mechanism with conjugate cam which they designed. A kinematic model of the transplanting mechanism was established on the bases

of analyzing its working principle. Visual Basic 6.0 was then used to develop an analysis and optimization software for the mechanism. The results obtained by the optimization software was compared with that of the simulation to validate the theoretical analysis.

Performance Evaluation of Vegetable Transplanters Compared to the Traditional Practice

The reasons that spark the development of various kinds of transplanters include minimizing the drudgery that vegetable farmers go through, reducing the number of labour required in vegetable cultivation and increasing the production of vegetables significantly. It is therefore imperative to assess the performance of these transplanters if they are really ahead of the traditional manual transplanting practice.

Singh (2010) carried out an experiment to evaluate the performance of a semi-automatic two-row unit (National Agro Industries, Ludhiana) vegetable transplanter compared to manual transplanting, and sowing seeds directly into the field. The vegetable seedlings used were brinjal, tomato and chili. The results showed that the use of the transplanter saves labour by 81.66 % for brinjal, 80.64 % for tomato and 80.70 % for chili. Plant mortality percentage was less in vegetable transplanter than in manual method. Plant height, number of branches, fruits per plant and yield were high in the transplanter method. However, percentage of missing plants was less in manual transplanting than the transplanter method. In terms of cost, the transplanter usage is significantly less expensive than the manual method as shown in Table 1.

Table 1: Cost of Transplanting Vegetable by Manual and by Transplanter Methods

Parameters	Vegetables		
	Brinjal	Tomato	Chilli
Cost of transplanting (Traditional) (Rs/ha)	3666.56	4059.41	3797.61
Cost of transplanting (Traditional) (Rs/ha)	3545.84	3888.18	3711.6
Saving in cost (Rs)	120.73	171.23	86.01
Saving in transplanting (%)	3.29	4.21	2.26

Source: (Singh, 2010)

Kumar and Tripathi (2016) conducted a research to study the performance of a tractor-operated two-row semi-automatic vegetable transplanter developed at Punjab Agricultural University (PAU), Ludhiana compared to the traditional manual practice. The transplanter was tested at an average speed of 1.0-1.2 km/h in a sandy loam soil with 8-9.5 % soil moisture content. The average time required by the transplanter for brinjal crop was 8.6 h/ha and for chillies crop was 1.17 h/ha. Comparing the machine transplanting to manual transplanting, the study revealed that the machine method had advantage in terms of time saving, labour saving, less cost of operation, plant height, number of branches per plant, yield per plant, and leaf area index. On the other hand, the manual transplanting method had advantage over the machine method in terms of percentage plant mortality and missing seedling. Table 2 shows details of some of the parameters.

Table 2: Effect of Transplanting Methods on Plant Height, Number of Branches & Leaf Area Index in Brinjal

		Effect of transplanting methods on plant height in brinjal					Performance parameters
Location	Method of transplanting	20	40	60	80	100	Mean
		DAT	DAT	DAT	DAT	DAT	
Village farmer field1	Manual	30.77	39.71	48.21	55.00	56.55	46.04
	Transplanter	30.32	40.71	51.32	58.38	59.77	48.10
	Mean	30.54	40.21	49.76	56.69	58.16	
Village farmer field2	Manual	28.66	37.93	47.71	54.55	56.77	
	Transplanter	30.31	40.71	51.32	58.38	59.77	
	Mean	29.48	39.32	49.51	56.46	58.27	
Location	Method of transplanting	Effect of transplanting methods on number of branches per plant in brinjal					Performance parameters
		20	40	60	80	100	Mean
Village farmer field1	Manual	4.31	10.27	14.60	19.16	20.21	13.71
	Transplanter	5.11	10.82	15.21	19.87	20.43	14.28
	Mean	4.70	10.54	14.90	19.52	20.32	
Village farmer field2	Manual	3.87	8.60	13.87	18.93	20.16	13.9
	Transplanter	4.55	9.49	15.32	20.10	21.11	14.11
	Mean	4.21	9.04	14.60	19.51	20.63	
Location	Method of transplanting	Effect of transplanting methods on leaf area index in brinjal.					Performance parameters
		20	40	60	80	100	Mean
Village farmer field1	Manual	3.91	8.02	12.02	14.20	15.32	10.69
	Transplanter	4.30	8.52	12.92	15.12	15.38	11.45
	Mean	4.11	8.27	12.47	14.66	15.84	
Village farmer field2	Manual	3.68	7.83	10.45	12.31	14.08	9.67
	Transplanter	3.80	7.76	11.09	13.13	14.38	10.03
	Mean	3.74	7.79	10.77	12.72	14.23	

Source: (Kumar and Tripathi, 2016)

CHAPTER THREE

MATERIALS AND METHODS

Introduction

The goal of the research was to develop and evaluate the performance of a semi-automatic pepper seedling transplanter for small scale farmers. It was intended to help reduce the delay, cost, and drudgery associated with manual transplanting of vegetables, especially pepper. This chapter presents the methods adopted to develop the semi-automatic pepper seedling transplanter, the materials selected, and the procedure followed to evaluate its performance under field conditions and its comparison to manual transplanting. The details include the experimental site and then the design and construction of the transplanter

Experimental Site Description

The experiment was conducted at the A.G Carson Technology Village of the school of Agriculture, University of Cape Coast, Central Region, Ghana. The mean temperature for the month of August, 2019 when the experiment was conducted was 24.25°C with 24.7 mm rainfall. The field was cleared, ploughed and harrowed to obtain a fine tilth with power tiller. Ridges of dimensions 0.60 m wide, 0.20 m high and 9 m long were then prepared. The soil properties of the experimental site are presented in Table 3

Table 3: Selected Soil Properties at the Experimental Site

Soil Property	Soil Depth	
	0-15 cm	15-30 cm
Sand (%)	60.30	58.10
Clay (%)	10.60	12.25
Silt (%)	29.10	29.65
Bulk Density (g/cm ³)	1.26	1.29
Particle Density (g/cm ³)	2.53	2.46
Saturated Hydraulic conductivity (cm ³ /s)	0.0127	0.0112
pH	6.2	6.5
Organic Carbon (%)	0.3	0.3
Total N (%)	0.04	0.05
P(ppm)	17.3	18.7
K(mg/100g soil)	0.27	0.22
EC(ds/m)	0.34	0.37

Source: Field survey Karimu (2019)

Materials and Tools

The main materials used in the manufacture of the power tiller drawn semi-automatic vegetable transplanter were: 50 mm x 25 mm mild steel U-channel, 50 mm x 50 mm galvanized angle iron, 40 x 40 mm galvanized angle iron, 30 x 30 mm galvanized angle iron, 50 mm x 25 mm galvanized pipe, 1.5 mm galvanized plate, 50 x 5 mm mild steel flat bar, 25 mm diameter mild steel shaft, and 50 mm mild steel pipe. Others included 207 and 205 pillow bearings, 6205 roller bearings, lugged tyres, chain and sprockets, bolts and nuts.

The equipment used in the manufacture of the transplanter include, a centre lathe machine, shaping machine, electric arc welding machine, drilling machines, and electric hand grinding machine. The hand tools used in

conjunction with the machines mentioned above were Vernier callipers, tape measure, try square, spanners, hacksaw, spirit level, sliding bevel, hammers, and centre punch.

Design considerations

The target group of the transplanter was small scale farmers, and as a result, the single axle tractor (also called power tiller) was chosen as the source of power for the transplanter, since it is less expensive. The transplanter was designed to be hitched to the drawbar of a VST Shakti 130 DI power tiller (13 Hp or 9.56 kW).

The furrow opener meant to receive and place the seedlings into the soil was designed by taking into consideration the average leaf spread diameter and height of the vegetable (pepper) seedlings. Maximum height of 130mm and top diameter of 65 mm were selected for the furrow opener.

The transplanter was to carry two people and two trays of seedlings at a time. The average weight of two people and that of the two seedling trays in addition to the weight of the transplanter's parts were considered in the design of the frame.

The speed ratio between the rotational speed (in revolutions per minute (rpm)) of the ground wheel axle and that of the crank shaft of the mechanism determines the inter-plant spacing. The average inter-plant spacing of common vegetables grown in Ghana informed the selection of a speed ratio of 1:2.5 through which the transplanter is able to make furrows at 60cm intervals.

Design Concepts

Mechanism for forward movement and up-and-down motion of the planting arm

The key planting technology for the movement of the semi-automatic vegetable transplanter under this study was based on crank-rocker mechanism. A crank-rocker mechanism is a 4-bar linkage (Figure 15) in which the shortest (driving) link revolves and the longest one (follower) rocks. For this to be achieved the linkage must comply with Grashof's law. The law states that for a planar 4-bar linkage, the sum of the shortest and longest links cannot be greater than the sum of the remaining links if one of the links (generally the shortest link) is to be able to revolve fully relative to the other links (Chang et al., 2014).

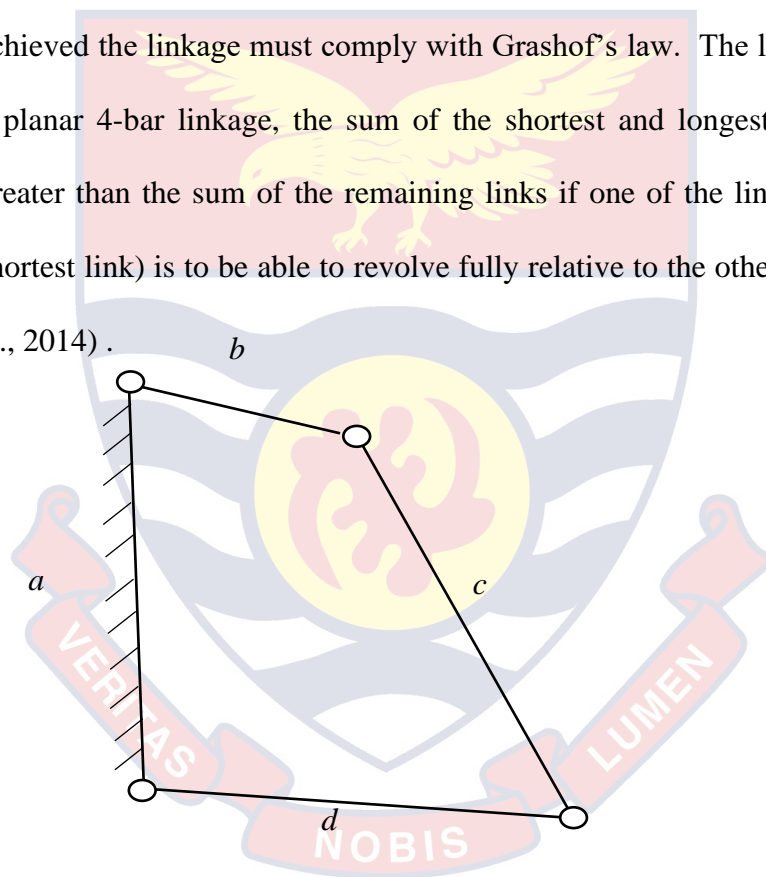


Figure 15: Crank-Rocker Mechanism (A 4-bar linkage)

In this design, the crank is driven by the ground wheels through chain and sprocket drive system, and the rocker drives a rocking shaft to which an arm that carry a furrow opener is attached. The furrow opener is opened at its lowest position by an actuator.

The transplanter, as part of the concept, was to carry two people (the operator of the power tiller and the person to be feeding the transplanter), transport the seedlings, make furrows at equal inter-plant spacing, deposit seedlings into the furrows in an upright position, and compact soil around the seedlings.

Apart from the mechanism, in order to meet the above requirements, the transplanter was planned to have a tray holder, seedling cup, a furrow opener, an actuator, four ground wheels, chain and sprocket system. Other components are two sets of foot rests, guards, a pair of compacting wheels, a frame, and then one-point hitching system.

Design mechanism for the opening-and-closing of the furrow opener

In order to come out with the best mechanism for the transplanter's furrow opening and closing for placing the seedling into the soil, three conceptual designs were selected. They were Cam-lever design (concept A), Chain-cam design (concept B), and Hydraulic plunger design (concept C). These designs were assessed using standard design evaluation parameters and the best one selected based on the scores.

The Cam-Lever Mechanism Design (Concept A)

This design comprised of a shaft with a cam, driven by power from the ground wheels through a chain and sprocket system, and a lever connected to the furrow opener (Figure 16). As the cam shaft rotates, when the cam is turned away from the direction of the furrow opener, the lever is pulled along, causing the furrow opener jaws to open. The jaws of the furrow opener are returned to the closed position by a tension spring when the cam is turned to face the opposite direction (Stanley, 1961).

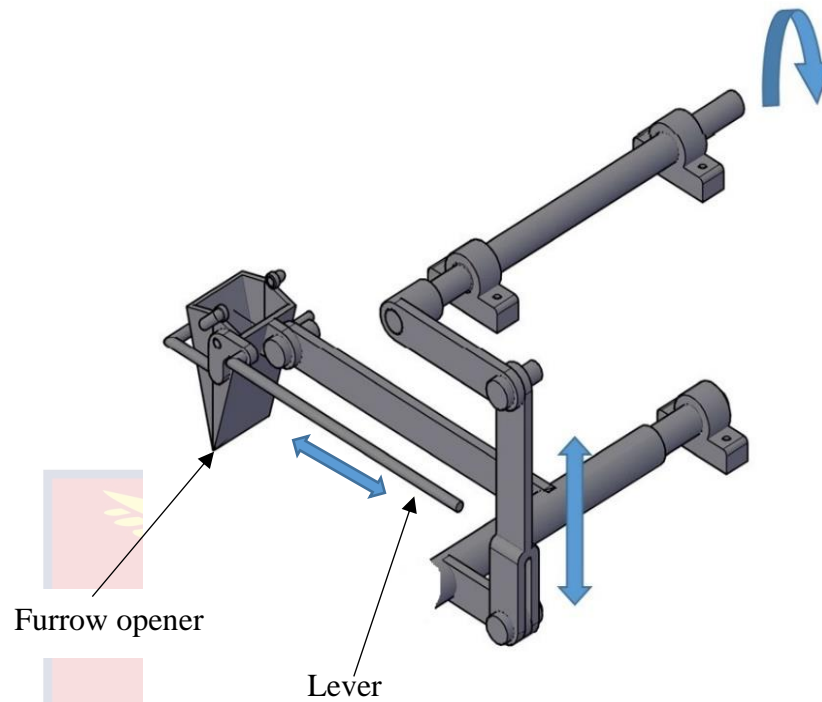


Figure 16: Cam-lever mechanism design

The Chain-Cam Mechanism Design (Concept B)

This design consists of a wheel cam attached to a shaft, mounted on the frame with roller bearings. The cam shaft is driven by power from the crankshaft through chain and sprocket drive system. There is a seedling cup into which the operator puts the seedling. The arm opens the cup in its upward travel, and the seedling released into the furrow opener (Figure 17). The rotation of the cam shaft is synchronized with the movement of the furrow opener arm such that the cam on the wheel presses against a finger on the furrow opener causing its jaws to open at its lowest position and release the seedling into the soil. The jaws are closed when the furrow opener starts to ascend and the cam is turned away from the furrow opener (Gladow, 1991).

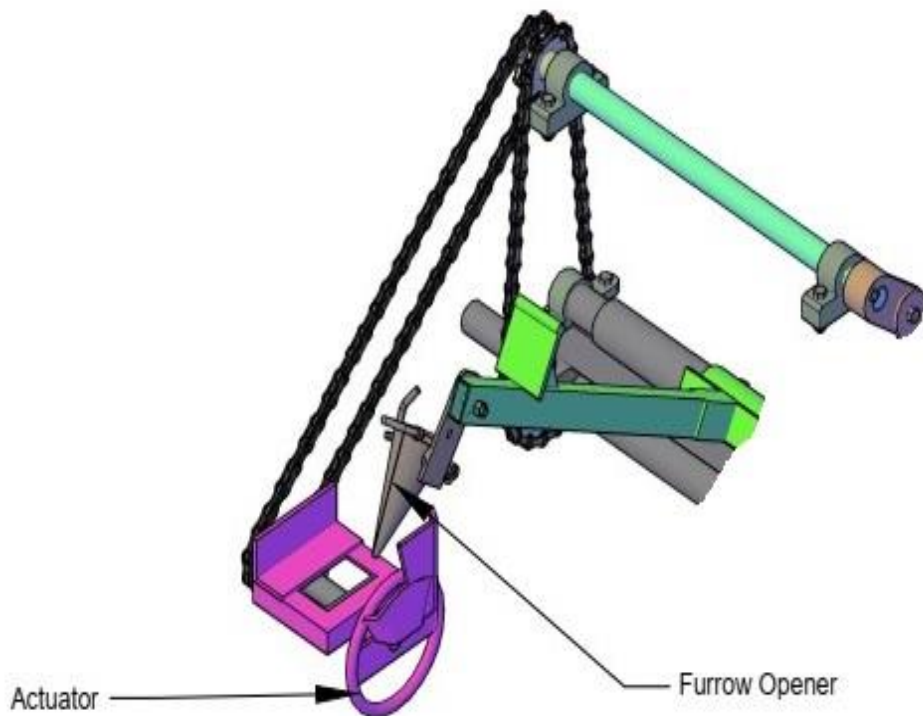


Figure 17: Chain-cam mechanism design

The Hydraulic Plunger Mechanism Design (Concept C)

This design is made up of a pump, a hydraulic plunger attached to the furrow opener jaws, a motor and a generator. The generator is driven by power from the ground wheels through belt and pulley system to produce electrical power. The hydraulic motor, driven by the electrical current, operates the hydraulic pump to drive the plunger. The plunger being attached to the furrow opener jaws, when pushed out, opens the jaws (Figure 18). This opening is programmed such that it occurs when the furrow opener is in the soil (Kershaw, Asquith and Shilton, 1995).

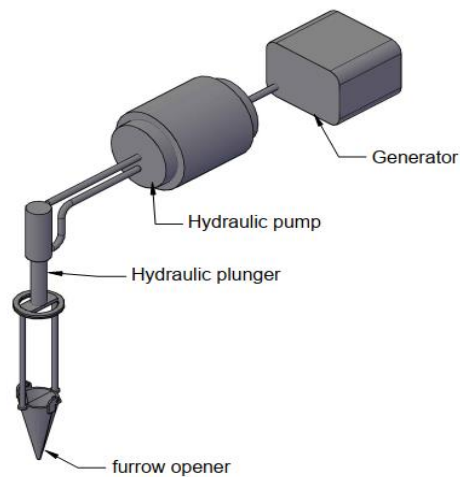


Figure 18: Hydraulic plunger design

Concept Evaluation

Evaluation parameters

The conceptual designs were evaluated based on general design parameters (i.e. cost of production, ease of maintenance, ease of operation and reliability). In addition, specific parameters related to transplanting machines (i.e. effectiveness in furrow opening and safety of seedlings) were also used.

Cost of production

This parameter considered the estimated total production cost of each conceptual design. This included the cost of materials, method/equipment to be used, the level of skills needed, the amount of energy, and labour required.

Ease of maintenance

This parameter considered the ease with which the transplanter could be maintained in the case of each conceptual design. It looked at the accessibility of all parts that need regular cleaning, the availability of parts for replacement, and the ease with which parts can be replaced.

Ease of operation

This parameter compared the operational process of each of the conceptual designs in order to determine the concept that was less complex and less tiring. It specifically looked at level of training that an operator will need before he/she can operate the machine for each case.

Reliability

This parameter analysed the features of the conceptual designs that strengthen the transplanter against failure. It specifically looked at the ability of the transplanter to transplant at the designed transplanting rate without failure, and effectively work for the projected lifespan.

Effectiveness in furrow opening

This parameter analysed how effective furrow opening will be in the case of each conceptual mechanism design. Specifically, it considered how quick-acting each concept will be and the timing of the opening relative to the position of the furrow opener.

Safety of seedlings

This parameter examined the features of each conceptual design with regard to the safety of the seedlings that it will handle. It looked at the features that will have less physical damage and less transplanting shock.

Evaluation criteria

The details of the criteria used to evaluate the conceptual designs are shown in Table 4. It indicates the parameter magnitudes and their corresponding values used for the evaluation.

Table 4: Evaluation Criteria

Parameters							
Cost of production	Magnitude(GHC)		≤4,000	4,100-5,000	5,100-6,000	6,100-7,000	≥7,100
	score		5	4	3	2	1
Ease of maintenance	Magnitude	Very easy	easy	normal	difficult	Very difficult	
	score	5	4	3	2	1	
Ease of operation	Magnitude	Very easy	easy	normal	complicated	Very complicated	
	score	5	4	3	2	1	
Reliability	Magnitude	Most reliable	Very reliable	reliable	unreliable	Most unreliable	
	score	5	4	3	2	1	
Effectiveness in furrow opening	Magnitude	Most Effective	Very Effective	Effective	Less effective	Ineffective	
	score	5	4	3	2	1	
Safety of seedlings	Magnitude	Safest	Very safe	safe	unsafe	Most unsafe	
	score	5	4	3	2	1	

Source: Field survey Karimu (2019)

Decision matrix

The score of each of the conceptual designs under the parameters used for the evaluation are shown in table 5.

Table 5: Decision Matrix

PARAMETERS		Design A	Design B	Design C
Cost of production	Magnitude (GHC)	6,500	6,000	8,500
	Score	4	5	2
Ease of Maintenance	Magnitude	Easy	Very easy	Normal
	Score	4	5	3
Ease of operation	Magnitude	Easy	Very easy	Easy
	Score	4	5	4
Reliability	Magnitude	Very Reliable	Most reliable	Very Reliable
	Score	4	5	4
Effectiveness in furrow opening	Magnitude	Most Effective	Very effective	Effective
	Score	5	4	3
Safety of seedlings	Magnitude	Very safe	Very safe	Safest
	Score	4	3	5
Total		25/30= 83 %	27/30=90 %	21/30= 70 %

Source: Field survey Karimu (2019)

From table 5, concept B (the Chain-cam mechanism design) had the highest total score. It was therefore selected as the key mechanism for opening the furrow as shown in the 3-Dimensional drawing in Figure 19.

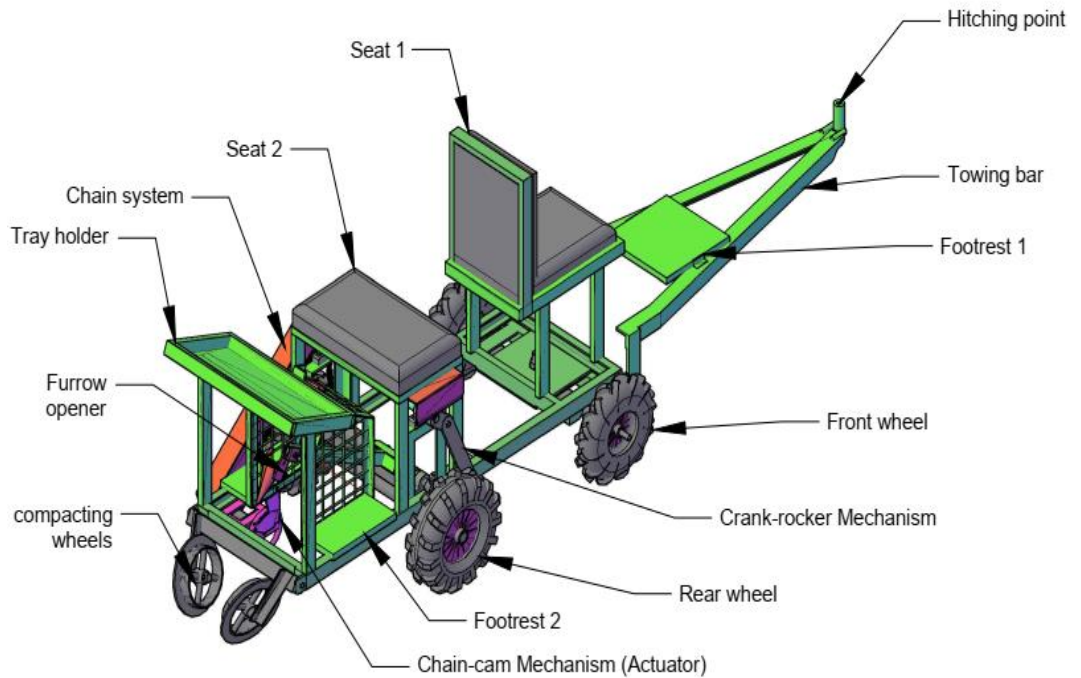


Figure 19: The 3-Dimensional drawing of the transplanter

Design of functional components of the vegetable transplanter

Design of the crank-rocker mechanism

The lengths of the links

Assuming in a 4-bar linkage (Figure. 20), *b* is the length of the shortest link, *d* the length of the longest link, *c* and *a* being the lengths of the other two links, Grashof's law states that, one link will be able to completely rotate if

$$d + b \leq c + a \dots\dots\dots \text{Equation 3.1}$$

and no link can have complete revolution if

$$d + b > c + a \dots\dots\dots \text{Equation 3.2}$$

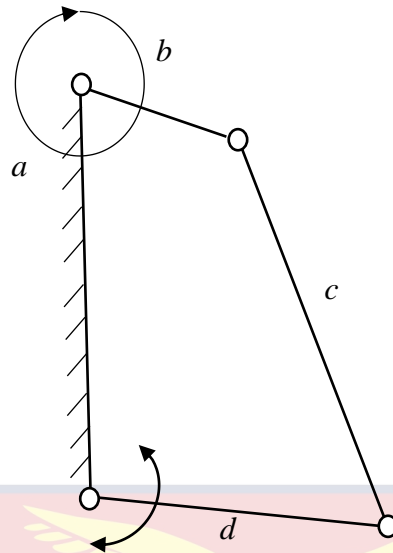


Figure 20: Parts of the Crank-Rocker Mechanism (a) Frame, (b) Crank, (c) Coupler (d) driven link, follower, or rocker.

In the design of this study, when the lengths of the various links were substituted into the inequality (Equation 3.1) and evaluated, it resulted in $253 \leq 570$. This implies the crank would be able to have full revolution according to Grashof's law (Chang et al., 2014).

Degree of freedom

For a planar mechanism, the degree of freedom can be determined using Gruebler's Equation: $F = 3(n - 1) - 2f_i$ Equation 3.3

Where F is the degree of freedom and n is the number of links (including a frame or ground link) and f_i represents the number of joints (Slocum, 2008)

The number of joints and links in this design when substituted into equation 3.3 also resulted in one (1) degree of freedom of movement. This implies all the links are constrained to move in one plane, minimizing energy losses caused by unwanted movements in other directions or planes.

The power transmission system

As the power tiller pulls the transplanter, power from the rotation of the ground wheels is used to operate the mechanism through sprocket and chain drive system. Sprocket and chain drive system was selected over gear and belt & pulley drive systems because the shaft centre distances are relatively unrestricted (can vary anywhere from 50 % to 300 % or more of their pitch diameters). Compared to gear drives, chain drives are relatively easy to install as assembly tolerances are less restrictive. Also, chains perform better than gears under shock loading conditions. Chain drives require less space for a given loading and speed condition as compared to belt drives. No slip takes place during chain drive unlike the case of belt drive, hence uniform velocity ratio is obtained (Gears Educational Systems, 2002).

Design of the chain and sprocket drive system for the crank-rocker mechanism.

The assumptions made for the crank-rocker mechanism chain sprocket calculations are presented in Table 6.

Table 6: Assumed Values for the Crank-Rocker Chain Sprockets

Parameter	Value
speed of transplanter (S_t) = Speed of power tiller	1 km/h = 16.67 m/min
Diameter of transplanter ground wheels (D_{gw})	0.38 m
Desired speed ratio between the ground wheels and the crank shaft	1:2.5
Distance between ground wheel and crank Shaft Centres (C_p)	0.38 m
Maximum HP of power tiller 13 hp @ 2400 rpm	9.698 kW
The power required by the mechanism	8 % of 9.698 = 0.776 kW

Source: Field survey Karimu (2019)

Rotary speed of crank shaft (high speed shaft)

$$\text{Rotary Speed of the ground wheels} = \frac{\text{speed of transplanter}}{\text{circumference of ground wheel}}$$

..... Equation (3.4)

The rotary speed of the crank shaft was calculated to be 35 rpm from Appendix C1

Application coefficient (service factor)

From the Application Coefficient (service Factor) Table (Appendix E3), for a machine powered by an internal combustion engine with smooth transmission, the Application coefficient is 1.2 if there is no fluidic mechanism (Misumi, 2009). This value is applied in the design since the Vegetable Transplanter is operated by a power tiller which is an internal combustion engine.

Corrected power transmission (design horsepower)

$$\begin{aligned} \text{Corrected power transmission} &= \text{Power Transmission (kW)} \times \text{Application} \\ \text{Coefficient} &= 0.776 \times 1.2 = 0.93 \text{ kW} \end{aligned}$$

Chain and number of small sprocket teeth

In order to minimize noise and ensure smooth transmission of power, the pitch of the chain should be kept as minimum as possible, provided the required power transmission efficiency is attained (Misumi, 2009). From the Chain and Sprocket Selection Guide Table (Appendix E1), the chain and number of small sprocket teeth that satisfy the calculated rotary speed of the high-speed shaft (35 rpm), and the corrected power transmission (0.93 kW), is CHE40 15T from Appendix C2 (Chain number 40 and small sprocket 15 teeth).

Number of large sprocket teeth

The number of large sprocket teeth was calculated as;

Number of Large Sprocket Teeth = Number of Small Sprocket Teeth \times Speed

Ratio = $15 \times 2.5 = 37.5$

Hence 37 teeth sprocket was selected.

Chain length for the Crank-Rocker mechanism

Chain length is measured in discrete units called links. The length of each link is the same as the pitch length. For a given chain drive system, the length of the chain is determined by equation 3.5.

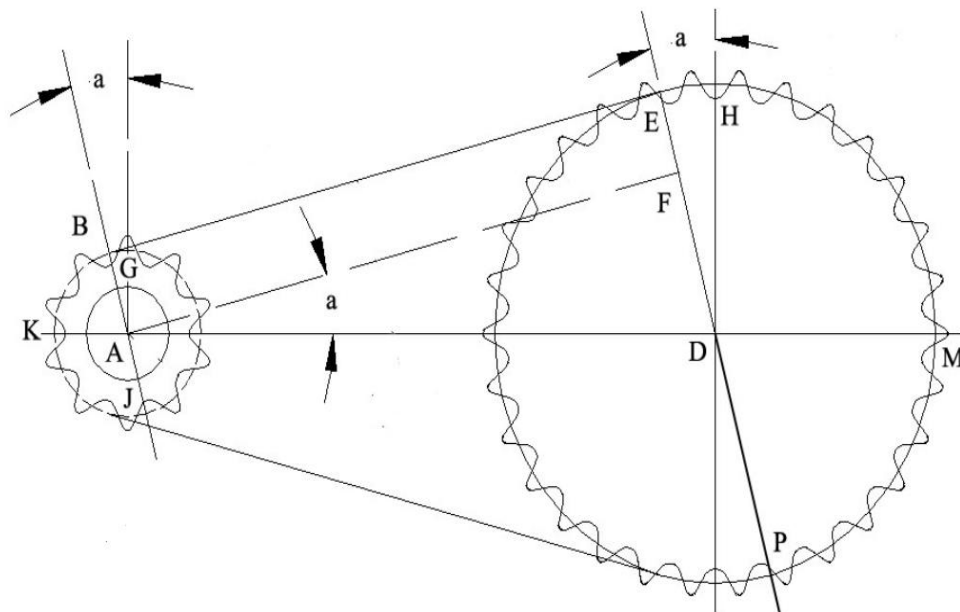


Figure 21: Chain drive system for the Crank-Rocker mechanism (Gears Educational Systems, 2002)

In Table 7 are assumed figures used for the calculation of the Crank-Rocker Mechanism chain length.

Table 7: Assumed Figures for the Crank-Rocker Chain Length

Item	Assumed Values
Pitch (P)	½” (12.7mm)
Small Sprocket (n)	15 Teeth
Large Sprocket (N)	37 Teeth
Center Distance (AD)	380mm or 380/12.7 = 30 pitch units

Source: Field survey Karimu (2019)

The mechanism chain length was given by

$$L_1 = 2 (BE + ME + BK) \dots\dots\dots \text{Equation 3.5}$$

Pitch circle radius of the small sprocket (Pr)

From Figure 21, the dimension AB = Pr

And Pr = ½ x pitch circle diameter of the small sprocket (Pd)

$$\text{However, } Pd = \frac{P}{\sin\left[\frac{180^\circ}{n}\right]} \dots\dots\dots \text{Equation 3.6}$$

$$AB = PR = \frac{1}{2} \times \frac{P}{\sin\left[\frac{180^\circ}{n}\right]}$$

Where PR is the pitch circle radius of the large sprocket.

Eventually from calculation and analysis, the small sprocket pitch circle radius used was 30.5 mm

Pitch circle radius for the large sprocket (PR) was determined using the relation,

$$PR = DE = \frac{1}{2} \times \frac{P}{\sin\left[\frac{180^\circ}{N}\right]} \dots\dots\dots \text{Equation 3.7}$$

Large sprocket pitch circle radius was 74.7 mm

The length of side DF was found to be 44.2 mm

The magnitude of angle “a” was determined to be 6.9° using the relation

$$\sin(a) = \frac{DF}{AD}$$

The length of chain between the pitch circle tangent points, BE was found to be 30 pitch units using the relation $BE = AF = AD \times \cos a$.

In the determination of the lengths of chain wrapped around each of the sprockets, half of the chain wrapped around the large sprocket, arc ME, was found to be 10 pitch units using the relation

$$ME = MH + HE = \frac{N}{4} + N \frac{a}{360} \dots\dots\dots \text{Equation 3.8}$$

Half of the chain wrapped around the small sprocket, arc KB, was also found to be 3.5 pitch units using the relation

$$KB = KG - BG = \frac{n}{4} - n \frac{a}{360} \dots\dots\dots \text{Equation 3.9}$$

Substituting the values of line BE, arc ME, and arc KB into equation 3.5 resulted in a chain length of 87 pitch units (links).

This value was rounded up to 88 links (an even number) since it is not convenient to work with odd number of links. Rounding down is discouraged because too tight chains damage sprockets, shafts, and lead to premature chain failure (Gears Educational Systems, 2002).

Design of the actuator chain and sprocket

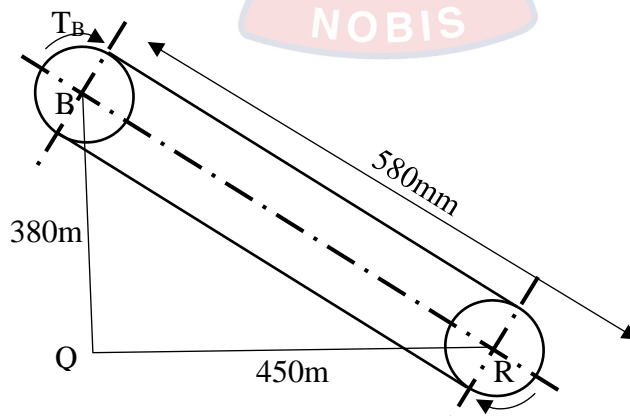


Figure 22: Actuator chain drive system

The parameters with known or selected values for the design of the actuator are as follows:

Pitch (P) = 1/2" = 12.7 mm

Distance between the crank shaft and the actuator shaft centres (C_d) = 580mm

Desired speed ratio between the crank shaft and the actuator shaft = 1: 1

Number of teeth of driving sprocket n₁ = 15

Actuator sprocket teeth

Since the speed ratio was 1:1, the number of teeth on the driving sprocket (n₁) and the driven sprocket (n₂) were equal,

$$n_1 = n_2 = 15$$

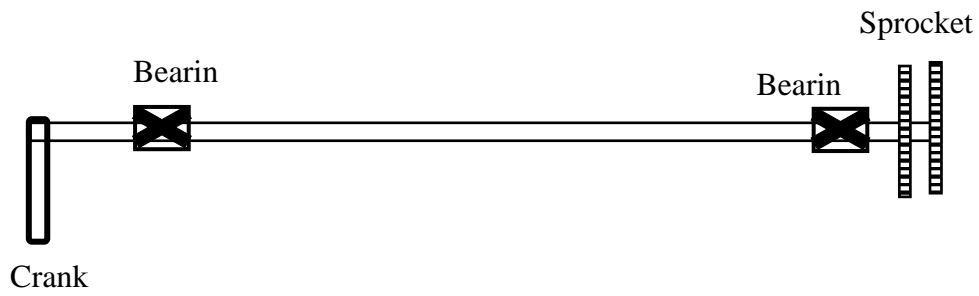
Actuator chain length

The length of the actuator chain was found to be 106 pitch units using the relation

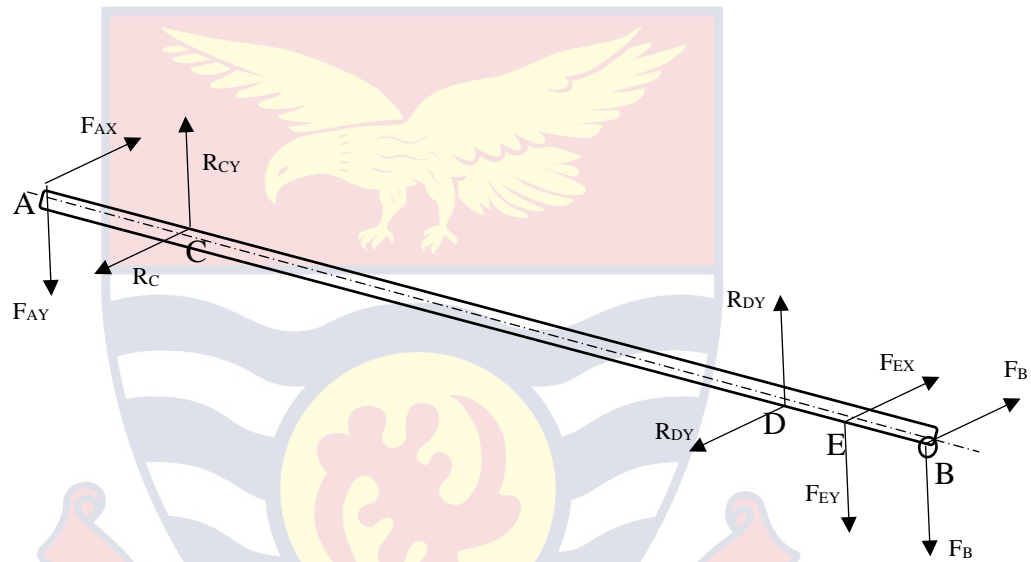
$$L_2 = 2C_d/p + n \text{ (in pitch units)} \dots\dots\dots \text{Equation 3.10}$$

Design of the crankshaft

This basically, is the determination of the correct diameter of the shaft to ensure satisfactory strength and rigidity when it is transmitting power under various loading and operating conditions. The length (L) of the shaft had been pre-determined as 650mm. It is shown in Figure 23 including its free body diagram showing the forces associated with it.



(a)



(b)

Figure 23: (a) Crank Shaft attachments (b) free body diagram

Properties of the selected material

The material from which the shaft was machined, selected from standard table is AISI 1020 low carbon steel. From the properties of AISI 1020 table (Appendix E2), the material has tensile yield strength (S_y) of 295 Mpa, ultimate tensile strength (S_u) 395 mPa, and density of 7.87 g/cm^3 . Its modulus of elasticity (E) is 200GPa, and its poisson's ratio (ν) is 0.290 (Azo Materials, 2015).

This design was based on the following assumptions:

- i. The shaft was circular in cross-section;

- ii. The Material being homogenous;
- iii. Material being linearly elastic or Hook's law is valid;
- iv. There are no internal stresses prior to loading;
- v. The design factor of safety (N) was taken to be 3.

Torque in the shaft (T)

The transplanter was to be drawn by a power tiller (VST Shakti 130 DI) with a maximum horse power of 13.0 HP @ 2400 rpm and a maximum torque of 4.2 kg-m @ 1600 rpm at an average speed of 1.0 km/h. The power requirement of the transplanter was determined as follows:

$$p = \frac{2\pi N \times T}{60 \times 10^3} \dots\dots\dots \text{Equation 3.11}$$

Where N is rotational speed of the driving shaft and T is the shaft torque (kNm). With P and N already known, the torque in the shaft was calculated to be 0.038kNm

Weight of the crank at point A in figure. 3.9 (b)

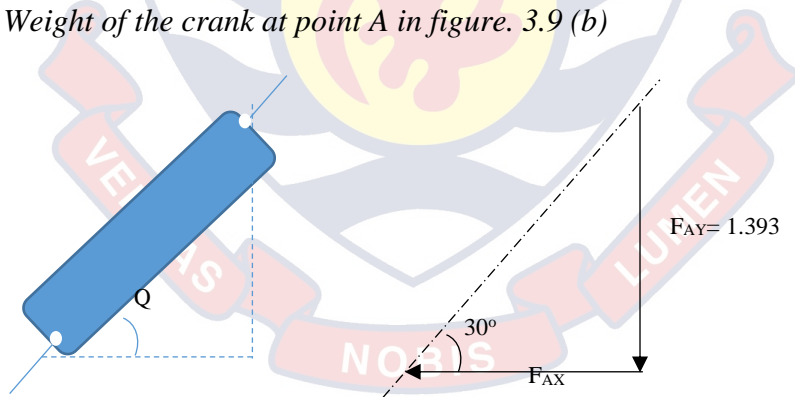


Figure 24 Free body diagram of the crank

The vertical weight of the crank (F_{AY}) was found by

$$F_{AY} = mg \dots\dots\dots \text{Equation 3.12}$$

Where g = acceleration due to gravity, m = mass of the crank = ρV

ρ = density of the crank material (AISI 1020) = $7.87g/cm^3$

The volume of the crank was determined as $18cm^3$ from the formula

$$V = l \times b \times h \dots\dots\dots \text{Equation 3.13}$$

By substitution and evaluation, the mass (m) of the crank was calculated as 0.142kg. Subsequently, F_{AY} was found to be 1.393kN.

The horizontal component of the crank weight was found to be 0.804kN with the relation,

$$F_{AX} = F_{AY} \tan 30 \dots\dots\dots \text{Equation 3.14}$$

Forces due to Chain and Sprocket

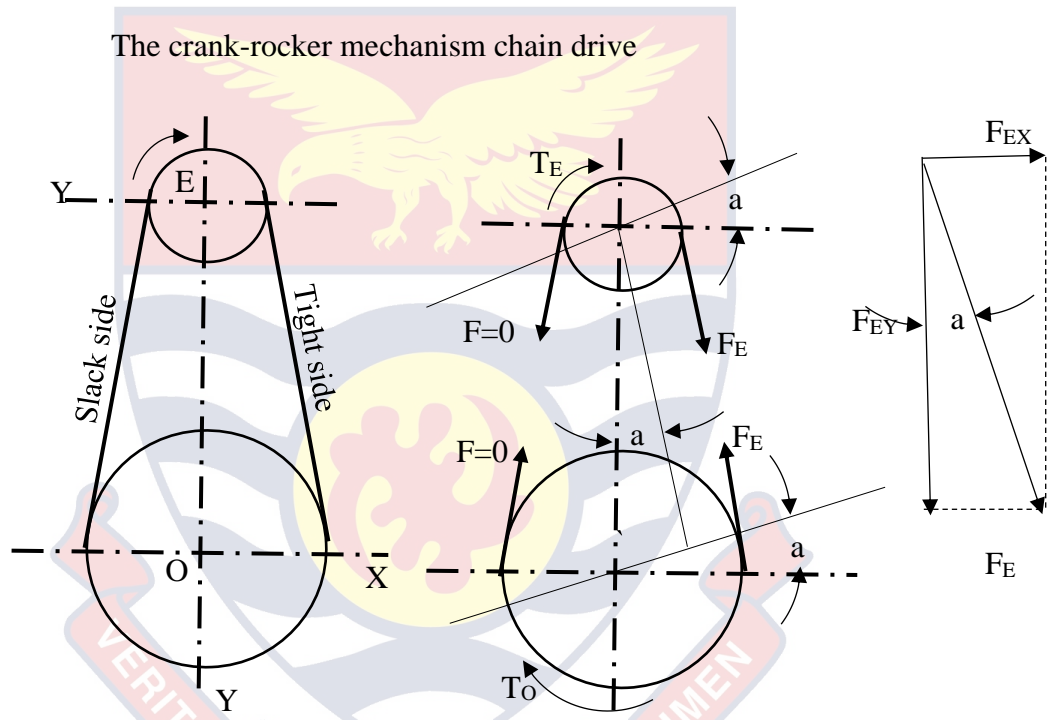


Figure 25: Free body diagram of the crank-rocker mechanism chain drive

The force due to the sprocket at point E on the shaft is given by

$$F_E = \frac{2T}{D} \dots\dots\dots \text{Equation 3.15}$$

Where T = torque (calculated above) = 0.038 kNm

D = Pitch circle diameter of sprocket on the shaft = 0.061 m = 0.1m

By substitution $F_E = 0.76$ kN. The horizontal component of the force F_E was calculated as $F_{EX} = 0.091$ kN using the relation

$$F_{EX} = F_E \sin a \dots\dots\dots \text{Equation 3.16}$$

The vertical component of the force F_E is calculated as $F_{EY} = 0.754\text{kN}$ using the relation

$$F_{EY} = F_E \cos a \dots\dots\dots \text{Equation 3.17}$$

The chain-cam (actuator) Chain drive

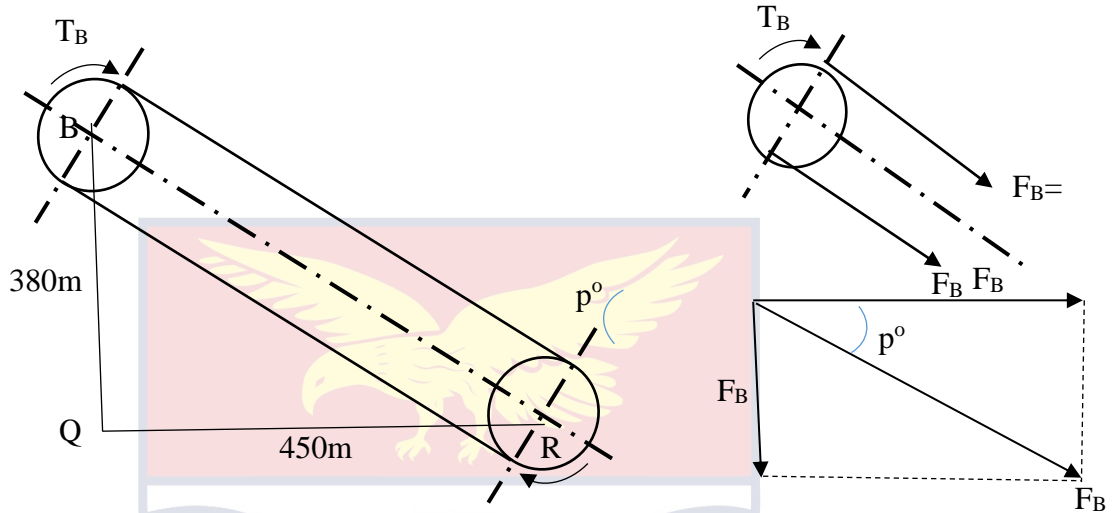


Figure 26: Free body diagram of the actuator chain drive

The force due to the sprocket at the point B on the shaft is given by

$$F_B = \frac{2T_B}{D} \dots\dots\dots \text{Equation 3.18}$$

Where T_B = torque = 0.038 kN

D = Pitch circle diameter of sprocket on the shaft =0.061 m = 0.1 m.

By substitution F_B was found to be 0.76 kN

The actuator chain drive inclination to the horizontal, angle p from Figure 26, was calculated as 40.2° using the relation

$$\tan p = \frac{BQ}{QR}$$

The horizontal component of the force F_B was calculated as $F_{BX} = 0.580$ kN using the relation

$$F_{BX} = F_B \cos p \dots\dots\dots \text{Equation 3.19}$$

The vertical component of the force F_B was calculated as $F_{BY} = 0.490$ kN using the relation

$$F_{BY} = F_B \sin p \dots\dots\dots \text{Equation 3.20}$$

Reactions at the bearings supporting the crankshaft

The vertical (YZ plane) forces acting on the crankshaft are represented by the free body diagram shown in Figure 27.

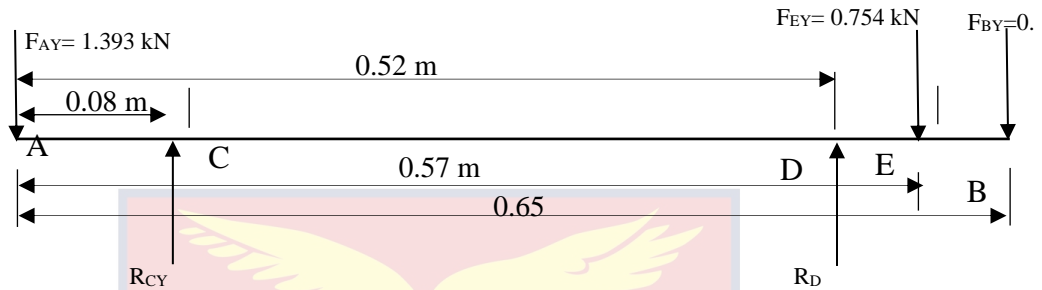


Figure 27: Vertical loading of the crank shaft

Taking moments about point C, and equating the sum of Clockwise Moments to the sum of Anticlockwise Moments in Figure 27 gave

$$(F_{AY} \times 0.08) + (R_{DY} \times 0.44) = (F_{EY} \times 0.49) + (F_{BY} \times 0.57)$$

This relation was used to calculate the reaction (R_{DY}) by the bearing at point D on the shaft as $R_{DY} = 1.221$ kN

Also for equilibrium, total upward forces were equated to total downward forces to give

$$R_{CY} + R_{DY} = F_{AY} + F_{EY} + F_{BY}$$

This relation was used to calculate the reaction (R_{CY}) by the bearing at point C on the shaft as $R_{CY} = 1.416$ kN

Taking the point A as the reference point, and using singularity function in Microsoft excel, the shearing forces and bending moments at the points A, C, D, E, and B were found to be

$$V_A = -1.393 \text{ kN}, V_C = 0.023 \text{ kN}, V_D = 1.244 \text{ kN}, V_E = 0.49 \text{ kN}, V_B = 0$$

$$M_A = 0, M_C = -0.11 \text{ kNm}, M_D = -0.102 \text{ kNm}, M_E = -0.039 \text{ kNm}, M_B = 0$$

Figure 28 presents the shearing force and bending moment diagrams for the YZ plane.

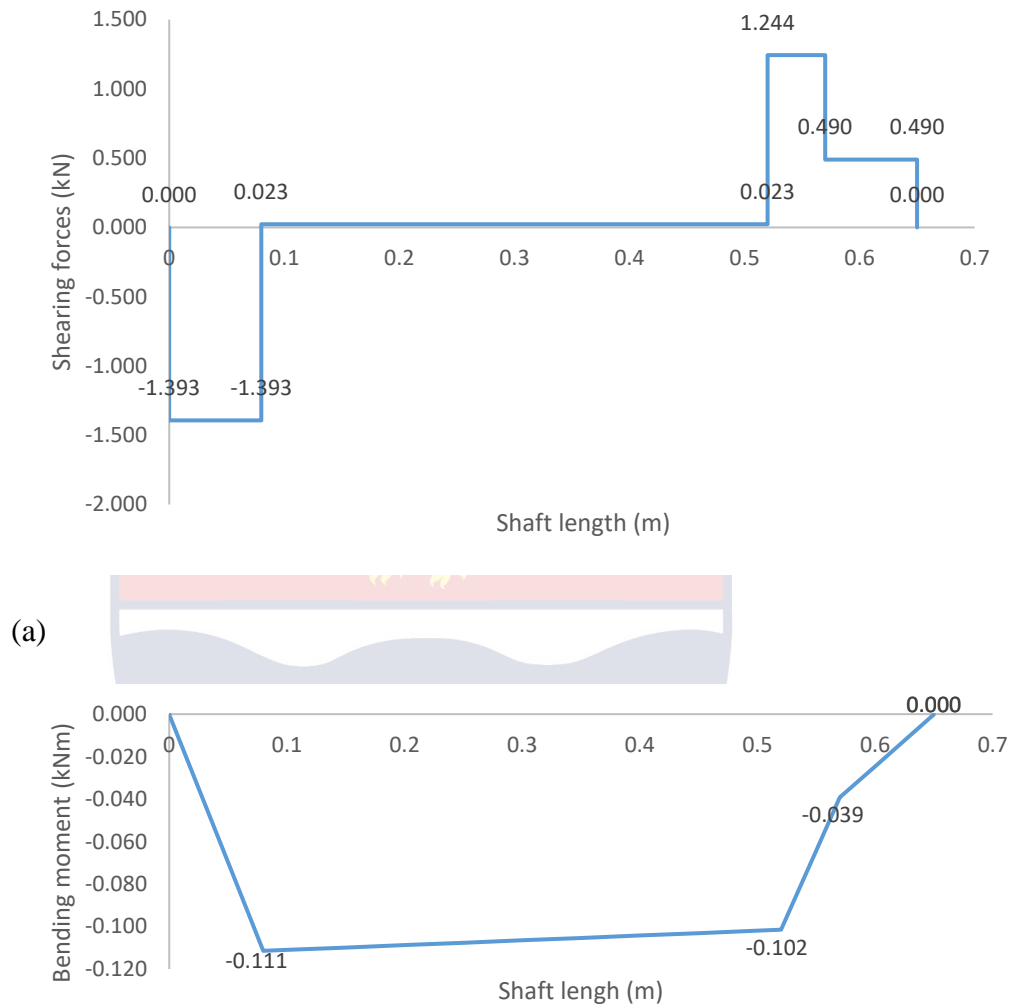


Figure 28: (a) Shearing force diagram (b) Bending moment diagram for the YZ plane

Horizontal forces (XZ plane)

Figure 29 represents the expected free body diagram of the horizontal forces acting on the crankshaft

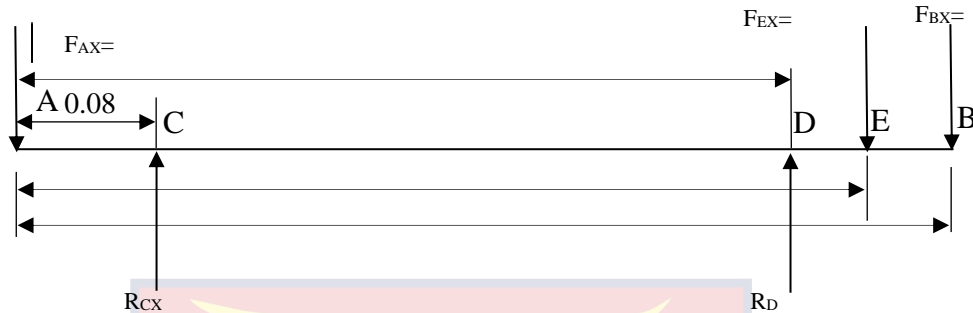


Figure 29: Horizontal loading of the crank shaft

Taking moments about point C, and equating the sum of Clockwise Moments to the sum of Anticlockwise Moments gave

$$(F_{EX} \times 0.49) + (F_{BX} \times 0.57) = (F_{AX} \times 0.08) + (R_{DX} \times 0.44)$$

This relation was used to calculate the reaction (R_{DX}) by the bearing at point D on the shaft as $R_{DX} = 0.707 \text{ kN}$

Also for equilibrium, total upward forces were equated to the total downward forces to give

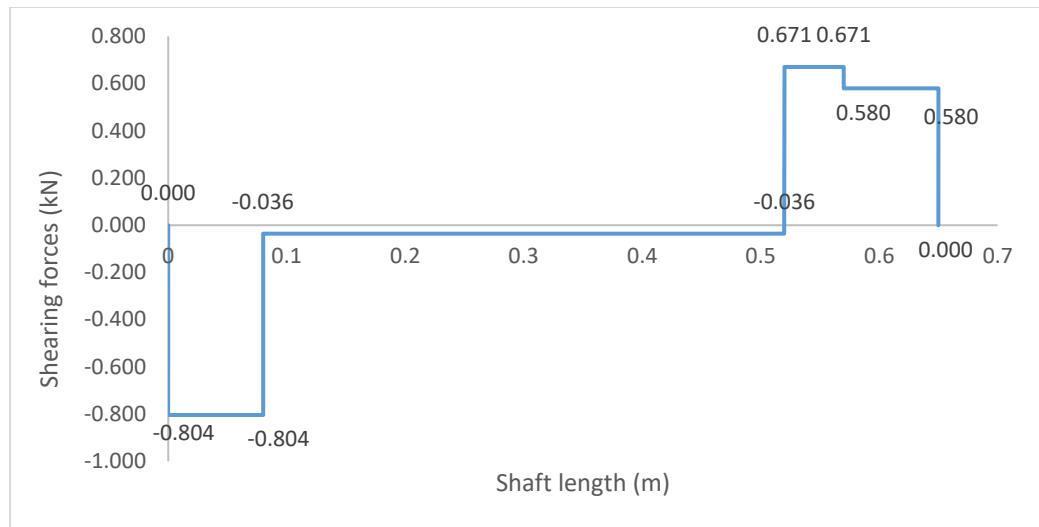
$$F_{CX} + F_{DX} = F_{AX} + F_{EX} + F_{BX}$$

This relation was used to calculate the reaction (R_{CX}) by the bearing at point C on the shaft as $R_{CX} = 0.768 \text{ kN}$

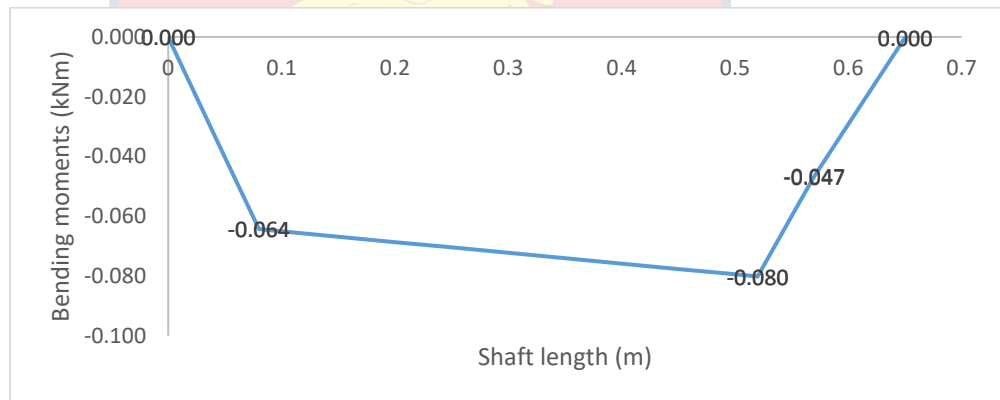
Taking A as the reference point, and using singularity function in Microsoft excel, the shearing forces and bending moments at the points A, C, D, E and B were calculated to be

$$V_A = -0.804 \text{ kN}, V_C = -0.036 \text{ kN}, V_D = 0.671 \text{ kN}, V_E = 0.580 \text{ kN}, \text{ and } V_B = 0$$

$$M_A = 0, M_C = -0.064 \text{ kNm}, M_D = -0.080 \text{ kNm}, M_E = -0.047 \text{ kNm}, \text{ and } M_B = 0$$



(a)



(b)

Figure 30: (a) Shearing force diagram (b) Bending moment diagram for XZ plane

Sizing the crankshaft

The crankshaft was designed on the basis of its strength. The shaft material was mild steel, and it was considered to be subjected to combined twisting and bending moments. Hence, maximum shear stress theory or Guest’s theory was applied. According to this theory, maximum shear (τ_{max}) stress is given by:

$$\tau_{max} = \frac{1}{2} \sqrt{[(\delta_b)^2 + 4\tau^2]} \dots\dots\dots \text{Equation 3.21}$$

(Khurmi and Gupta, 2005)

Where δ_b = stress due to bending moment, and τ = stress due to twisting moment

From equation (3.21), the equivalent twisting moment equation 3.22 is drafted and used to calculate the diameter of the shaft.

$$T_e = \sqrt{(M^2 + T^2)} = \frac{\pi}{16} \times \tau \times d^3 \dots\dots\dots (3.22)$$

(Khurmi and Gupta, 2005)

Where

T_e is equivalent twisting moment

M is maximum bending moment found to be -111 kNm at point C on the shaft

T is applied torque on the shaft calculated earlier to be 0.038 kNm

d is the shaft diameter

τ is allowable shear stress

The allowable shear stress was taken as 42 MPa (42 N/mm²) since that is the maximum permissible shear stress for shafts with allowance for keyways (Khurmi and Gupta, 2005).

Substituting the values of the maximum bending moment, applied torque, and allowable shear stress into equation (3.22) and evaluating, resulted in a shaft diameter (d) of 23.8 mm. however, a standard shaft diameter of 25 mm was selected in order to ensure safety.

Deflection of the Shaft

The angle of twist was computed from the relation;

$$\phi = \frac{TL}{JG} \dots\dots\dots \text{Equation 3.23}$$

Where: T is the torque applied to the shaft = 0.038 kNm, L = Length of the shaft = 650 mm

J- polar moment of inertia of solid shaft = $\frac{\pi D^4}{32}$ Equation 3.24

(Rao, 2007)

Using shaft diameter of 0.025, we have,

$$J = \pi \times \frac{0.025^4}{32} = 3.835 \times 10^{-8} m^4$$

G - Modulus of rigidity = $\frac{E}{2(1+\nu)}$ Equation 3.25

(Beer, Johnston Jr and DeWolf, 2001)

Substituting the values of the modulus of elasticity (E) and poisson's ratio (V) of the material (from the Properties of AISI 1020 Low Carbon Steel in Appendix E2) into equation (3.25) gives a modulus of rigidity (G) of 77.5 GPa. Consequently, with "G" known, the deflection of the shaft was determined using equation (3.23) to be $(8.31 \times 10^{-6})^\circ$.

Bearing selection

Round ball bearings were used for the rocker shaft on which the furrow opener arm is mounted, whilst pillow block bearings were used for the crank shaft since the mount surface is opened and parallel to the rotation axis. However, both bearings have ball rollers and with the same bore of 25mm. The factors considered during the bearing selection included; the mount surface condition, bearing life, strength, rigidity, and the design of the shaft that carries the bearing.

Natural deterioration is not the only cause of bearing failure. It was noted that since situations such as errors in the selection process, improper design of bearing surroundings, incorrect mounting, and insufficient maintenance may also lead to conditions such as heat-seizure, fracture, scoring of bearing rings, and damage of seals or the cage (NSK, 1998), we carefully

selected the bearings to fit the design requirements of the machine after determining the speed factor, bearing load, and bearing life.

From the concept, the known parameters to be used in the calculation included the following:

Single groove ball bearing bore inside diameter = 25mm, Outside diameter <100 mm,

Radial Load, $F_r=1.256$ kN, Speed, $n = 37$ rpm, Basic Rating life, $L_h \geq 10,000$ hrs

Hence the speed factor (f_n) was determined using the formula,

$$f_n = \left(\frac{10^6}{500 \times 60n} \right)^{\frac{1}{3}} = (0.03n)^{1/3} \dots \dots \dots \text{Equation 3.26}$$

where n = rotational speed of the shaft

Putting the value of n (as stated above) into Equation (3.26) gives a speed factor of 1

Also, the bearing load (P) is given by

$$P = F_r \times F_w$$

Where F_r = Radial load = 1.256 kN,

For operations under vibration and shock conditions, according to the Bearing Load Factor Values Table (Appendix E4), F_w = load factor = 3

By substitution, $P = 1256 \times 3 = 3768$ N

The eventual bearing life was calculated by assuming the nominal life at 10 % probability of failure for ball bearings and using Equation (3.27)

$$L_{10} = \left(\frac{C}{P} \right)^3 \dots \dots \dots \text{Equation 3.27}$$

Where C = basic load rating (N), P = bearing load or equivalent load (N)

For bearings running at constant speed, the fatigue life is appropriately presented in hours instead of mileage as generally found in automobiles.

Basic rating life in hours is given by

$$L_h = \frac{10^6}{60n} \left(\frac{C}{P} \right)^{\frac{1}{3}} = 500F_h^3 \dots\dots\dots \text{Equation 3.28}$$

Where f_h is fatigue life factor given by

$$f_h = f \frac{C}{P} \dots\dots\dots \text{Equation 3.29}$$

According to NSK (1998), the fatigue life factor f_h of ball bearings having fatigue life rating longer than 10000 hours is 2.72. substituting the values of f_h , and P, into equation (3.29) gives a basic load rating (c), of 10249 N. And from Bearing Selection Table for Bore Diameter 25-45 mm (Appendix E5), the safer bearing number that satisfies the above condition was 6205.

Design of the seedling handling system

The seedling tray holder

Standard 98 square plug cell trays with configuration of 7x14 cells, cell top diameter of 32mm, cell depth of 50.8 mm, cell centre-centre distance of 36x37mm, and overall dimensions of 260 mm x 530 mm, was used to nurse the seedlings. For the tray holder to be able to contain two of these trays at a time, the size of its platform was calculated as follows:

$$\begin{aligned} \text{The tray platform size} &= (\text{tray width} + \text{desired clearance}) \times (\text{tray length} + \text{desired clearance}) \\ &= (260 + 40) \text{ mm} \times (530 + 40) \text{ mm} \\ &= 300 \text{ mm} \times 570 \text{ mm} \end{aligned}$$

The maximum height of the tray holder was assumed to be 500mm as a convenient height for picking and dropping seedlings while sitting on the transplanter chair.

Simulation Procedure of the Designed Semi-Automatic Vegetable

Transplanter

The designed semi-automatic vegetable transplanter drawn with AutoCAD was imported into COMSOL Multiphysics 5.2 version for simulation to ascertain the motion patterns of moving parts and the forces acting at critical joints in the design.

Setting up the model environment

The type of simulation conducted was a multibody dynamics simulation under Structural Mechanics module. To set up a model environment for this type of simulation, after launching the application, the model wizard was selected, and 3D selected under Space Dimensions. Multibody Dynamics (mbd), an extension of Structural Mechanics, was then selected and added as the desired physics. Finally, under the select study window, Time Dependent option was selected as the desired suitable study.

Setting up the geometry

The design was modelled in AutoCAD and saved as dwg file onto the computer. Under the geometry tap, through the Import button, the geometry (the transplanter mechanism subassembly), was imported into the COMSOL geometry area. Since there are several parts coming into contact with each other to form the geometry, the Form Assembly option was selected to create the required geometry.

Definition of boundaries

Boundaries that are essential for creation of contact pairs were selected and grouped. This was done by going to explicit button under definitions tap and creating the required Explicit.

Specification of material properties

Under the Home tap, “Add Material” was selected and from the built in library, structural steel was selected. The default material model is a linear elastic material which was maintained as the analysis to be performed was flexible multibody analyses.

Definition of physics

The groups of boundaries necessary to form the joints and frames were selected and the appropriate type of joints and constraints applied. This was done by creating the necessary attachments under Boundaries button in the Physics tap, and choosing the appropriate joint type from the Global button, also in the Physics tap. Under the Domain button, gravity node was selected and added to the component to account for its weight.

Creation of mesh and running of the simulation

Under home tap, “Build mesh” was selected and the appropriate mesh that best suits the component was built. Under the time-dependent node, time settings were adjusted to solve for 3s, at 0.025s intervals. The required analysis was performed on the solved module by clicking on the Compute button in the Home tap.

Post-processing of the results

Usually after running the simulation, the default plot created are for displacement and the component velocity. To plot the joint forces with respect to time graph, Add plot group button was selected in the Home tap and 1D plot added. Then at Global plot, joint forces for the joint to be analysed was selected and the Y and Z coordinate settings specified as rotation is about the X-axis. The Plot button was then clicked and the joint forces graph plotted.

To plot the tip trajectory, another 1D plot was added and this time, point plot was selected. A pot at the bottom of the furrow opener was selected and the Y and Z coordinate settings specified since the rotation was about the X-axis. Finally, the plot button was clicked and the tip trajectory graph plotted.

Manufacture of the Pepper Transplanter

The raw materials used were all purchased locally from Cape Coast and Accra. The manufacture of the transplanter was done at the workshop of GRATIS Foundation in Cape Coast, Ghana. The manufacturing process started in December 2018 and ended in July, 2019. The major processes adopted in the manufacture of the pepper transplanter included measuring and marking-out, punching and drilling, pressing, cutting and welding, turning, shaping, bending, rolling, grinding, and fastening. The transplanter was broken into ten (10) sub-assemblies for convenience during the manufacturing process. They were the structure, steering system, mechanism, tray holder, seedling cup, furrow opener, actuator, the compacting system, chain drive system, and wheels sub-assemblies. The manufacturing processes of the major sub-assemblies are described below:

The structure sub-assembly

The frame was made of 25 x 50mm mild steel U-channel of thickness 4mm, 40 x 40mm mild steel angle iron of thickness 4mm, 1.5mm and 5mm galvanized plates, and then 20 x 40mm galvanized rectangular pipe. Two pieces, each of lengths 1330mm and 515mm, were cut from the U-channel and then welded to form a rectangular structure of length 1330mm and width 515mm. Another piece of length 507mm was cut from the U-channel and welded across the rectangular structure 285 mm from one end. A diameter 30

mm hole was drilled in the middle of the 5 x 290x290 mm galvanized plate and the plate attached to the middle of the cross member and the front to form the upper steering plate. A piece of length 507 mm was cut from the 40 x 40 mm mild steel angle iron and also welded across the rectangular structure 815mm from the same end taken as the front.

A pair of 245 mm high by 185 mm long platform was fabricated from the 40x40 mm mild steel angle iron, and welded 810 mm from the front end. Also, a pair of 150x300 mm footrest fabricated from the 40x40 mm galvanized pipe and the 1.5 mm galvanized plate, and welded onto the frame 1084mm from the front end. A seat of height 370 mm and sitting area of 350 x 500 mm, fabricated from the 40x20 mm galvanized pipe, with a leather covered 78 mm high cushion top and back rest, was mounted at the front end. Another seat of height 425 mm and sitting area of 300x515 mm, fabricated from the 40x20 mm galvanized pipe, also with a leather-covered 78 mm high cushion top was mounted 751 mm from the front end (Figure 31).

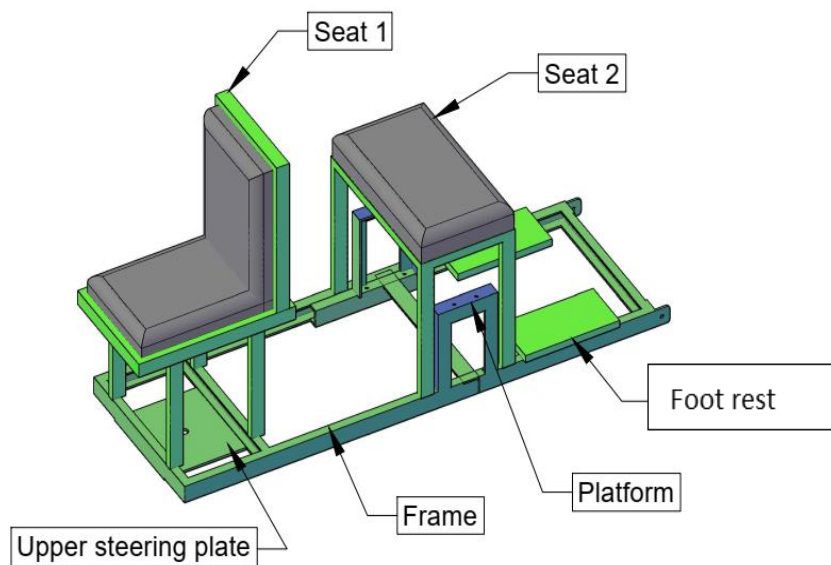


Figure 31 Structure sub-assembly

Steering system sub-assembly

From a 50 x 50 x 5 mm galvanized angle iron, two pieces each of two lengths, were cut and welded together to form a rectangular frame of 460 x 270 mm. A diameter 30mm hole was drilled in the middle of a 290 x 290 x 5 mm galvanized plate and attached to the middle of the rectangular frame to form the lower steering plate.

From the 50 x 50 x 5 mm galvanized angle iron, two pieces were cut and welded together to form an “A” shaped towing bar, parallel over a length of 160 mm and tapered over the remaining 1080 mm length. The parallel end is 460 mm wide with 200 mm long flat bars welded vertically at each side to couple the rectangular steering unit with the aid of bolt and nut. The Tapered end of the towing bar carries a 35 x 90 mm diameter cylindrical hollow shaft which serves as a hitching point. Four pieces of 300 mm length cut from a 25 x 25 x 3 m galvanized angle iron, were used to frame a square and 1.5 mm galvanized plate 300 x 300 mm welded onto of the square shape to form a footrest. This was placed 674 mm from the hitching point of the towing bar (Figure 32).

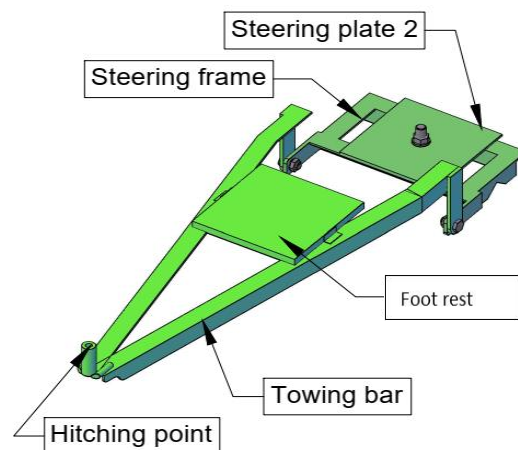


Figure 32: Steering system sub-assembly

The mechanism sub-assembly

The 4-bar linkage of the mechanism was made with 50 x 5 mm mild steel flat bar. The flat bar was cut into 370 mm, 240 mm, and 113 mm lengths. A hub of diameter 50 x 30 mm with an internal diameter of 25 mm and a keyway, was welded to one end of the 113 mm long flat bar to form the Crank. Another hub of the same dimensions but without a keyway was also welded to the 240 mm long flat bar to form the Rocker. The 370 mm long flat bar had 10 mm diameter holes drilled on both of its ends to form the Coupler. The free ends of the Crank and Rocker were also drilled with diameter 10 mm holes and assembled to the Coupler. The linkage was completed by attaching the hub end of the Crank to a diameter 30 x 595 mm crank shaft mounted on 205 pillow block bearings, and the hub end of the Rocker to a 50 x 535 mm diameter rocker shaft mounted on ball bearings. The fixed distance between the crank shaft and the rocker shaft formed the fourth (4th) link.

A length of 510 mm was cut from a galvanized pipe with a cross section of 40 x 20 mm. One of its ends was covered with 1.5 mm galvanized plate, and a pipe flange welded across the other end to form the furrow opener arm. A wedge of 80 mm height and 70 mm width was welded 99 mm from the covered end of the furrow opener arm. This part was bolted to the rocker shaft (Figure 33).

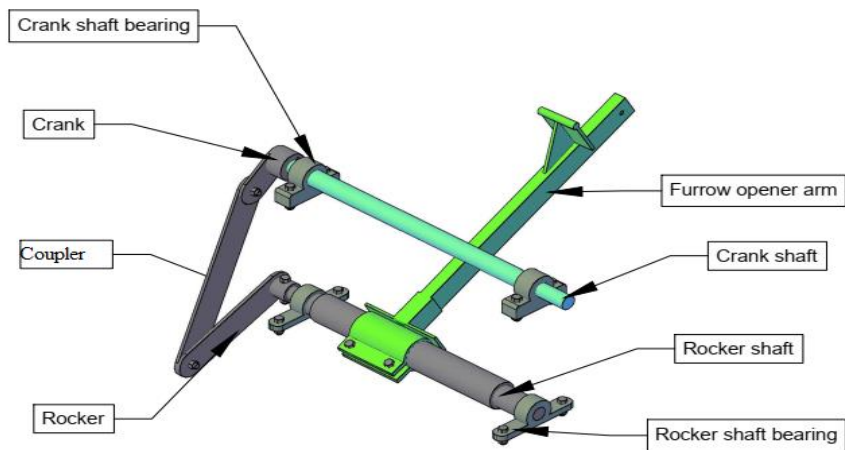


Figure 33: Mechanism Sub-Assembly

The furrow opener sub-assembly

A 2 mm galvanized plate was cut and formed into a right cone of base diameter 65 mm and height of 130 mm. The cone was then cut into two halves along its height and hinged together at the top to form the furrow opener jaws. Attached to the middle of the hinge is a vertical finger which the actuator presses to open the jaws. A tension spring was hinged to the jaws to serve as a return spring after the jaws are opened. A 40 x 4 mm mild steel flat bar of length 120 mm, was cut and welded to the top of one of the jaws. The flat bar which serves a flange for attaching the opener to the arm, has three 8 mm diameter holes spaced at 20 mm for adjusting the transplanting depth (Figure 34).

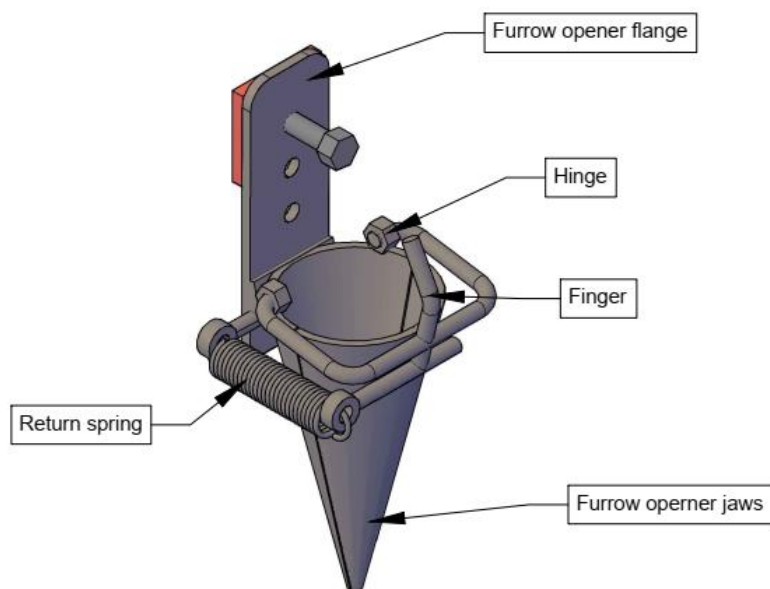


Figure 34: Furrow opener sub-assembly

Actuator sub-assembly

The actuator was fabricated by cutting 5 pieces of 135 mm length from a 25 x 25 x 5 mm galvanized angle iron. Four of the pieces were welded together to form a square, and the fifth one welded on one side of the square as a flange. This formed the frame of the actuator. A 14 mm diameter iron rod was rolled into a 160 mm diameter circular shape. A 40 x 5 mm flat bar was welded across the middle of its diameter with a 26 mm long hub having internal diameter of 20 mm and outside diameter of 40 mm welded in the middle of the flat bar to the cam wheel. A 20 mm high, 113 mm long, and 124 mm wide cam made of 5 mm thick mild steel plate was welded on a segment of the cam wheel. The cam wheel was then mounted at one end of a diameter 25 x 210 mm mild steel shaft attached to the actuator frame through two pieces of size 6204 ball bearings (Figure 35).

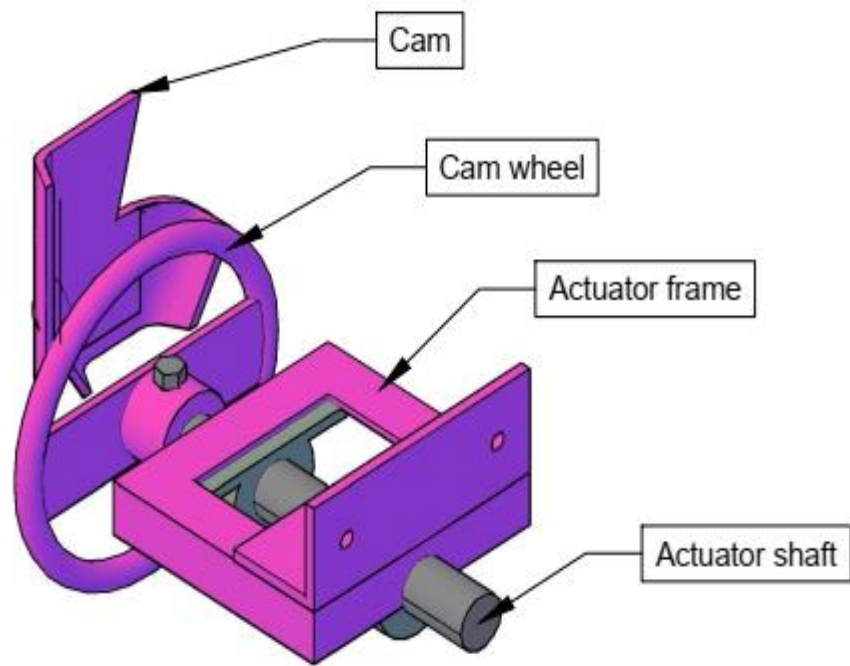


Figure 35: The actuator sub-assembly

The compacting wheels' sub-assembly

A 40 x 2.5 mm mild steel flat bar was cut and rolled into two wheels of outside diameter 185 mm. A flange of inside diameter 185 and outside diameter 245 mm was machined from a 3 mm mild steel plate and welded to each edge of the wheels. Held in the middle of each wheel was a 40mm long hub of outside diameter 40mm and inside diameter 30mm, by four pieces $\varnothing 15$ mm mild steel iron rods. These two wheels were mounted on a 505 mm wide frame. The frame was fabricated from a 40 x 40 x 5 mm galvanized angle iron. It had 166 mm long legs welded at its ends, inclined at an angle of 25° towards each other. At the end of each leg was a perpendicularly welded diameter 30 x 75 mm mild steel shaft on which the compacting wheels were mounted (Figure 36).

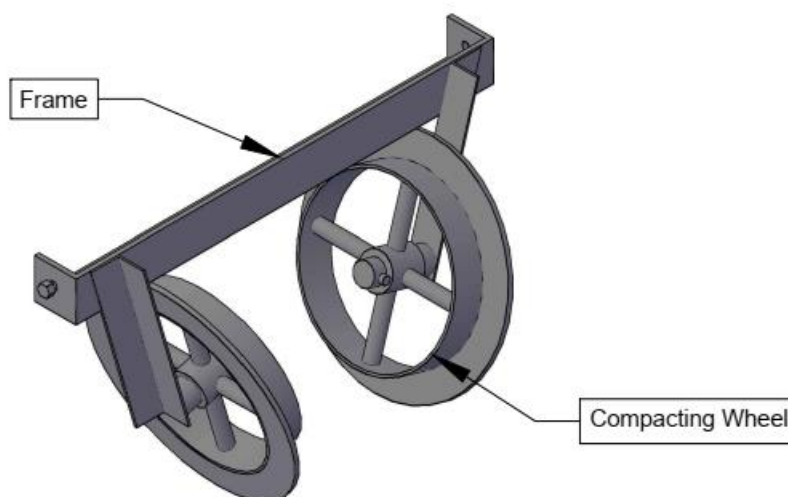


Figure 36: The compacting wheel sub-assembly

Evaluation of the Manufactured Vegetable Transplanter

Experimental design and field layout

The experiment to evaluate the performance of the manufactured Vegetable Transplanter was done using a factorial arrangement in randomized complete block design (RCBD). There were two factors (method and depth of transplanting). Two methods were considered – manual and machine transplanting. Also, three transplanting depths were used – 4 cm, 6 cm and 8 cm. Three replicate blocks were also used. This resulted in a 2 x 3 x 3 factorial design in RCBD with eighteen experimental plots. Each experimental plot was a 9 m long, 0.6 m wide and 0.2m high ridge. The inter-ridge spacing (buffer zone) was 0.5 m and inter-block spacing was 1.5 m.

The theoretical field capacity (C_{th}) of the transplanter

Theoretical field capacity (C_{th}) is the rate of field performance recorded for a given time if 100 % of the time and its operating width were used in performing its function at its rated operating speed. It was calculated using equation (3.30).

$$C_{th} = \frac{v \cdot w}{10} \dots\dots\dots \text{Equation 3.30}$$

C_{th} = theoretical field capacity

Where,

v = Operating/forward speed, and w = Operated width.

Operating speed (V)

The operating speed was determined by multiplying the number of revolutions of the driving wheel in travelling over the 9 m long bed, by its circumference, and then diving by the average of the time (Equation (3.31)).

The average operating speed was found to be 0.9 km/h

$$\text{Average speed, } V = \frac{\pi D \times N}{t} \dots\dots\dots \text{Equation 3.31}$$

Field efficiency

Field efficiency (e) of a machine is the percentage of its theoretical field capacity actually attained under real conditions. It is usually lower than 100% due to overlapping, and time losses due to turning, loading and unloading of materials, cleaning a plugged machine, making adjustments, and waiting at operator rest stops. The efficiency of the transplanter was calculated using Equation 3.32.

$$e = \frac{T_a}{T_a + T_l} \times 100 \% \dots\dots\dots \text{Equation 3.32}$$

Where T_a = Actual time used for performing the activity operating at full width.

T_L = Time loss due to various interruptions,

The effective field capacity of the transplanter

The actual performance rate of a machine in terms of land covered or crop processed in a given time based on the total field time is the effective field capacity. Unlike the theoretical field capacity, this takes into

consideration, the time lost during the field operation. The effective field capacity of the transplanter was calculated using Equation (3.33).

$$C_e = \frac{V \cdot W \cdot e}{10} \dots\dots\dots \text{Equation 3.33}$$

Where, C_e = Effective field capacity (hah^{-1}), v = Travel speed of the transplanter (kmh^{-1})

w = Width of work (m), and e = efficiency (Alizadeh, 2011)

Field capacity of the manual transplanting

The field capacity of the manual transplanting was calculated using the area covered, the total time used for the transplanting and the non-productive time (time spent at rest stops). Equation 3.34 below was used.

$$C_{em} = \frac{A}{T_p - T_n} \times 100 \dots\dots\dots (3.34)$$

where C_{em} = Effective field capacity of manual transplanting,

A = total transplanted area, T_p = total time used for the transplanting,

T_n = non-productive time (Murali, Anantachar, and Devojee, 2019)

Percentage transplanting success

Transplanting success is the number of seedlings successfully transplanted out of the number of seedlings which were attempted to be transplanted. The percentage transplanting success was calculated as

$$\text{Transplanting success} = \frac{\text{number of successfully transplanted seedlings}}{\text{Number of seedlings removed from tray for seeding}} \times 100\% \dots\dots \text{Equation 3.35}$$

Wheel slip (S)

Wheel slip, which is the reduction in travel for a given drawbar load, is a key factor in farm machinery performance (Zoerb and Popoff, 1967). During the experiment the number of revolutions of the wheels driving the

transplanting mechanism for a fixed distance (9 m) under varying loads, was recorded and the percentage slip calculated using Equation (3.36).

$$S = \frac{N_l - N_u}{N_u} \times 100 \% \dots\dots\dots \text{Equation 3.36}$$

where N_l = Number of revolutions under loading condition; N_u = Number of revolution under unloaded condition (Hoque and Miah, 2015)

Force prediction of the furrow opener in the soil

In this study, equations developed for the depth/width (d/w) ratio of simple blades passing through the soil as reported by Godwin and O’Dogherty (2007) were used as follows:

- I. Wide (blades) tine have $d/w < 0.5$
- II. Narrow (chisel) tine have $1 < d/w < 6$
- III. Very narrow (knife)tine have $6 < d/w$ (Godwin and O’Dogherty, 2007)

For this study, the depth (d) is about 2/3 of the furrow opener height

$$d = \frac{2}{3} \times 130 = 86.7 \text{ mm}$$

And the width (w) = 65 mm = 0.065 m

$$\text{Therefore } \frac{d}{w} = \frac{86.7}{65} = 1.33$$

The furrow opener was found to be narrow tine since the depth/ width ratio (1.33) is less than 6.

Equations for narrow tine force prediction

The following equations were also used to determine the draught (H) and vertical (V) forces:

Draught force,

$$H = (\gamma d_c^2 N_\gamma + c d_c N_c + q d_c N_q) \times \left[w + d \left\{ m - \frac{1}{3}(m - 1) \right\} \right] \sin(\alpha + \delta)$$

..... Equation 3.37

Vertical force,

$$V = (\gamma d_c^2 N_\gamma + c d_c N_c + q d_c N_q) \times \left[w + d \left\{ m - \frac{1}{3}(m - 1) \right\} \right] \cos(\alpha +$$

$\delta)$ Equation 3.38

Where γ = Bulk density of soil (kN/m³), d_c = critical depth of tine (m), c = Cohesion (kN/ m²), d = depth of tine (m), δ = soil-metal friction = 20°

q = surcharge pressure on the soil - free surface (kN/m²), w = width of tine (m), m = rupture distance ratio (= r / d_c) with r = crescent radius (m)

$$N_\gamma = N_{\delta=0} \left[\frac{N_{\delta=\phi}}{N_{\delta=0}} \right]^{\delta/\phi} = \text{gravitational earth pressure coefficient,}$$

$$N_c = N_{\delta=0} \left[\frac{N_{\delta=\phi}}{N_{\delta=0}} \right]^{\delta/\phi} = \text{cohesive/adhesive earth pressure coefficient,}$$

$$N_{q=\delta} = N_{\delta=0} \left[\frac{N_{\delta=\phi}}{N_{\delta=0}} \right]^{\delta/\phi} = \text{surcharge earth pressure coefficient.}$$

[(Godwin and O'Dogherty, 2007) and (Kirisci and Blackmore, 1994)]

Prediction of forces

In Table 8 are the results of the narrow tine force calculations. The gravitational, cohesive, and surcharge dimensionless earth pressure coefficients were found to be 2.228, 5.495, 4.312 respectively as indicated in Table 8. The draught force and its vertical component were found to be 0.996kN, and -0.267kN respectively. This implies the draught power is approximately 0.25 kW (draught force x operating speed) which is within the capacity of the power tiller with maximum power of 9.561kW.

Table 8: Narrow Tine Force Calculations

Design Property	Input Parameters	Result
Gravitational pressure coefficient (N_γ)	Earth $\phi=28^\circ, \delta=20, N_{(\delta=0)} = 0.9, N_{(\delta=\phi)} = 3.2$	2.228
Cohesive/Adhesive pressure coefficient (N_c)	Earth $\phi=28^\circ, \delta=20, N_{(\delta=0)} = 0.3, N_{(\delta=\phi)} = 7$	5.495
Surcharge coefficient (N_q)	Earth pressure $\phi=28^\circ, \delta=20, N_{(\delta=0)} = 2.7, N_{(\delta=\phi)} = 5.2$	4.312
Draught force (H)	$N_\gamma= 2.228, N_c= 5.495, N_q= 4.312,$ $\gamma= 12.4\text{kN/m}^3, d_c= 0.08\text{m}, c=10 \text{ kN/}$ $\text{m}^2, q= 5 \text{ kN/ m}^2, w=0.065\text{m}, 0.08\text{m},$ $m= 1.44, \alpha= 85^\circ, \delta=20^\circ$	0.996kN
Vertical force (V)	$N_\gamma= 2.228, N_c= 5.495, N_q= 4.312,$ $\gamma= 12.4\text{kN}^3, d_c= 0.08\text{m}, c=10 \text{ kN/}$ $\text{m}^2, q= 5 \text{ kN/ m}^2, w=0.065\text{m}, 0.08\text{m},$ $m= 1.44, \alpha= 85^\circ, \delta=20^\circ$	0.267kN

Source: Field survey Karimu (2019)

where w = Width of tine, d = Depth of tine or furrow opener, γ = Dry Bulk Density, c = Cohesion, q = Surcharge, α = Rake angle, ϕ = Angle of soil-soil friction, δ = Angle of soil-metal friction,

m = Rapture distance ratio

Cost analysis

The cost of using the transplanter was analyzed taking into consideration both the ownership (fixed) cost and operating (variable) costs.

Ownership cost

The total ownership cost (TOC) or fixed cost was estimated by adding depreciation, interest, taxes, insurance and housing cost using the assumptions made in Table 9. The manufacturing cost from the bill of quantities presented in Appendix C7 was GHC2,787.98

Depreciation was calculated using Equation (3.39) as indicated in the ASABE Standard (2005).

$$Depreciation = \frac{Purchase\ Price - Salvage\ Value}{Economic\ life} \dots\dots\dots Equation\ 3.39$$

Insurance and Tax charges were estimated using the prevailing rates and government policies regarding agricultural machinery in Ghana.

Table 9 Assumptions for ownership cost calculation

Item	Assumption
The purchase price	120% of the manufacturing cost
The economic life of the transplanter	10 years
Salvage value of the transplanter	40% of the purchase price (Lazarus, 2009)
The Bank of Ghana Interest rate	16%
Taxes on agricultural machinery in Ghana	Tax-free
Insurance cost	0.25% of the purchase price (Srivastava, Goering, Rohrbach and Buckmaster, 1993)
Cost of housing	0.75% of its purchase price (Srivastava et al., 1993)
Annual usage	100 days per year, and 6 hours per day

Source: Field survey Karimu (2019)

Operating cost

The operating (variable) cost was determined by adding the repair and maintenance, fuel, lubrication, and operator labour cost. Repair and Maintenance cost of one machine can vary from one geographical location to another due to soil and atmospheric conditions. Within the same geographical location, repair and maintenance cost can also vary due to difference in operator skills and management strategies. Apart from these factors, the cost of repairs and maintenance is proportional to the size and complexity of the machine. The operator's own past record is therefore the best data for estimating the cost of repairs. Since there is no past record of the newly developed Vegetable Transplanter, 15 % of the purchase price was estimated as cost of repairs (Aikins, 2018). The assumptions made for the operating cost analysis are presented in Table 10.

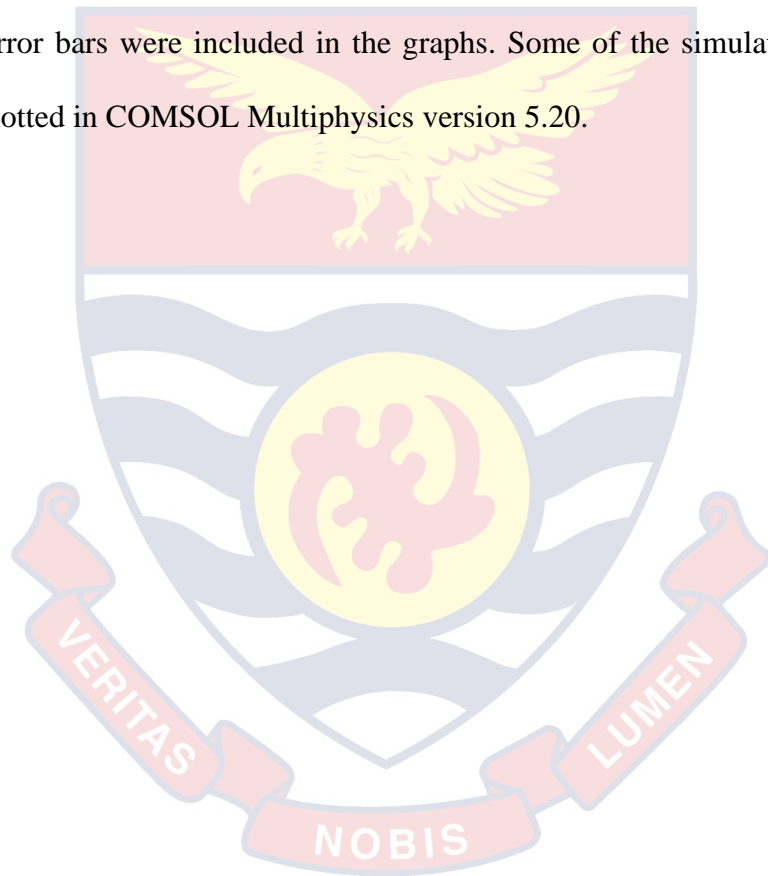
Table 10: Assumptions for Operating Cost Calculation

Item	Assumption
The repair and maintenance cost	15 % of the purchase price
Fuel price per litre	Prevailing price (GH¢ 5.195)
The cost of lubrication	15 % of the fuel cost (Ajit K. Srivastava, Carroll E. Goering, Roger P. Rohrbach, & Dennis R. Buckmaster, 2013)
The operator labour cost	GH¢10.00 per hour

Source: Field survey Karimu (2019)

Statistical analyses

Data on transplanting time, percentage seedlings survived and field capacity gathered from the experiment were analysed using analysis of variance (ANOVA) in GenStat Statistical Package 12th Edition. Means were separated using the Tukey HSD test at a significant level of 5 %. The rest of the data was processed using simple statistical techniques in Microsoft Excel (2016), such as calculation of percentages, means and construction of graphs. Error bars were included in the graphs. Some of the simulation graphs were plotted in COMSOL Multiphysics version 5.20.



CHAPTER FOUR

RESULTS AND DISCUSSION

Introduction

The main aim of the research was to develop a semi-automatic vegetable transplanter for small scale farmers and evaluate its performance using pepper as a test crop. This chapter presents and discusses the results of the research. The discussion includes results of the simulation in COMSOL Multiphysics, and the performance parameters of the developed transplanter. The chapter also presents two dimensional drawings of the designed transplanter, and then pictures of the transplanter after it was manufactured. Transplanting cost analyses for the machine and the manual transplanting methods are also presented in this chapter. Finally, the machine transplanting was evaluated and compared to the manual transplanting method.

Design and Construction of the Semi-Automatic Pepper Transplanter

The transplanter was designed and manufactured for use by pepper farmers for transplanting pepper seedlings in the field. Two views of the transplanter, plotted in AutoCAD 2016 version, are shown in Figure 37. From the design calculations, the crankshaft diameter was 23.8 mm but a standard shaft diameter of 25 mm was selected to ensure safety. Details of all the design calculations are found in Appendix C. Figure 38 shows pictures of the transplanter after manufacturing was completed.

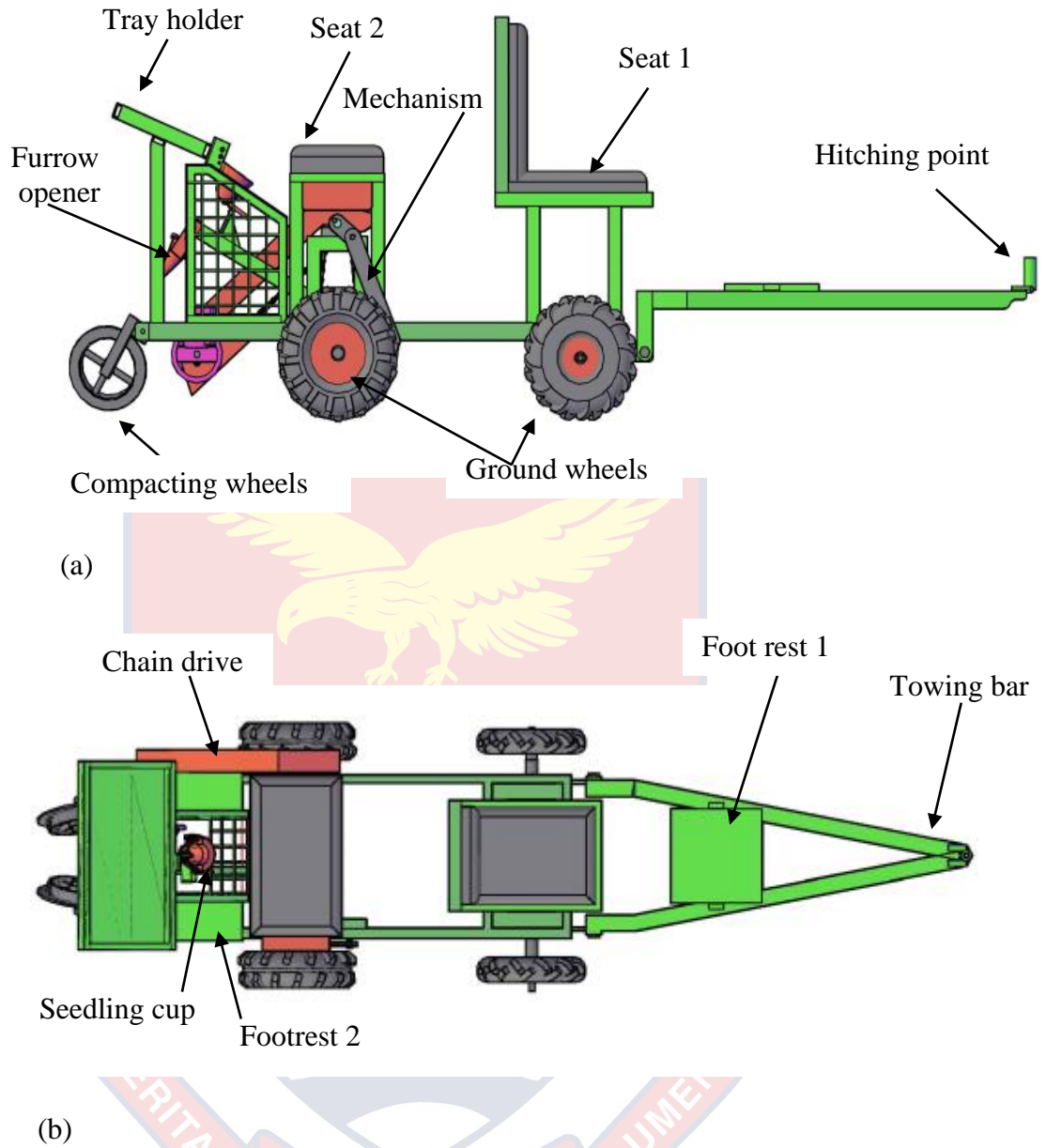
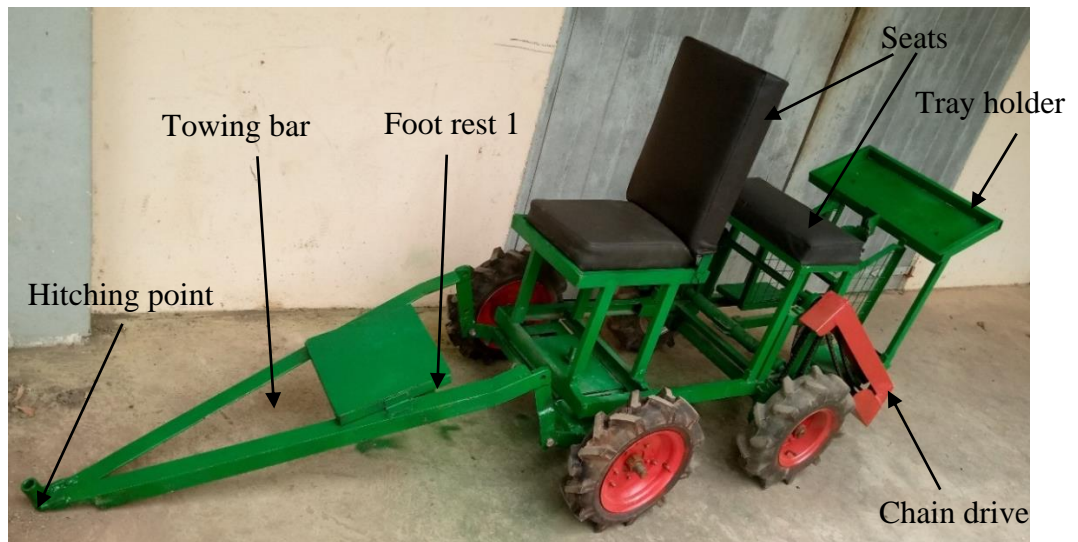


Figure 37: Two dimensional views of the transplanter (a) Side view (b) Top view



(a)



Figure 38: (a) The manufactured vegetable Transplanter (b) the furrow opener section

Design Simulation

Material properties and meshing of the geometry

When the geometry for the study (transplanting mechanism) in CAD format was imported into COMSOL Multiphysics, structural steel was selected from the material library as the suitable material. The properties of this material were given as shown in Appendix D2. After the definition of physics and application of all constraints, the default meshing (Tetrahedral)

was applied, since the geometry was complex, and the result shown in Figure 39. Meshing is necessary in order to make the problem solvable by finite element analysis (FEA), the principles on which COMSOL Multiphysics works. Since continuous objects have infinite degrees of freedom making them impossible to solve, finite element method reduces the degrees of freedom from infinite to finite through discretization or meshing (Gokhale, 2008). After the mesh was built, calculations were made at only limited number of points and the results interpolated for the entire volume of the object.

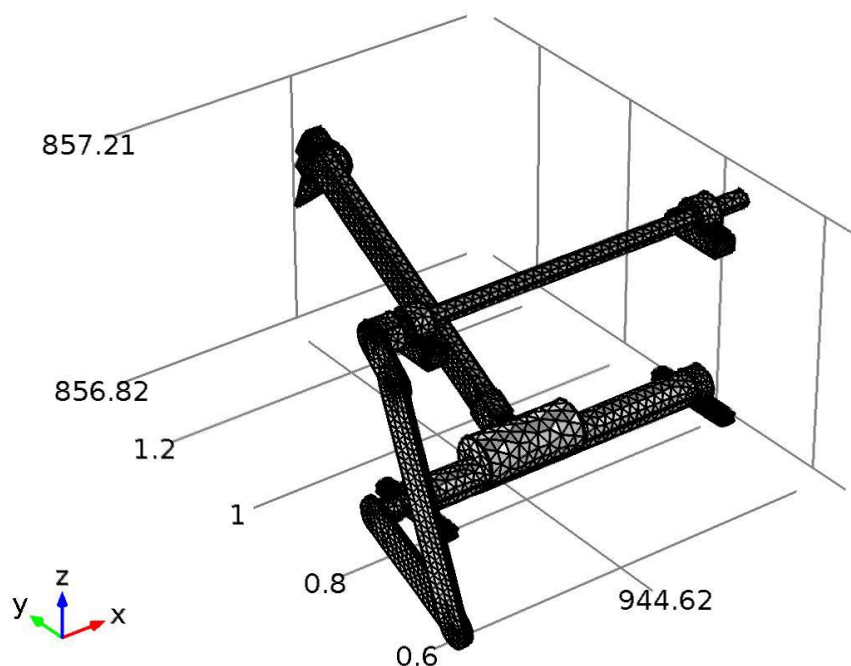


Figure 39: Tetrahedral meshing of the planting arm geometry under study.

Stress concentrated areas

Under structural mechanics, a multibody dynamics study was run on the geometry, and colours were used by the system to indicate the levels of stress concentration on the various parts of the mechanism. The most stressed

parts of the design were coloured red, less stressed parts coloured yellow, and parts with almost no stress coloured blue. From Figure 40, it can be seen that the furrow opener tip is the most stressed part of the transplanter followed by the crank-coupler joint.

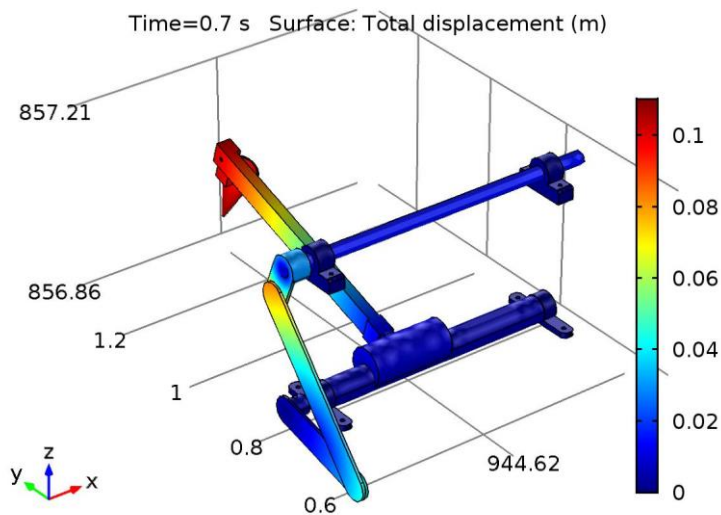


Figure 40: Multibody dynamics displacement results indicating stress concentrations

Joint Forces at the crank-coupler joint

After the simulation, the results of the joint forces acting at the crank-coupler joint, as presented in the graph of Figure 41, showed that the majority of forces at the joint acted in the downward direction. This is understandable because the shaft driven by the crank (the rocker shaft) is below the crank shaft hence the reason for the downward direction of the forces. The only instant at which there was an upward force occurred at about 1.1 seconds during the 3 seconds simulation computed. This was the time the crank pointed upwards, as it rotates through 360° in its operation.

It was also discovered from the graph that at the initial state of the operation of the machine, the forces at the joint were much greater than the

latter part. This explains the fact that much force is needed to start the rotation of the crank shaft. It could further be explained that when the rotation stabilizes, only small amount of force is needed to maintain the rotational motion. Also, the rotation of the crankshaft was about the X-axis, as a result, it was seen from the graph (Figure 41) that the X-axis component of the joint force was constant.

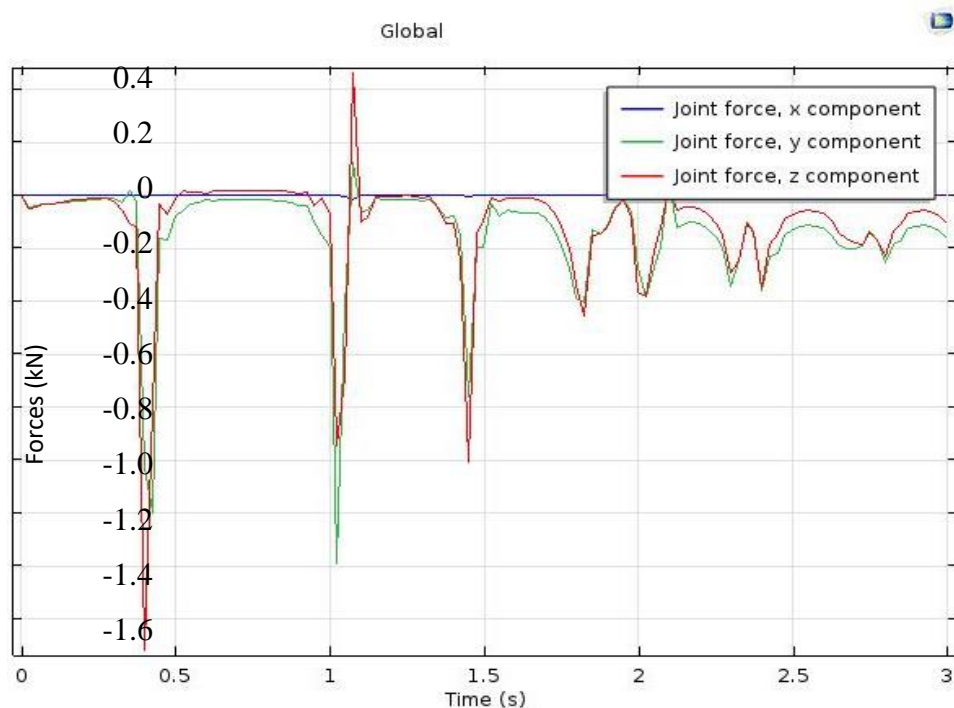


Figure 41: Forces at the crank-coupler joint

Joint forces at the rocker-coupler joint

The forces at the rocker-coupler joint was also studied. The results are presented in the graph of Figure 42 show that all the joint forces were acting in the upward direction. This is so because, unlike the crankshaft which rotated 360° , the rocker shaft only rocked without making complete revolution (about 90° of turning). Similar to the case of the crank-coupler joint, the joint forces at the initial stage were greater than the latter part of the machine operation and this confirms the fact that much force is needed to start the rocking motion

than is needed to maintain the motion when it stabilizes. In the design calculation, the maximum initial forces acting on the crankshaft was determined to be 1.393 kN and in the simulation results in Figure 42, the initial force needed to act and rotate the crankshaft was found to be 1.39 kN. This gives a strong agreement between the design calculation and the simulation. The x-component of the joint forces at this joint was constant, an evidence that the rocking motion at the joint was about the x-axis.

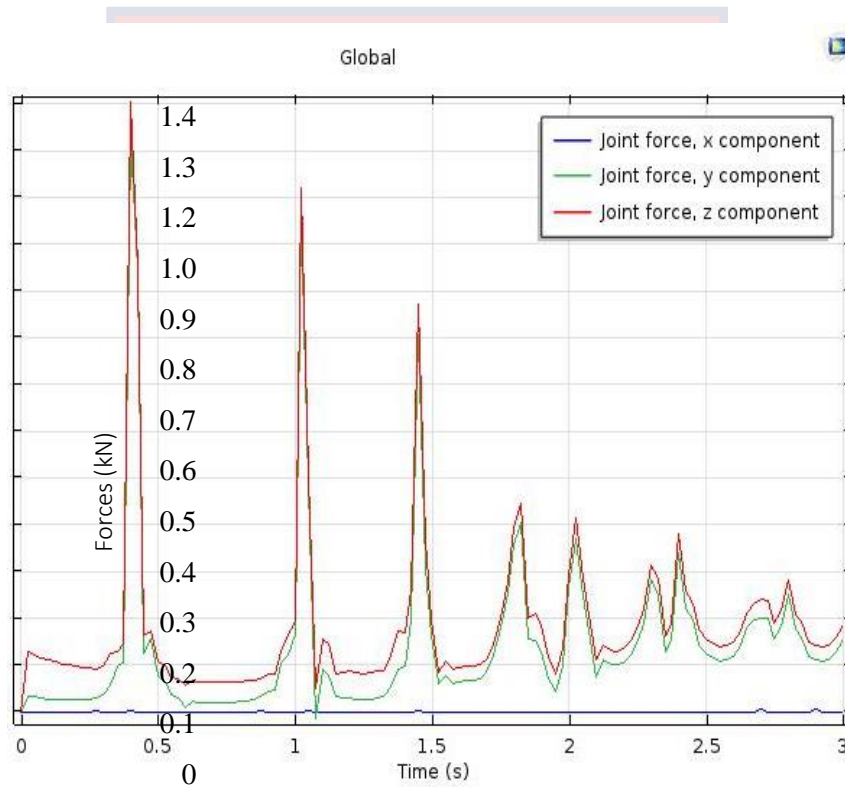


Figure 42: Forces at the rocker-coupler joint

The trajectory of the furrow opener tip

The trajectory of the furrow opener tip was studied and the results represented by the graph shown in Figure 43. From the graph, the tip reciprocated along a semi-parabolic path. It represents three trajectory paths. As pointed out by Hu et al (2014), the transplanter’s robotic arm undergoes a number of motion processes which forms its motion trajectory. For this

mechanism, for a single transplanting cycle, the planting arm undergoes two motion processes: downwards arc motion (for the furrow opener to enter the soil, create the furrow and release the seedlings into it) and vertical return motion (for it to come back to the position of feeding it with the seedlings). This continues until all the seedlings are transplanted. The Figure. 43 shows three successive movement of the transplanter's furrow opener.

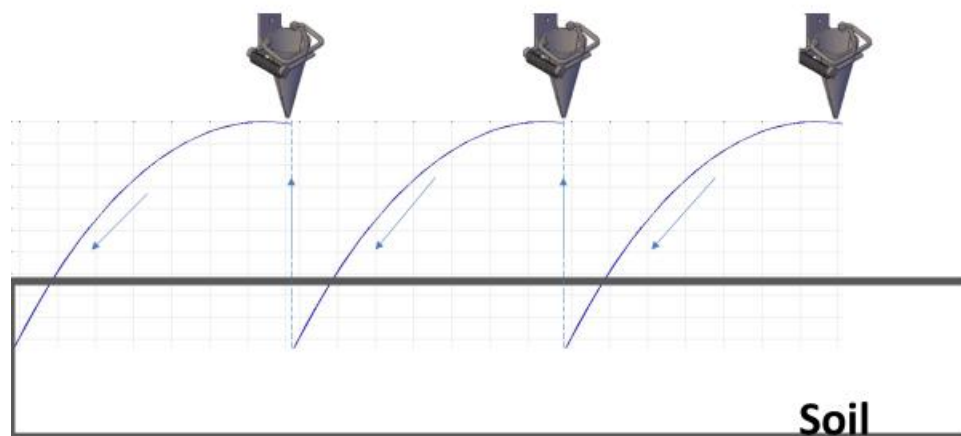


Figure 43: Trajectory of the furrow opener tip

Performance Evaluation of the Transplanter Under Local Field Condition Preliminary testing and machine modifications

The developed Semi-Automatic Single Row pepper Transplanter was first tested with dummy seedlings in a test field. This was to ascertain the release of seedlings by the furrow opener and the covering action of the compacting wheels. The machine was modified after field trial testing conducted using dummy seedling first and later, actual pepper seedlings. Figure 44 shows the dummy seedlings used in the preliminary testing. In the initial trial, there were difficulties in the release of the seedling into the furrow

because the opening of the tip of the furrow opener interfered with the seedling leaves thus making it unable to be released into the furrow. It was found that it was needful to incorporate a mechanism that delays the closure of the furrow opener which makes the seedling to be fully released without any interference with the leaves of the seedling. With this and other modifications, the second field trial was successfully conducted and based on its success, the prototype was modified and subjected to the actual field evaluation.

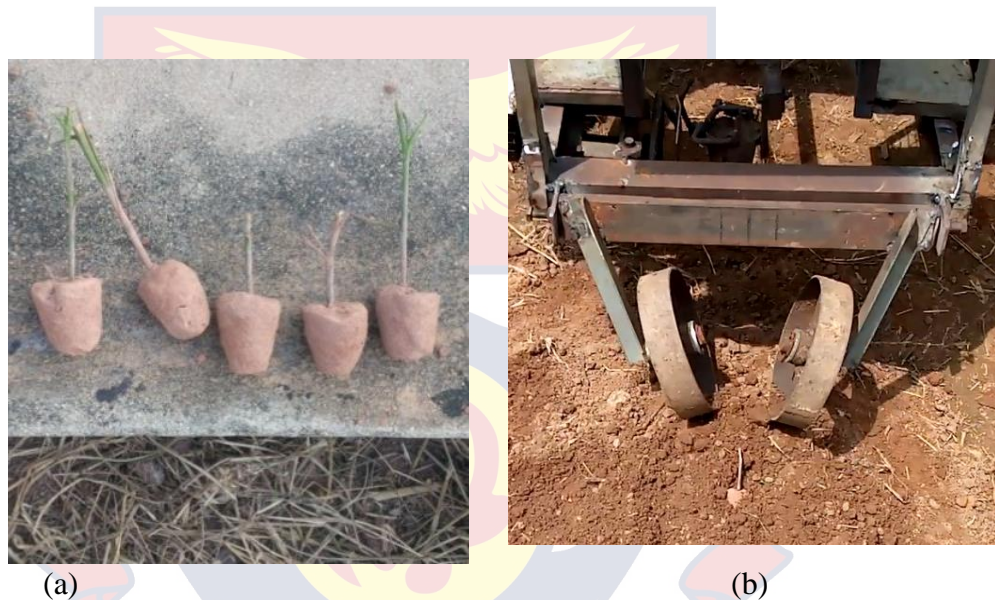


Figure 44: (a) Dummy seedlings, (b) preliminary testing with dummy seedling

Field experiment

After attaining satisfactory performance result in the preliminary testing, the performance of the Semi-Automatic Single Row Pepper Transplanter was evaluated under field conditions (Figure 45 (a)). After 28 days, the nursed seedlings of green pepper (*Capsicum Annum*), had well-developed root system as shown in Figure 45 (b), and were used for the experiment. The performance parameters measured were the transplanting time, the theoretical field capacity, effective field capacity, field efficiency, transplanting success,

slip of the driving wheels. After 21 days of transplanting, the percentage seedlings survived was also recorded.



Figure 45: (a) Actual field testing, (b) pepper seedling with well-developed root system

Field capacities

Theoretical field capacity is the rate of field performance recorded for a given time if 100 % of the time and its operating width were used in performing its function at its rated operating speed. With an average speed of 0.9 km/h and operating width of 0.6 m, the theoretical field capacity was calculated to be 0.054 ha/h.

On the average, 0.04 ha/h effective field capacity, 71.75 % field efficiency and planting rate of 25-30 plants per minute were realised, especially at the 8 cm depth. This is comparable to the report of Dihingia et al. (2017). By conversion, 0.04 ha/h is equivalent to 25 h/ha. The analysis of variance results showed a high significant difference between the methods – manual and machine ($p < 0.001$) while the planting depth showed no significant differences ($p = 0.071$) (Appendix A3). Also, the interaction effects of the methods and the planting depths was also highly significant ($p < 0.001$).

Kumar and Raheman (2011) reported the field capacity to be 0.026 ha/h for their fully automated vegetable seedling transplanter which is close to the average field capacity for the manual transplanting in this work (0.021 ha/h). This gives an indication that the developed semi-automatic transplanter gives an appreciable field capacity (Figure 46).

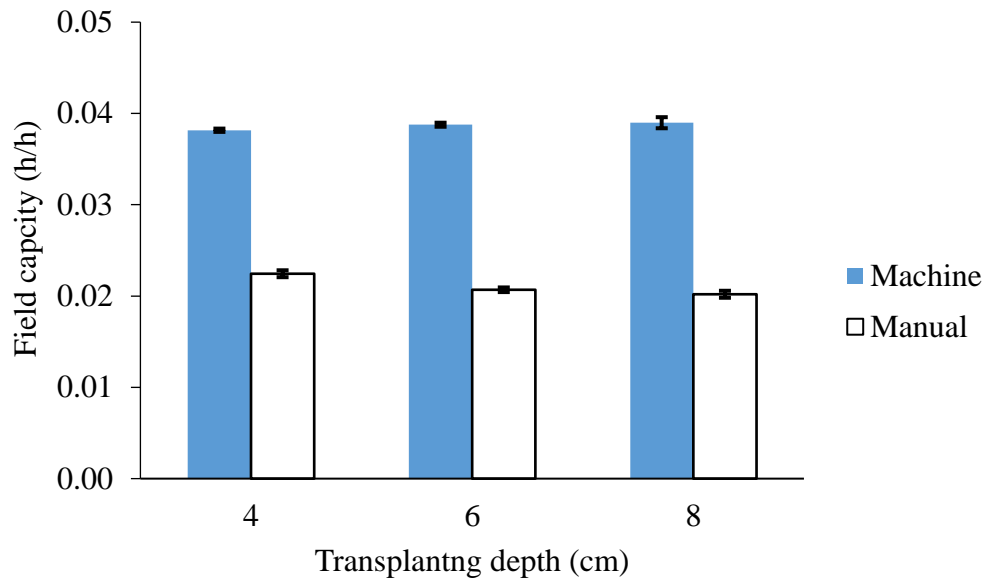


Figure 46: Effect of transplanting depth on the field capacity

Field efficiency

The field efficiency of a machine is the percentage of its theoretical field capacity actually attained under real conditions. It is usually lower than 100 % due to overlapping, and time losses due to turning, loading and unloading of materials, cleaning a plugged machine, making adjustments, and waiting at operator rest stops. The efficiencies for varying transplanting depths were determined and the results given in Figure 47. The results show that the transplanting depth has effect on the field efficiency of the machine, the efficiency increase with increased depth. The smaller depth (4 cm) had the lowest efficiency of 0.707 (70.7 %) and the deepest depth (8 cm) had the

highest efficiency of 0.723 (72.3 %). The average field efficiency of the transplanter was found to be 71.75 % which is close to the 72.20 % achieved by Sahoo, Mahapatra, Swain, and Behera (2018) when they developed and evaluated the performance of a single row semi-automatic bullock-drawn vegetable transplanter in India.

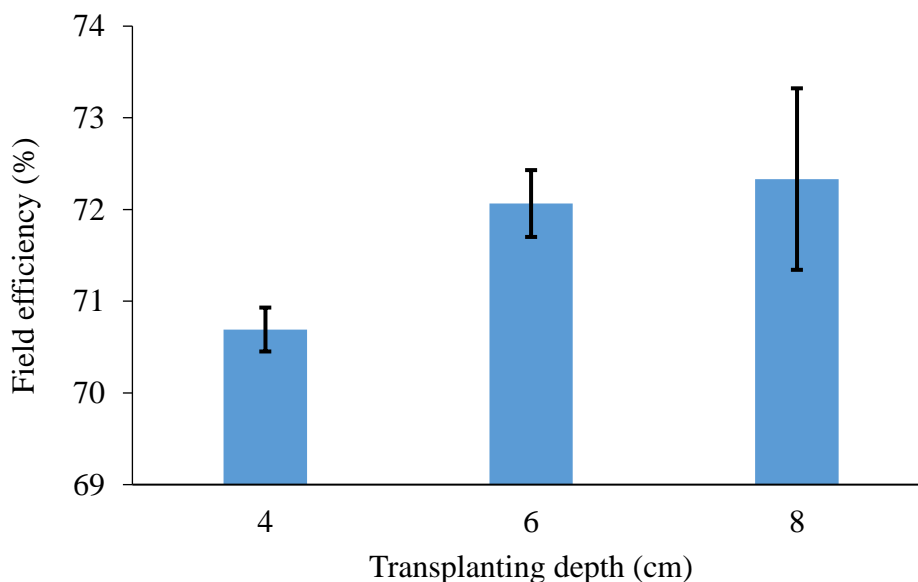


Figure 47: Effect of transplanting depth on field efficiency

Generally, the transplanter was found to have performed satisfactorily with appreciable average field efficiency of 71.75 % under actual field conditions (Kumar and Raheman, 2008). Also, the planting rate ranged between 25 and 30 seedlings per minute which is not too far from the reports of Kumar and Raheman (2012) and Satpathy and Gaggs (2008) who reported an average of 35 seedlings per minute.

Machine transplanting success

The percentage transplanting success which is the number of seedlings successfully transplanted out of a particular number of attempts, for various transplanting depths was recorded and the results presented in Figure 48. It

can be seen from the graph that depth might have influence on the transplanting success. There was a vast difference between the percentage success of 4 cm depth and that of 6 cm depth. However, the percentage success of 6 cm depth was very close to that of 8 cm depth. Generally, the percentage of transplanting success increased as the transplanting depth increased. The highest percentage of transplanting success was 84.45 % which is in line with the 85-90 % success achieved by Narang (2011) when he developed a two-row vegetable transplanter with a revolving magazine type metering mechanism, and a three-point hitch system for mounting it on a tractor.

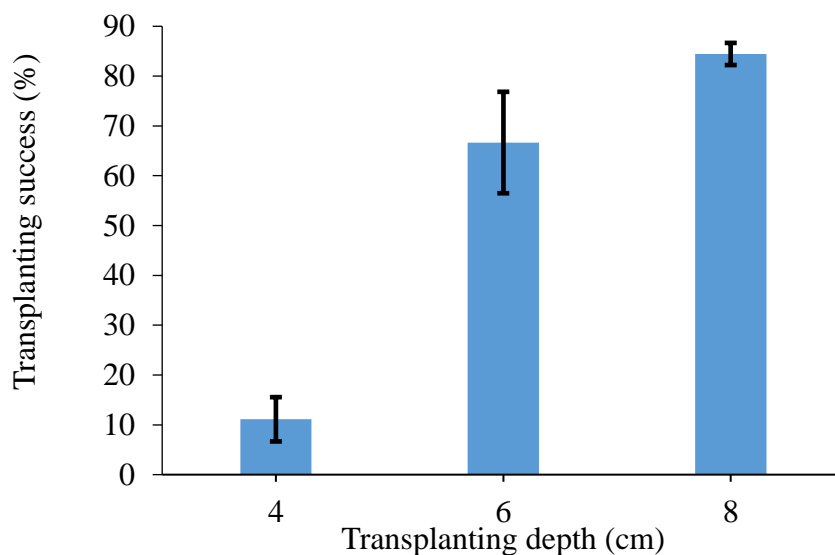


Figure 48: Effect of transplanting depth on transplanting success.

Percentage slip

For maximum tractive efficiency, the percentage slip of drive wheels should be between 10 % and 15 % (Zoerb et al., 1967). When the percentage slip is above 15 %, tractive efficiency reduces resulting in increased fuel cost. The highest percentage slip achieved in this study was 13.8 % at 8 cm depth, which is within the acceptable range. This can be seen from the results plotted

in Figure 49. It can also be deduced from the results that percentage slip increases as the transplanting depth increased.

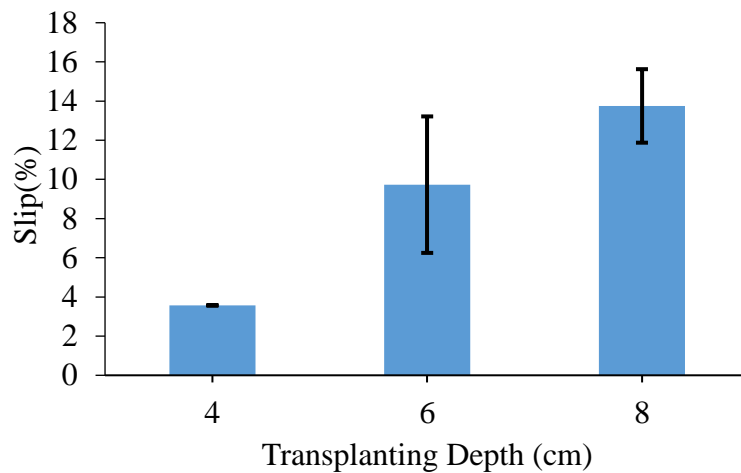


Figure 49: Effect of transplanting depth on wheel slip

Survival of transplanted seedlings

The results on the percentage of transplanted seedlings which survived after 21 days of transplanting, are presented in figure 50. There was no significant difference between the methods ($p=0.232$), planting depths ($p=0.335$) as well as their interaction ($p=0.215$) with respect to the percentage of seedlings survived (Appendix A2). Generally, for the machine, the survival of the seedlings increased with increasing depth while almost the reverse (but for 8 cm depth) was observed for the manual method. For the case of the transplanter machine, at 4 cm depth it was observed that the furrow had difficulty in releasing the seedlings into the furrow and might have damaged some of the seedlings in the process. That probably might have affected the survival of the seedlings on the field after 21 days of transplanting. Additionally, the average percentage of survived seedlings was 81.23 % which is not too different from the 84.48 % achieved by Singh (2010) when he

evaluated the performance of a two row semi-automatic vegetable transplanter.

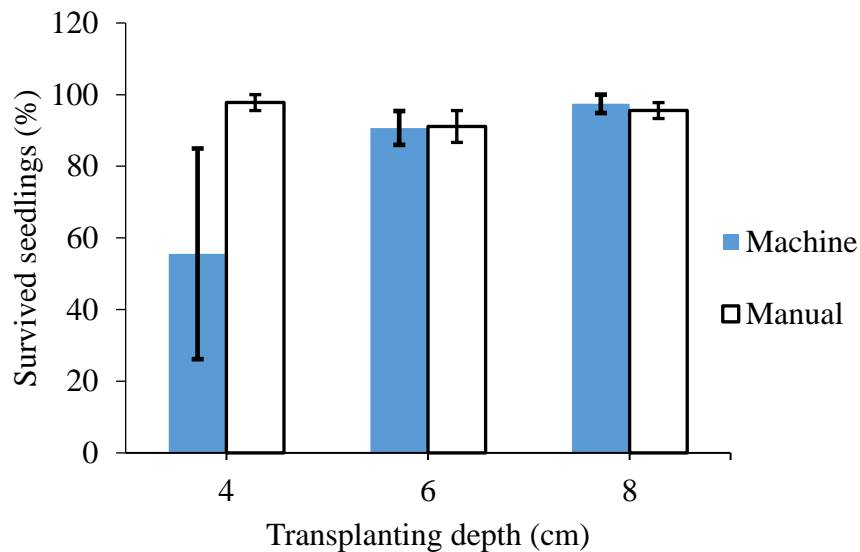


Figure 50: Effect of transplanting depth on seedling survival

Comparison of Machine Transplanting to the Manual Method

The performance of the developed semi-automatic single row pepper transplanter in the field, was compared to the traditional manual method in terms of transplanting time and cost of usage and the parameters measured are discussed in this section. The transplanter was pulled by the VST SHAKTI 130DI power tiller at an average forward speed of 0.9km/h in sandy loam soil.

Transplanting time

The actual time for transplanting 10 pepper seedlings at constant intervals of 0.6m, without taking into consideration the time loss due to interruptions, was recorded for both machine and manual methods and then assessed. It was observed from the ANOVA results that there was high significant difference between the transplanting time of the two methods ($p < 0.001$) Appendix A1). The transplanting depths were also significantly influenced ($p = 0.003$). However, there was no significant difference in their

interaction (($p=0.090$) Appendix A1). Figure 51 represents the relationship between the actual transplanting time and transplanting depth. It is evident from the graph that in both methods the transplanting time increased as the transplanting depth increases. In the case of the machine transplanting, the minimum time recorded was 33.2 at 4 cm depth and the maximum time was 36.2 seconds at 8 cm depth. While in the manual method the minimum time was 86.7 s at 4cm depth and 96.3 s at 8 cm depth.

The effective field capacity of the transplanter was found to be 0.04 ha/h equivalent to 25 h/ha, while that of the manual transplanting was 0.014 ha/h. This implies that the transplanter will require just one (1) hour to cover the area manual transplanting covered in three (3) hours, resulting in saving of about 67 % of the manual transplanting time. Compared to the time (29.79 man-h/ha) required by the single row hand –operated transplanter developed by Rudragouda (2017), this transplanter, being semi-automatic justifiably used less time (25 h/ha).

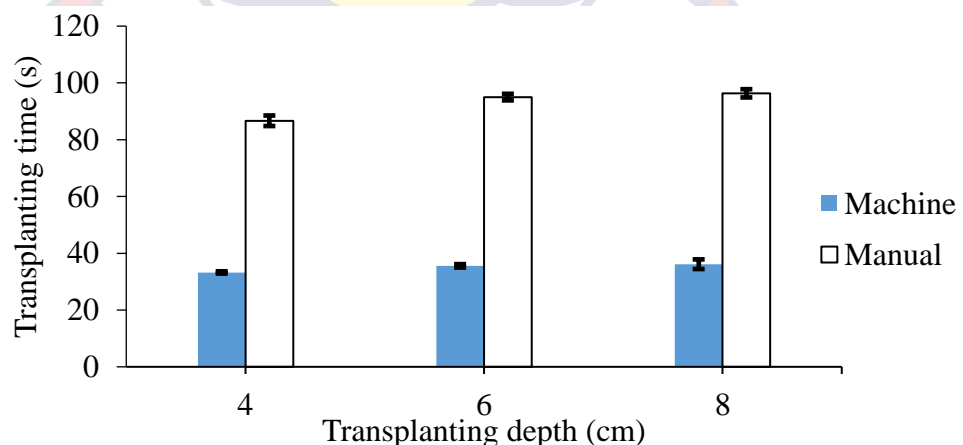


Figure 51: Effect of depth and method on actual transplanting time

Moreover, comparing the activities that take place in the use of the manual and the transplanter, the manual method involves walking throughout the transplanting area, carrying of seedling trays in the hands throughout the

process, and then bending at acute angles to manually make holes and plant seedlings. However, with the machine method, the operators are comfortably seated on the machine, no manual handling of trays, and no acute bending during the transplanting process.

Transplanting cost estimation

Machine transplanting cost

The transplanter cost was estimated taking into consideration the ownership cost also known as fixed cost, and the operating variable) cost.

Ownership cost

The total ownership cost (TOC) or fixed cost, which was estimated by adding depreciation, interest, taxes, insurance and housing cost was GH¢1.11 per hour (Table 11). The purchase price (PP) was found to be GH¢3,345.58 using the assumption that it is 120% of the manufacturing cost, and the salvage value found to be GH¢1,338.23 through the assumption that it is 40% of the purchase price.

Table 11: Results of Ownership Cost Estimation

Cost item	Input figures	Cost value
Depreciation (D)	$(PP-S)/L = [GH¢ (3,345.58 - 1,338.23)]/10 \text{ years}$	GH¢200.74
Interest cost (I_N)	$[(PP + S + D)/2] \times R_{IN} = [(3,345.58 + 1,338.23 + 200.74)/2] \times 16\%$	GH¢ 390.76
Taxes (T)		0.00
Insurance (I_S)	$R_{IS} \times PP = 0.25\% \times GH¢ 3,345.58$	GH¢8.36
Housing (H)	$R_H \times PP = 0.75\% \times GH¢ 3,345.58$	GH¢ 25.09
Total ownership cost per annum (TOC_a)	$D + I_N + T + I_S + H = GH¢(200.74 + 390.76 + 0 + 8.36 + 25.09)$	GH¢624.95
Total operating time (TOT)	90 days / yr x 6 h/day	540 h/yr
Ownership cost per hour (TOC_h)	$TOC_a / TOT = GH¢624.95 / 540 \text{ h/yr}$	GH¢1.16

Source: Field survey Karimu (2019)

Operating cost

The operating (variable) cost which was determined by adding the repair and maintenance, fuel, lubrication, and operator labour cost, was found to be GH¢1,654.25 (Table 12).

Table 12: Results of operating cost calculation

Cost item	Input figures	Cost value
Maintenance cost per hour (C_M)	$(15 \% \times PP) / TOT = (0.15 \times \text{GH}¢3,345.58) / 540$	GH¢0.93
Fuel cost per hour (C_F)	= cost per liter x consumption per hour = GH¢5.19 x 7.4 L/h	GH¢38.41
Lubrication cost per hour (C_{LU})	= 15 % x C _F = 0.15 x GH¢38.41	GH¢5.76
Labour cost per hour (C_{LA})	= rate per person x number of people = GH¢10 x 2	GH¢20.00
Total operating cost per hour (TOC_h)	= C _M + C _F + C _{LU} + C _{LA} = GH¢0.93 + GH¢38.41 + GH¢5.76 + GH¢20.00	GH¢65.10

Source: Field survey Karimu (2019)

Total cost of machine transplanting

Finally, the ownership cost of GH¢1.16 was added to the Operating cost of GH¢65.10 to give a total cost of GH¢66.26 per hour of the machine transplanting. This cost was then divided by the Effective field capacity of the transplanter (0.04 ha/h) to give an amount of GH¢1,720.51 as the cost per hectare of the machine transplanting.

Manual transplanting cost

The manual transplanting cost per hectare was found to be GH¢1,816.20. The assumptions made for the estimation of the manual transplanting cost are presented in Table 13, and the details of the cost estimation results presented in Table 14

Table 13: Assumptions for Manual Transplanting Cost Calculation

Item	Assumption
The labour cost per person	GH¢10.00 per hour
Resting time	15 minutes after every hour

Table 14: Results of Manual Transplanting Cost Estimation

Item	Input Figures	Value
Time for activity	Actual transplanting time + Time for marking and making holes + Time for seedling trays replacement = 831s + 1600 s + 10 s	0.68 h
Time spent at rest stops	Resting time per hour x Time for Activity = 15 min x 0.68 h	10.2 min
Total time spent	Time for activity + Time spent at rest stops = 0.68 h + 10.2 min	0.85 h
Time required per hectare	(Total time spent x Area of a hectare)/ Area covered = (0.85 h x 10000m ²)/ 93.6 m ²	90.81h
Cost per hectare	(Rate for manual transplanting x Number of people x Time required per hectare) = (GH¢10.00 x 2 x 90.81 h)	GH¢1,816.20

Source: Field survey Karimu (2019)

As can be seen in section 4.5.2.1.3, the total transplanting cost of using the machine was found to be GH¢1,720.51 per hectare, while the manual method costs GH¢1,816.20 per hectare (Table 14). This means the use of the transplanter is cheaper compared to the manual method. Other cost analysis reported by Kumar and Raheman (2011) on the other hand showed otherwise since they considered the cost of fully purchasing the power tiller. In this

work, the initial cost of the power tiller was not considered a major parameter because it is assumed that smallholder farmers in Ghana might not be able to buy the power tiller but rather rely on hiring services at the Agricultural Mechanisation Centres in Ghana. Moreover, since the machine has relatively high field capacity, it would be economical for use by farmers since they may break-even in the shortest possible time.



CHAPTER FIVE

CONCLUSIONS AND RECOMMENDATIONS

Conclusions

Semi-automatic pepper seedling transplanter design, simulation and manufacture

A single row semi-automatic pepper seedling transplanter was designed with a simple technology (crank-rocker and actuator-cam mechanisms) in AutoCAD 2016 version. The design was imported into Comsol Multiphysics version 5.2 and simulated to identify stress concentrations and the nature of forces acting on it. The designed transplanting machine was then manufactured using locally available materials.

Field performance of semi-automatic pepper seedling transplanter

The performance of the single row semi-automatic pepper seedling transplanter was evaluated at 4 cm, 6cm, and 8 cm transplanting depths. And it can be concluded that 8 cm was the optimum transplanting depth since it was at that depth maximum outputs of 97.43 % transplanting success, and 73.72 % mean field efficiency were achieved. This was followed by 6 cm, with 4cm being the depth at which least performance of 71.12 % mean field efficiency was attained.

Comparison of time requirement and cost of the transplanter and manual methods

The machine transplanting was faster than the manual transplanting and saves up to 67 % of the time required by manual transplanting for the same size of work. By this, the machine is able to solve the problem of the

delay associated with manual transplanting which causes non-uniform growth in plants consequently leading to reduction in yield.

The cost of using the transplanter (GH¢1,720.51) was found to be cheaper compared to the cost of manual transplanting (GH¢1,816.20), resulting in a saving of GH¢95.69 per hectare.

Recommendations

The following recommendations could be considered for future work:

1. Further research should be done to improve on the uprightness of transplanted seedlings and the covering of the root area or soil block of the seedlings.
2. The performance of the pepper seedling transplanter should be evaluated with seedlings of different crops such as tomato and eggplant and at different soil moisture contents.
3. The design should be modified to make the inter-plant spacing adjustable in order to suit different crop spacing requirements and preferences.
4. It is recommended that future work should evaluate the performance of the transplanter up to the yield stage since the current study, due to scarcity of funding and time, ended at the establishment stage after transplanting. This will help reveal trends that might be very important.

REFERENCES

- Aikins, S. H. M. (2018). Estimating Farm Machinery Field Operation Costs. *Farm Machinery Management, University of Cape Coast*, 7–14.
- Ajit K. Srivastava, Carroll E. Goering, Roger P. Rohrbach, & Dennis R. Buckmaster. (2013). Engineering Principles of Agricultural Machines, Second Edition. In *Engineering Principles of Agricultural Machines, Second Edition*. <https://doi.org/10.13031/epam.2013>
- Alizadeh, M. R. (2011). Field performance evaluation of mechanical weeders in the paddy field. *Scientific Research and Essays*, 6(25), 5427–5434.
- AZO Materials. (2015). AISI 1020 Low Carbon/Low Tensile Steel. *AZoM.Com Limited*, 1–3. Retrieved from www.azom.com
- Beer, F. P., Johnston Jr, E. R., & DeWolf, J. (2001). Stress and strain–Axial loading. *Plant J, Ed. Mechanics of Materials, 3rd Ed. New York: McGraw-Hill*, 48–57.
- Chagomoka T, Drescher A, Glaser R, Marschner B, Schlesinger J, and G. N. (2015). Vegetable production, consumption and its contribution to diets along the urban – rural continuum in Northern Ghana. *African Journal of Food, Agriculture, Nutrition and Development*, 15(4), 10352–10367. <https://doi.org/10.6094/UNIFR/12089>
- Chang, W., Lin, C., & Wu, L. (2014). A note on Grashof's theorem. *Journal of Marine Science and Technology*, 13(4), 239–248.
- DAI, N. A. (2014). CHILLIMARKET DIAGNOSTICS DFID Market Development (MADE) in Northern Ghana Programme. In *CHILLIMARKET DIAGNOSTICS*. Retrieved from www.dai.com
www.nathaninc.com

- Demirel, N., & Gölbasi, O. (2011). Stress distribution investigation on a dragline bucket using finite element analysis. *Madencilik*, 50(3), 3–9.
- Dihingia, P. C., Kumar, G. V. P., Sarma, P. K., & Neog, P. (2017). Production of soil block seedlings in plug trays for mechanical transplanting. *International Journal of Vegetable Science*, 23(5), 471–485.
- Dihingia, P. C., Kumar, G. V. P., Sarma, P. K., & Neog, P. (2018). Hand-Fed Vegetable Transplanter for Use with a Walk-Behind-Type Hand Tractor. *International Journal of Vegetable Science*, 24(3), 254–273. <https://doi.org/10.1080/19315260.2017.1413477>
- Eshbaugh, W. H. (1983). The genus *Capsicum* (Solanaceae) in Africa. *Bothalia*, 14(3/4), 845–848.
- FAOSTAT, F. (2017). Statistics of the Food and Agriculture Organization of the United Nations. *FAOSAT*. Retrieved from <http://www.fao.org/faostat/en/#data>
- Gears Educational Systems, LLC (2002). Chain Drive Systems. 105 Webster St. Hanover Massachusetts 02339, 1–15. Retrieved from www.gearseds.com. Accessed on April 19, 2019.
- Gladow, D. E. (1991, October 22). *Chain cam*. Google Patents.
- Godwin, R. J., & O'Dogherty, M. J. (2007). Integrated soil tillage force prediction models. *Journal of Terramechanics*, 44(1), 3–14. <https://doi.org/10.1016/j.jterra.2006.01.001>
- Gokhale, N. S. (2008). *Practical finite element analysis*. Finite to infinite.
- Gonzalez, Y. R. S., Dijkxhoorn, Y., Elings, A., Glover-Tay, J., Koomen, I., van der Maden, E., ... Obeng, P. (2014). *Vegetables Business Opportunities in Ghana: 2014*. GhanaVeg.

- Hoque, M. A., & Miah, M. S. (2015). Evaluation of different tillage methods to assess BARI inclined plate planter. *Agricultural Engineering International: CIGR Journal*, 17(3).
- Hu, J., Yan, X., Ma, J., Qi, C., Francis, K., & Mao, H. (2014). Dimensional synthesis and kinematics simulation of a high-speed plug seedling transplanting robot. *Computers and Electronics in Agriculture*, 107, 64–72.
- Hwang, H., & Sistler, F. E. (1986). Robotic Pepper Transplanter. *Applied Engineering in Agriculture*, 2(1), 2–5. [https://doi.org /10.13031 /2013.26695](https://doi.org/10.13031/2013.26695)
- IRRI. (2003). Manual Transplanting. In *Machine Transplanting* (Vol. 1, p. 1). Retrieved from <http://www.knowledgebank.irri.org/tropRice>
- IRRI. (2007). *Planting technique: Translanting*. 2(4). Retrieved from [http://www.knowledgebank.irri.org/ericeproduction/II.4_Transplanting .htm](http://www.knowledgebank.irri.org/ericeproduction/II.4_Transplanting.htm)
- Ishak, W. I. W., Awal, M. A., & Elango, R. (2008). Development of an automated transplanter for the gantry system. *Asian Journal of Scientific Research*, 1(4), 451–457.
- Jin, X., Li, D. Y., Ma, H., Ji, J. T., Zhao, K. X., & Pang, J. (2018). Development of single row automatic transplanting device for potted vegetable seedlings. *International Journal of Agricultural and Biological Engineering*, 11(3), 67–75. [https://doi.org /10.25165 /j.ijabe.20181103.3969](https://doi.org/10.25165/j.ijabe.20181103.3969)
- Kershaw, K., Asquith, J. D., & Shilton, P. (1995, January 10). *Hydraulic manipulator*. Google Patents.

- Khetigaadi. (2016). India Vs World Farm Mechanization and Technology. *Khetigaadi*. Retrieved from <https://blog.khetigaadi.com/author/admin/>
- Khurmi, P. S., & Gupta, J. K. (2005). Shafts. In *A Textbook of Machine Design* (Vol. 7361, pp. 509–556).
- Kirisci, V., & S.Blackmore, R. J. G. (1994). A field method for predicting the draught forces of tillage implement. Cranfield University, Silsoe College.
- Kumar, D., & Tripathi, A. (2016). “ Performance Evaluation of Tractor Operated Two-Row Vegetable Transplanter .” *IOSR Journal of Agriculture and Veterinary Science (IOSR-JAVS)*, 9(1), 1–5. <https://doi.org/10.9790/2380-09110105>
- Kumar, G. V. P., & Raheman, H. (2011). Development of a walk-behind type hand tractor powered vegetable transplanter for paper pot seedlings. *Biosystems Engineering*, 110(2), 189–197.
- Kumar, P., & Raheman, H. (2008). International Journal of Vegetable Transplanters for Use in Developing Countries — A Review. *International Journal of Vegetable Science*, 14(3)(July). <https://doi.org/10.1080/19315260802164921>
- Kumar, P., & Raheman, H. (2012). Automatic feeding mechanism of a vegetable transplanter. *International Journal of Agricultural and Biological Engineering*, 5(2), 20–27.
- Kumar, V., & Dixit, J. (2018). Design , Development and Fabrication of A Single Row Manual Vegetable Transplanter. *Indian Journal of Hill Farming*, 31(1), 177–182. Retrieved from www.kiran.nic.in

- Lazarus, W. F. (2009). Machinery cost estimates. *University of Minnesota Extension, St. Paul.*
- Lei, Y. D., Ur, W., & Obeng, P. (2014). Export Vegetable Sector in Ghana Identifying opportunities for development. *GhanaVeg Export Reports*, (September), 1–48. Retrieved from www.wageningenUR.nl/cdi
- Lin, S., Chou, Y., Shieh, H., Ebert, A. W., Kumar, S., Mavlyanova, R., ... Gniffke, P. A. (2013). Pepper (*Capsicum* spp.) germplasm dissemination by AVRDC–The World Vegetable Center: an overview and introspection. *Chronica Horticulturae*, 53(3), 21–27.
- Mahapatra, M. (2006). Design, development and evaluation of a power tiller operated vegetable transplanter. *Doctoral Dissertation, Bidhan Chandra Krishi Vishwavidyalaya; Nadia*, 1–266.
- Mahesh Kumar Narang, IS Dhaliwal, G. S. M. (2011). *Development and evaluation of a revolving magazine type transplanting mechanism for vegetable crops* (pp. 1–7). pp. 1–7. New Delhi: Doctorial Dissertation, Punjab Agricultural University.
- Manilla, R. D., & Shaw, L. N. (1987). A high-speed dibbling transplanter. *Transactions of the ASAE*, 30(4), 904–908.
- Martin. (2016). Sprocket Engineering Data. *Martin*, 184–192. Retrieved from <https://anyflip.com/wict/zaej/basic>
- Misumi. (2009). Designing of Chain Drive Mechanism 1. *Technical Calculations*, 2815–2816. Retrieved from http://www.misumiusa.com/categoryimages/metric_2009_pdf/p2815.pdf
- Mkomwa, E. S., Mkoga, Z., Pembe, E. R., Kinyaga, E. I., Shetto, E. R., & Temu, F. (2008). Improving Rice Productivity through Promotion of

- Mechanised Rice Transplanting Technologies in Mbarali District. *ReseachGate*, (November 2008), 1–15.
- Murali, M., Anantachar, M., & Devojee, B. (2019). Performance evaluation of four row self propelled paddy transplanter for black cotton soil. *Journal of Pharmacognosy and Phytochemistry*, 8(2), 452–454.
- Nishida, C., Uauy, R., Kumanyika, S., & Shetty, P. (2004). The Joint WHO/FAO Expert Consultation on diet, nutrition and the prevention of chronic diseases: process, product and policy implications. *Public Health Nutrition*, 7(1a), 245–250. <https://doi.org/10.1079/PHN.2003592>
- NSK. (1998). NSK Rolling Bearings Catalogue. *Motion and Control*, 1, 1–279.
- Orzolek, M. D. (1996). Stand establishment in plasticulture systems. *HortTechnology*, 6(3), 181–185.
- Panel, M. M. (2018). Mechanised: Transforming African’s Agricultural Value Chains. *Dakar: Malabo Montpellier Panel*. Retrieved from www.mamopanel.org
- Penella, C., & Calatayud, A. (2018). Pepper crop under climate change: Grafting as an environmental friendly strategy. *Climate Resilient Agriculture: Strategies and Perspectives*. *IntechOpen, London*, 129–155.
- Prasanna Kumar, G. V., & Raheman, H. (2012). Automatic feeding mechanism of a vegetable transplanter. *International Journal of Agricultural and Biological Engineering*, 5(2), 20–27. <https://doi.org/10.3965/j.ijabe.20120502.00?>

- R Kavitha and R Karunanithi TNAU, C. D. A. K. V. D., & Introduction. (2008). Tractor Operated Three Row Plug Type Vegetable Transplanter. *Central Institute of Agricultural Engineering Nabi Bagh, Bhopal-462 038, India* :
- Rijk, M., & Beatrixlaan, P. (2014). Factsheet–Vegetables Ghana. *Netherlands-African Business Council*, 5(31), 12.
- Rudragouda, C. (2017). Manually Operated Single Row Vegetable Transplanter for Vegetable Seedlings. *International Journal of Agriculture Sciences*, 9(53), 4911–4914. Retrieved from <http://www.bioinfopublication.org/jouarchive.php?opt=&jouid=BPJ0000217>
- Sahoo, A. U., Mahapatra, M., Swain, S., & Behera, D. (2018). Development and Evaluation of a Bullock Drawn Vegetable Transplanter. *Int. J. Curr. Microbiol. App. Sci*, 7(1), 1584–1589.
- Shaw, L. N. (1998). Automatic transplanter for vegetables. *Proceedings of the... Annual Meeting of the Florida State Horticultural Society*.
- Singh, A. K. (2010). *Performance Evaluation of Two Row Semi-Automatic Vegetable Transplanter* (pp. 1–53). pp. 1–53. Birsa Agricultural University, Kanke, Ranchi, Jharkhand.
- Slocum, A. (2008). Fundamental of Design Topic 4 Linkages. *Jan*, 1, 62.
- Srivastava, A. K., Goering, C. E., Rohrbach, R. P., & Buckmaster, D. R. (1993). *Engineering principles of agricultural machines*.
- Standard, A. (2005). Terminology and Definitions for Soil Tillage and Soil-Tool Relationships. In *St. Joseph, Michigan: ASABE*.

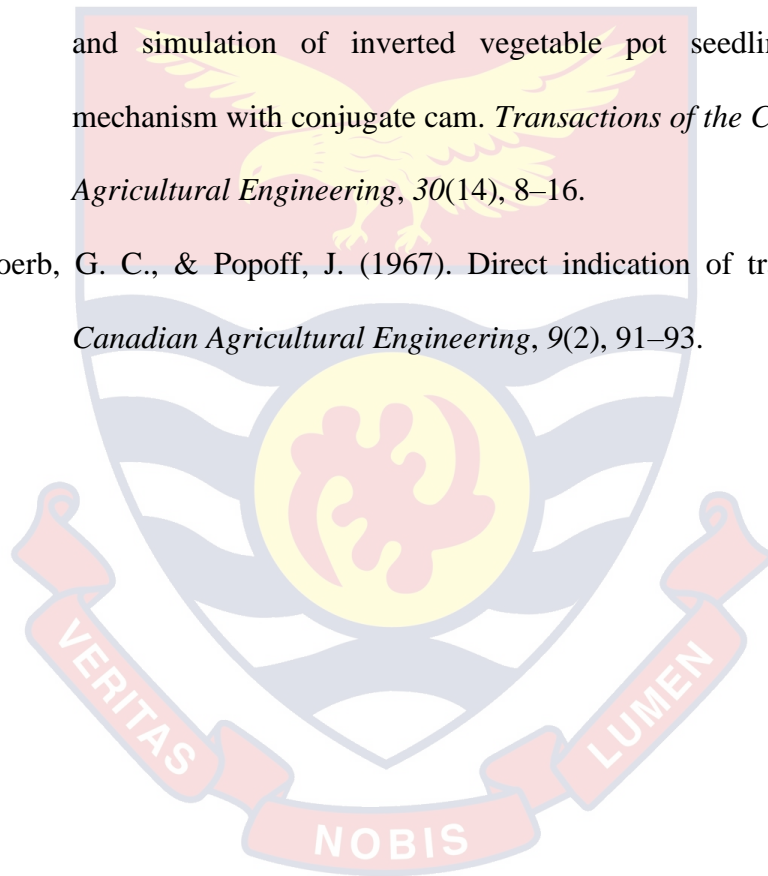
- Stanley, S. M. (1961, January 17). *Ball detent fastener with cam lever actuating means*. Google Patents.
- Statista. (2019). Global production of vegetables in 2017. *Statista*. Retrieved from www.statista.com/statistics/264065
- Tian, S., Qiu, L., Kondo, N., & Yuan, T. (2010). Development of automatic transplanter for plug seedling. *IFAC Proceedings Volumes (IFAC-PapersOnline)*, 3(PART 1), 79–82. <https://doi.org/10.3182/20101206-3-jp-3009.00013>
- Tripodi, P., & Kumar, S. (2019). The capsicum crop: an introduction. In *The Capsicum Genome* (pp. 1–8). Springer.
- Tsuga, K. (2000a). Development of fully automatic vegetable transplanter. *Japan Agricultural Research Quarterly*, Vol. 34, pp. 21–28.
- Tsuga, K. (2000b). Development of fully automatic vegetable transplanter. *Japan Agricultural Research Quarterly*, 34(1), 21–28.
- U.S. Department of Health and Human Services. (2011). State indicator report on fruits and vegetables, 2009. In *Eating Right: The Consumption of Fruits and Vegetables* (pp. 139–156). Retrieved from www.cdc.gov/nutrition
- University, R. (2007). Shaft Design. *PoLAR*, 1–7.
- Utkalini Sahoo, A., Mahapatra, M., Swain, S., & Behera, D. (2018). Development and Evaluation of a Bullock Drawn Vegetable Transplanter. *International Journal of Current Microbiology and Applied Sciences*, 7(1), 1584–1589. <https://doi.org/10.20546/ijcmas.2018.701.192>

Yujie, S., & Jun, H. (2016). *The structure design and simulation analysis for the corn seedling mechanism of transplanting machine*. (Ameii), 1224–1228.

Zamani, D. M. (2014). Development and evaluation of a vegetable transplanter. *International Journal of Technical Research and Applications*, 2(6), 40–46. Retrieved from www.ijtra.com

Zhao, Y., Fan, F., Song, Z., Na, M., Zuo, Y., Feng, Y., & Ji, H. (2014). Design and simulation of inverted vegetable pot seedling transplanting mechanism with conjugate cam. *Transactions of the Chinese Society of Agricultural Engineering*, 30(14), 8–16.

Zoerb, G. C., & Popoff, J. (1967). Direct indication of tractor-wheel slip. *Canadian Agricultural Engineering*, 9(2), 91–93.



APPENDICES

Appendix A: Analysis of Field Data

Appendix A1: Analysis of variance

Variate: Transplanting Time

Source of variation	d.f.	s.s.	m.s.	v.r.	F pr.
Block stratum	2	3.200	1.600	0.27	
Block.*Units* stratum					
Method	1	14798.881	14798.881	2479.90	<.001
Transplanting Depth	2	129.923	64.962	10.89	0.003
Method.Transplanting_Depth	2	36.930	18.465	3.09	0.090
Residual	10	59.675	5.968		
Total	17	15028.610			

Source: Field survey Karimu (2019)

Information summary

All terms orthogonal, none aliased.

Message: the following units have large residuals.

Block 1 *units* 5 3.88 s.e. 1.82

Tables of effects

Variate: Transplanting Time

Block.*Units* stratum

Method response 57.35, s.e. 1.152, rep. 9

Planting Depth effects, e.s.e. 0.997, rep. 6

Planting Depth	4	6	8
	-3.70	1.12	2.58

Method.Planting_Depth effects, e.s.e. 1.410, rep. 3

Method	Planting_Depth		
	4	6	8
Machine	1.96	-0.54	-1.42
Manual	-1.96	0.54	1.42

Source: Field survey Karimu (2019)

Tables of means

Variate: Trans Time

Grand mean 63.66

Method	Machine	Manual
	34.99	92.33

Planting_Depth	4	6	8
	59.95	64.78	66.24

MethodPlanting_Depth	4	6	8
Machine	33.24	35.57	36.15
Manual	86.67	94.00	96.33

Source: Field survey Karimu (2019)

Standard errors of differences of means

Table	MethodPlanting_Depth		
	Method Planting_Depth		
rep.	9	6	3
d.f.	10	10	10
s.e.d.	1.152	1.410	1.995

Source: Field survey Karimu (2019)



Appendix A2: Seedling survival

Variate: Seedling_survival

Source of variation	d.f.	s.s.	m.s.	v.r.	F	pr.
Block stratum		2	411.9		206.0	0.40
Block.*Units* stratum						
Method		1	829.6		829.6	1.62 0.232
Planting_Depth		2	1253.5		626.8	1.22 0.335
Method.Planting_Depth		2	1847.4		923.7	1.80 0.215
Residual		10	5125.2		512.5	
Total		17	9467.6			

Source: Field survey Karimu (2019)

Information summary

All terms orthogonal, none aliased.

Message: the following units have large residuals.

Block 2 *units* 6	38.5	s.e. 16.9
Block 3 *units* 6	-49.8	s.e. 16.9

Tables of effects

Variate: Seedling_surv

Block.*Units* stratum

Method response 13.6, s.e. 10.67, rep. 9

Planting_Depth effects, e.s.e. 9.24, rep. 6

Planting_Depth	4	6	8
	-11.4	2.9	8.5

Method.Planting_Depth effects, e.s.e. 13.07, rep. 3

MethodPlanting_Depth	4	6	8
Machine	-14.3	6.6	7.7
Manual	14.3	-6.6	-7.7

Source: Field survey Karimu (2019)

Tables of means

Variate: Seedling_surv

Grand mean 88.0

Method	Machine	Manual
	81.2	94.8

Planting_Depth	4	6	8
	76.7	90.9	96.5

MethodPlanting_Depth	4	6	8
Machine	55.6	90.7	97.4
Manual	97.8	91.1	95.5

Source: Field survey Karimu (2019)

Standard errors of differences of means

Table	MethodPlanting_Depth		
	Method		Planting_Depth
rep.	9	6	3
d.f.	10	10	10
s.e.d.	10.67	13.07	18.48

Source: Field survey Karimu (2019)

Appendix A3: Field Capacity

Variate: Field_Capacity

Source of variation	d.f.	s.s.	m.s.	v.r.	F	pr.
Block stratum		2	2.618E-06		1.309E-06	5.89
Block.*Units* stratum						
Method		1	1.382E-03		1.382E-03	6217.32 <.001
Planting_Depth		2	1.548E-06		7.739E-07	3.48 0.071
Method.Planting_Depth		2	7.568E-06		3.784E-06	17.03 <.001
Residual		10	2.222E-06		2.222E-07	
Total		17	1.396E-03			

Source: Field survey Karimu (2019)

Information summary

All terms orthogonal, none aliased.

Tables of effects

Variate: Field_Capacity

Block.*Units* stratum

Method response -0.01752, s.e. 0.000222, rep. 9

Planting_Depth effects, e.s.e. 0.000192, rep. 6

Planting_Depth	NOE4	6	8
	0.00041	-0.00013	-0.00028

Method.Planting_Depth effects, e.s.e. 0.000272, rep. 3

MethodPlanting_Depth	4	6	8
Machine	-0.00089	0.00027	0.00062
Manual	0.00089	-0.00027	-0.00062

Source: Field survey Karimu (2019)

Tables of means

Variate: Field_Capacity

Grand mean 0.02986

Method	Machine	Manual
	0.03862	0.02110

Planting_Depth	4	6	8
	0.03027	0.02973	0.02958

MethodPlanting_Depth	4	6	8
Machine	0.03813	0.03877	0.03897
Manual	0.02240	0.02070	0.02020

Source: Field survey Karimu (2019)

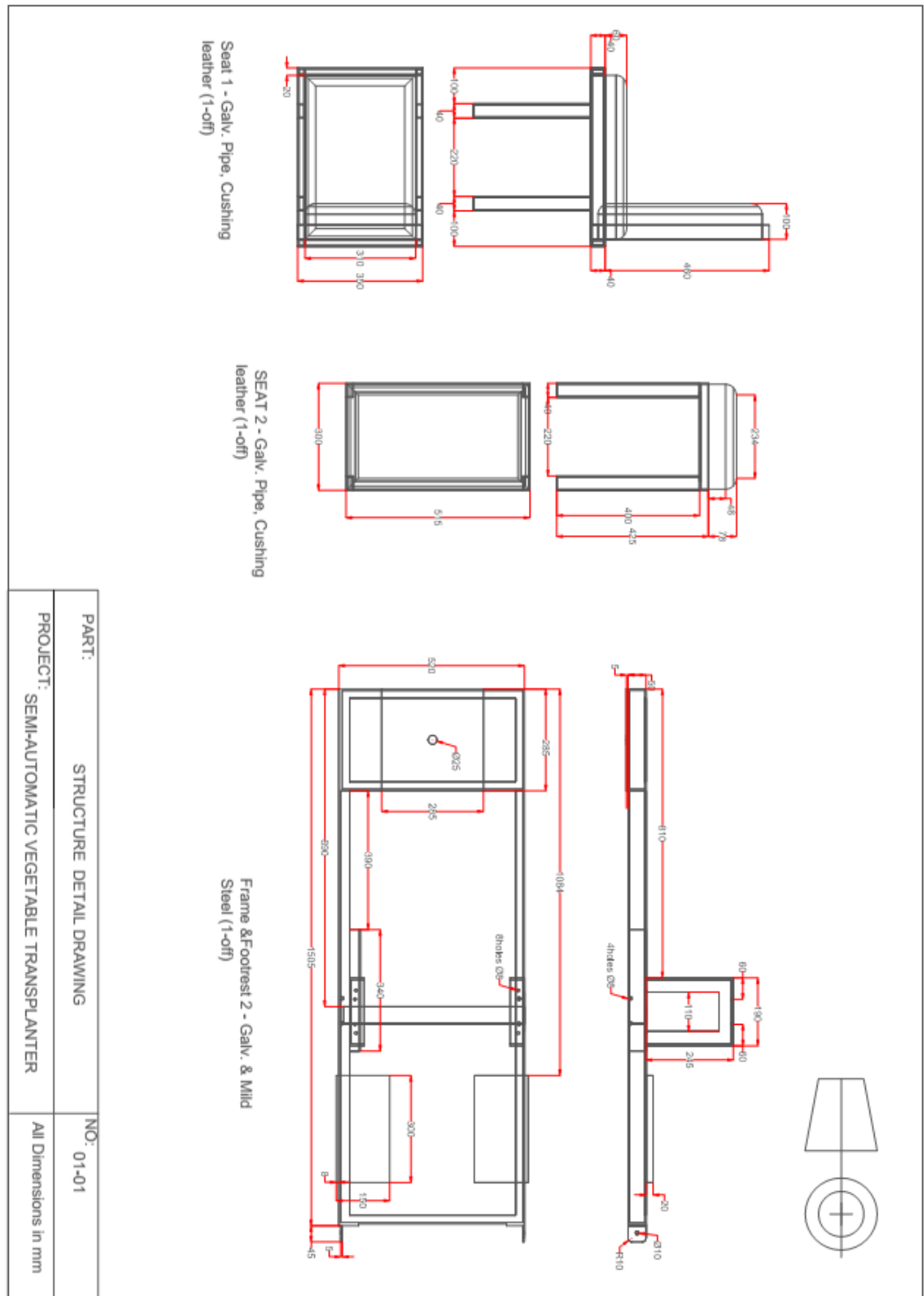
Standard errors of differences of means

TableMethodPlanting_Depth	Method		
	Planting_Depth		
rep.	9	6	3
d.f.	10	10	10
s.e.d.	0.000222	0.000272	0.000385

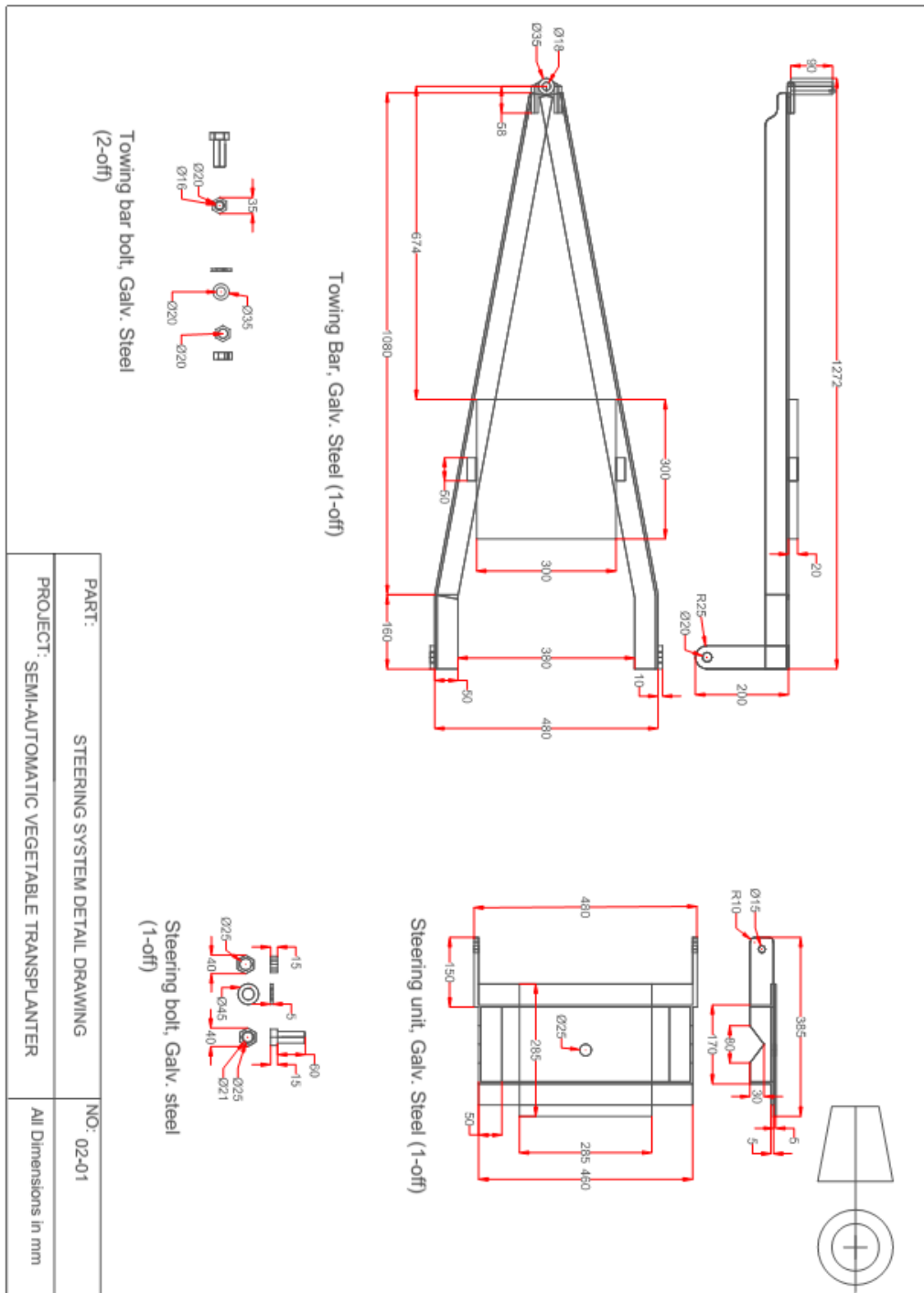
Source: Field survey Karimu (2019)

Appendix B: Detail Drawings

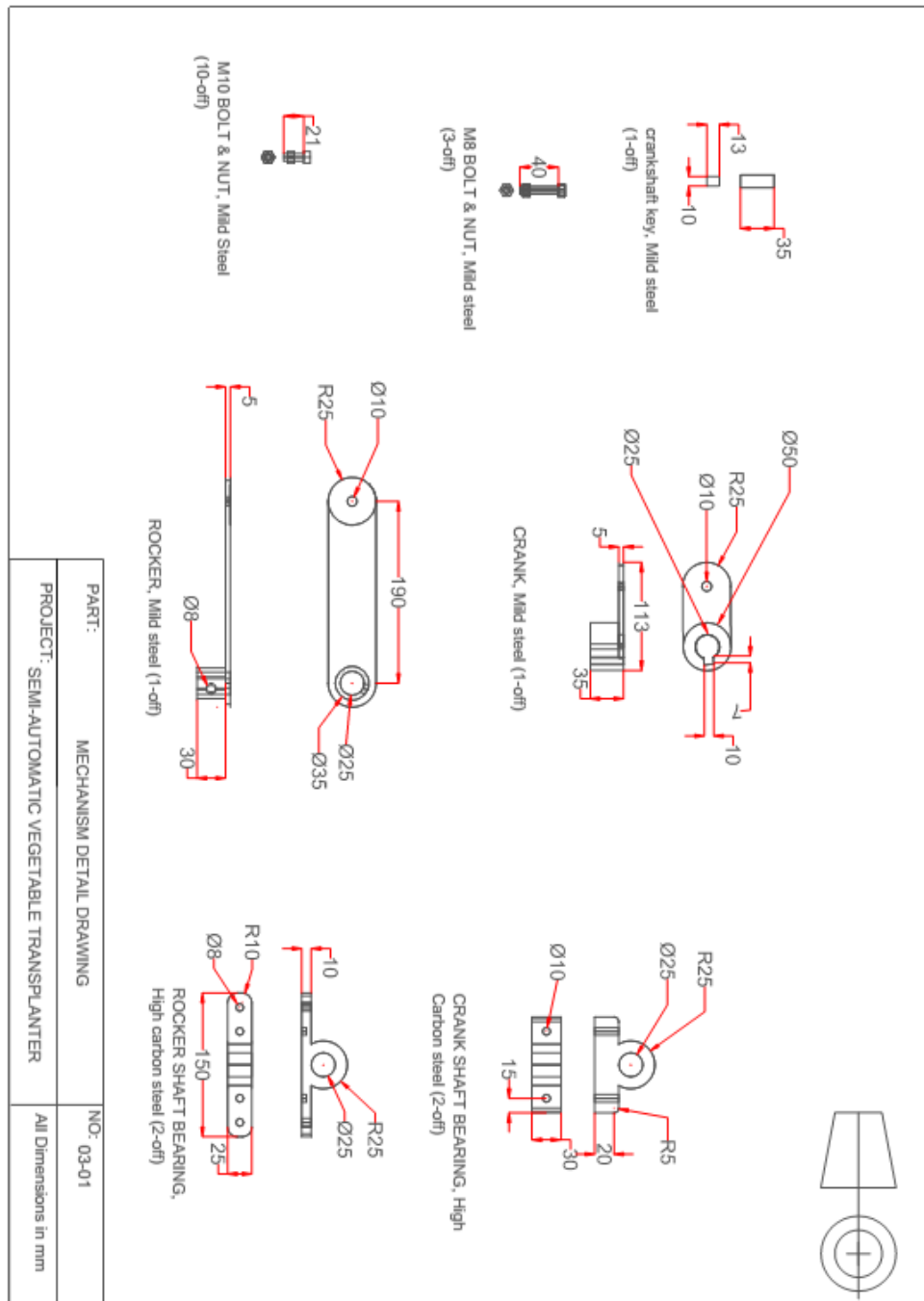
Appendix B1: Detail drawing of the structure sub assembly



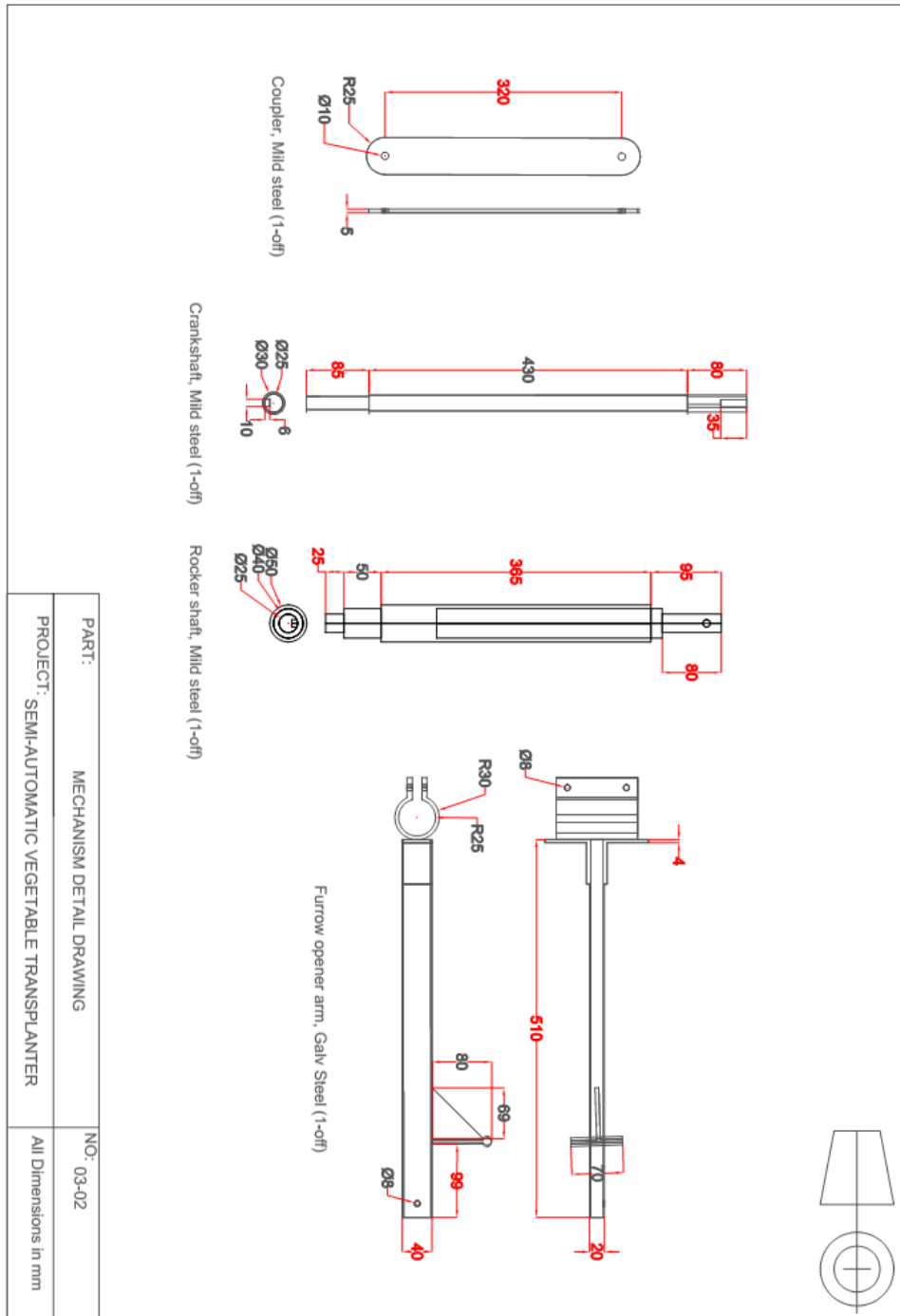
Appendix B2: Detail drawing steering system subassembly



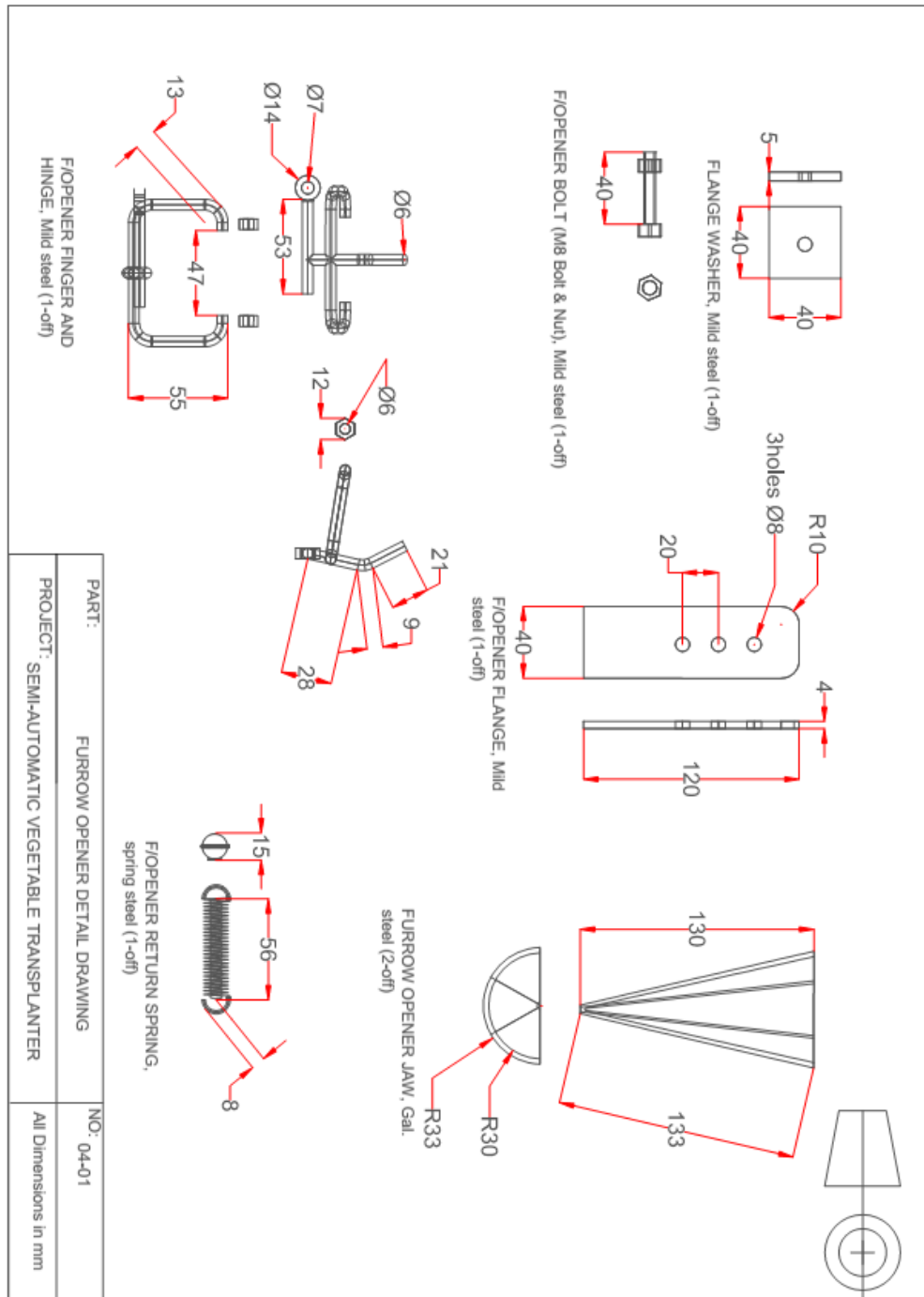
Appendix B3: Detail drawing of the mechanism sub-assembly



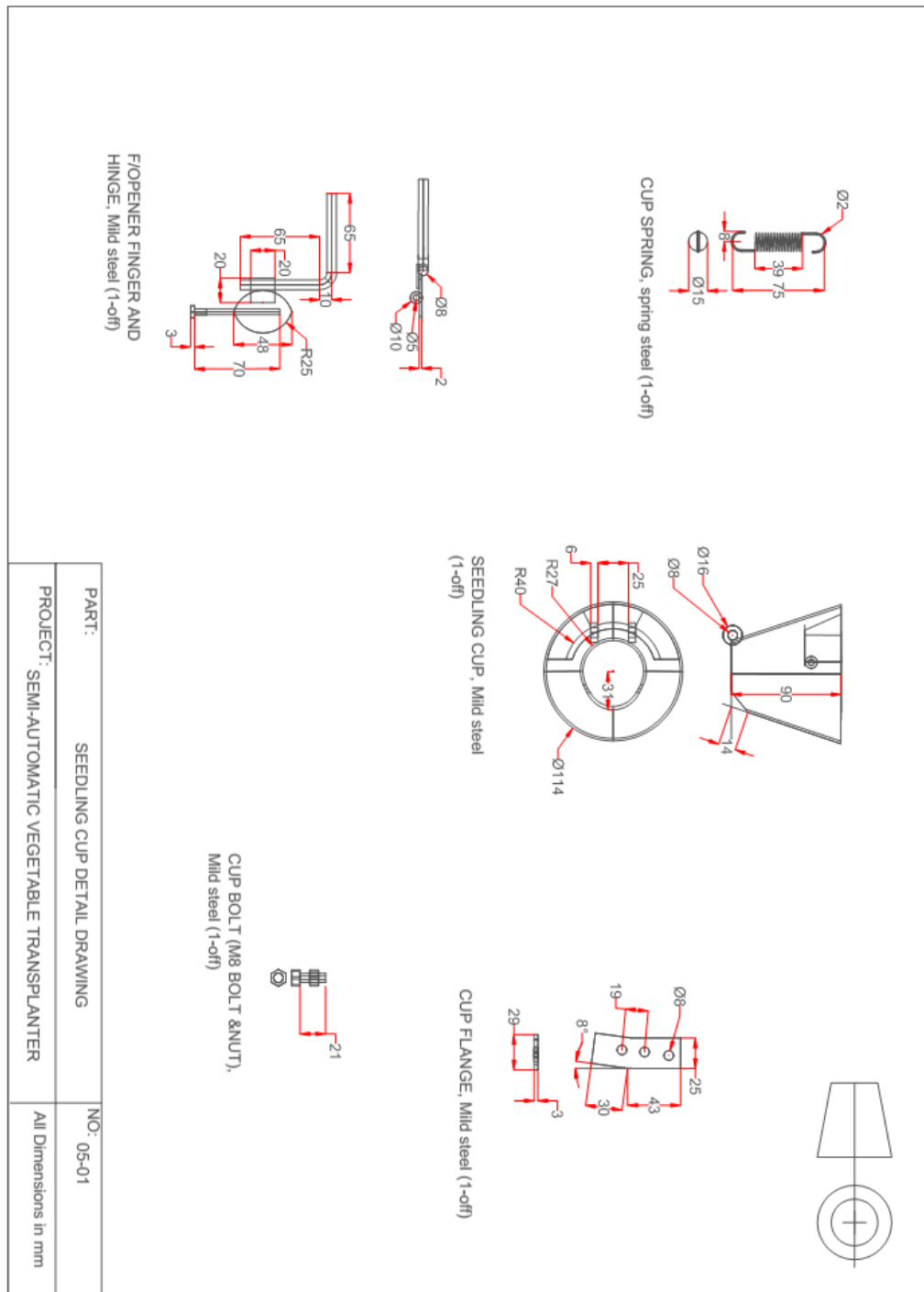
Appendix B4: Detail drawing of the mechanism sub-assembly cont.



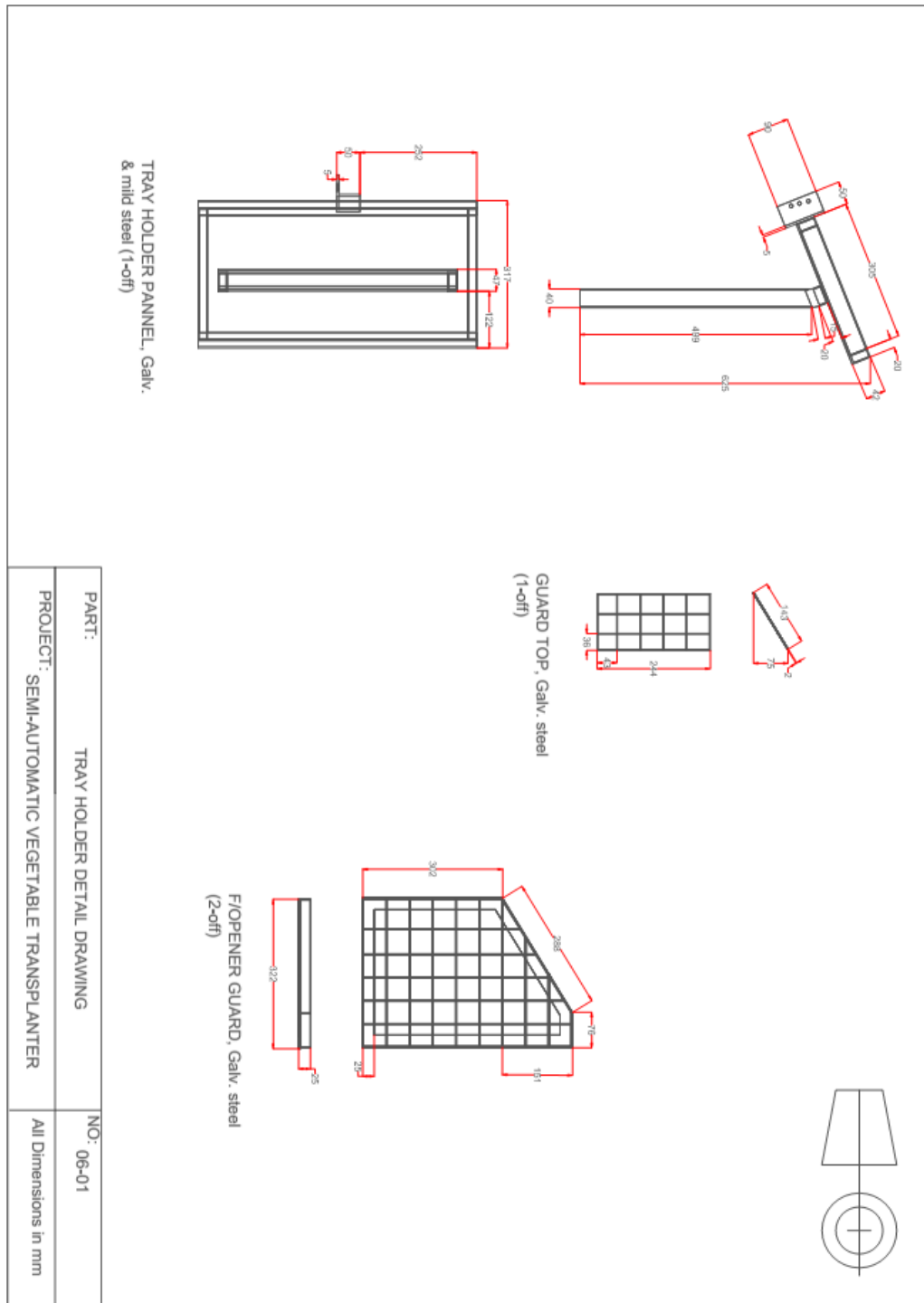
Appendix B5: Detail drawing of the furrow opener sub-assembly



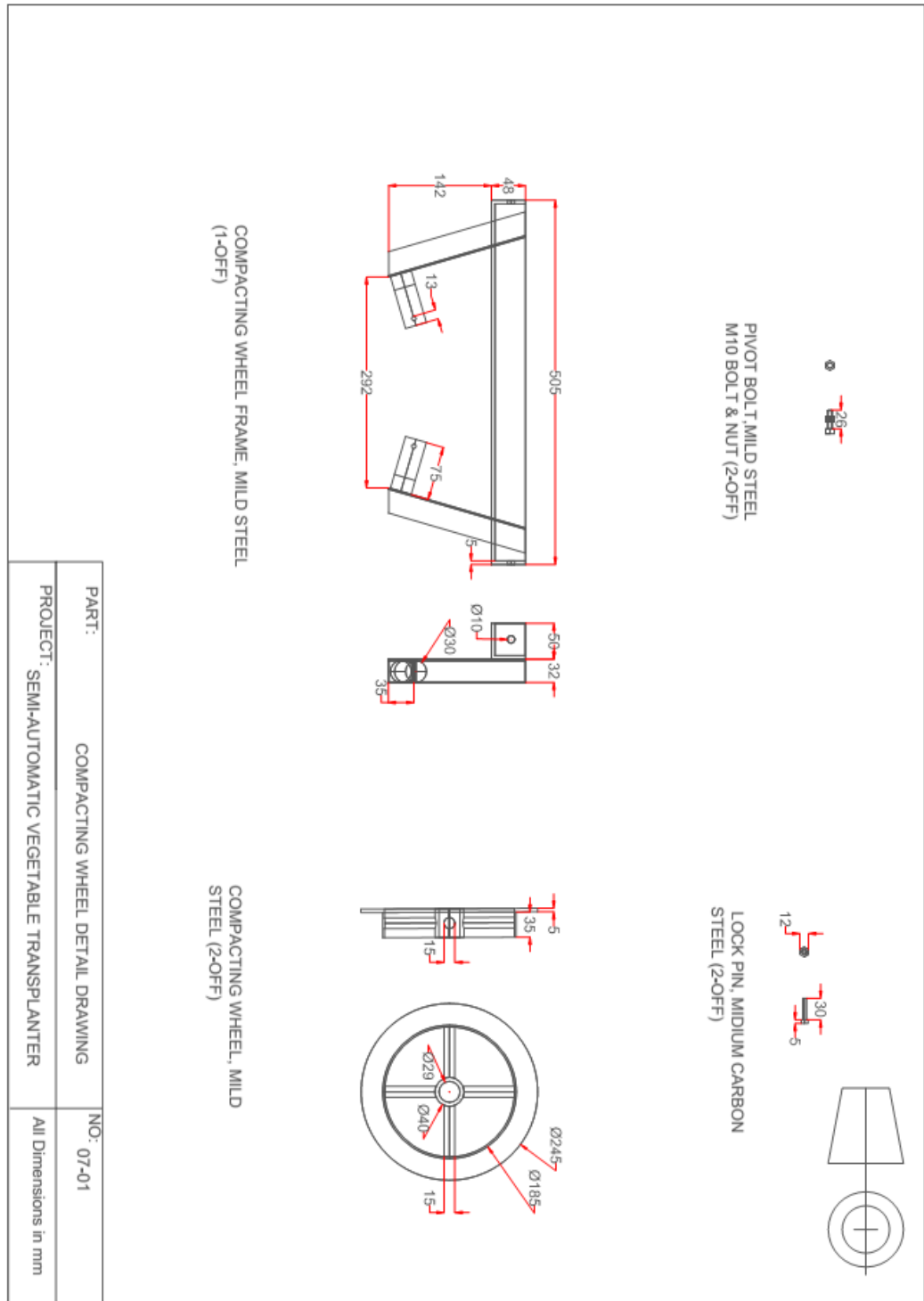
Appendix B6: Detail drawing of the seedling cup sub-assembly



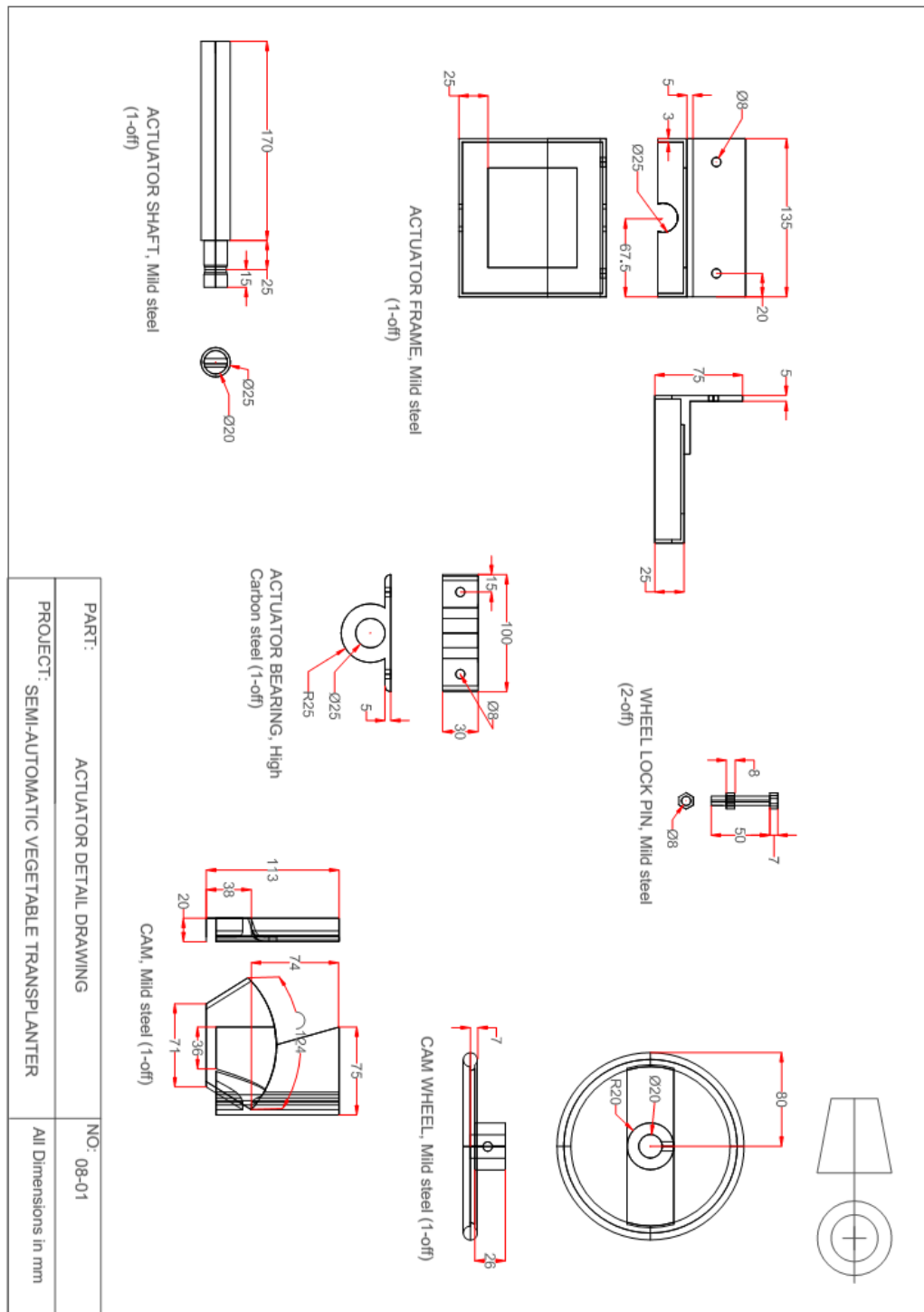
Appendix B7: Detail drawing of the tray holder sub-assembly



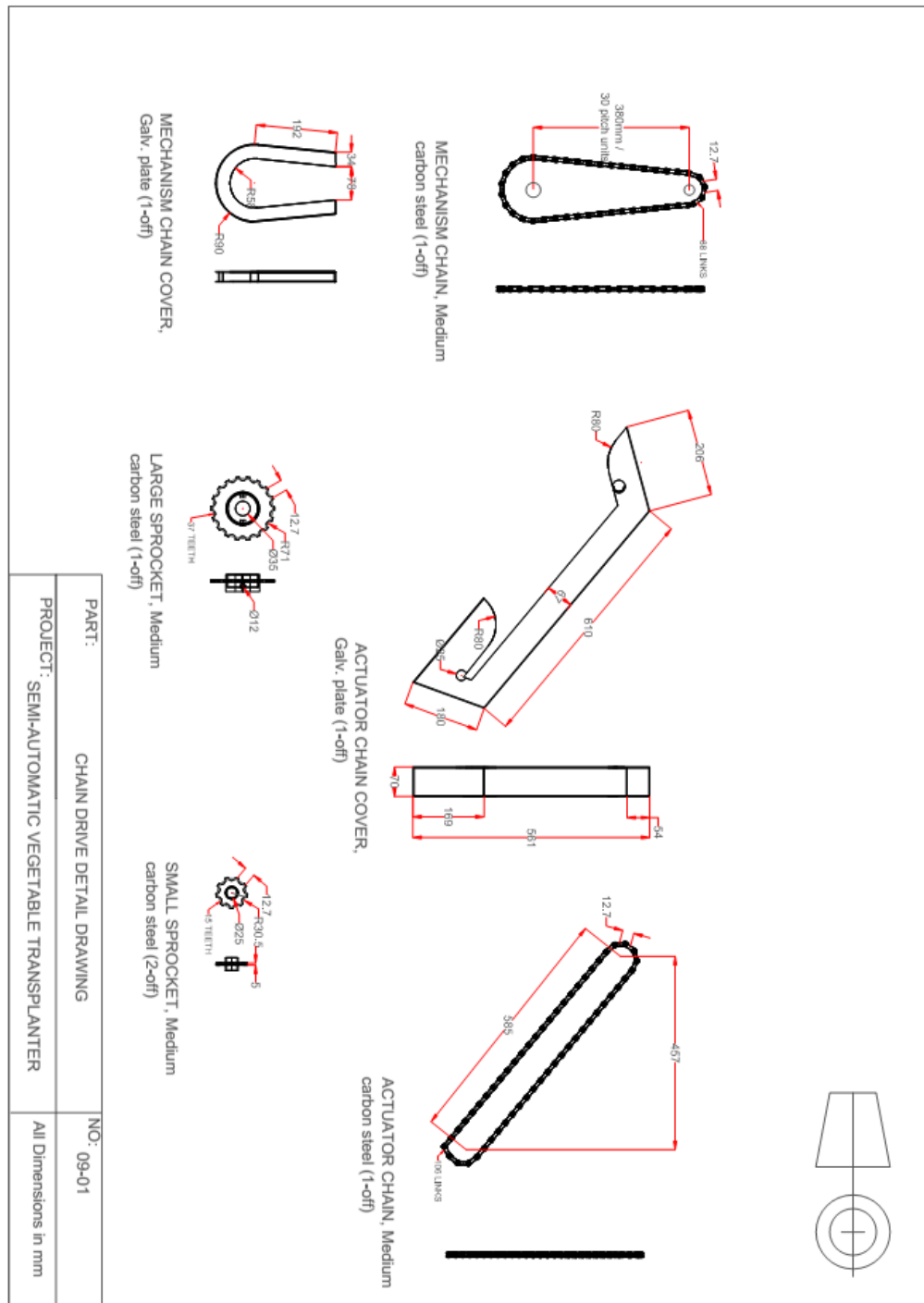
Appendix B8: Detail drawing of the compacting wheel sub-assembly



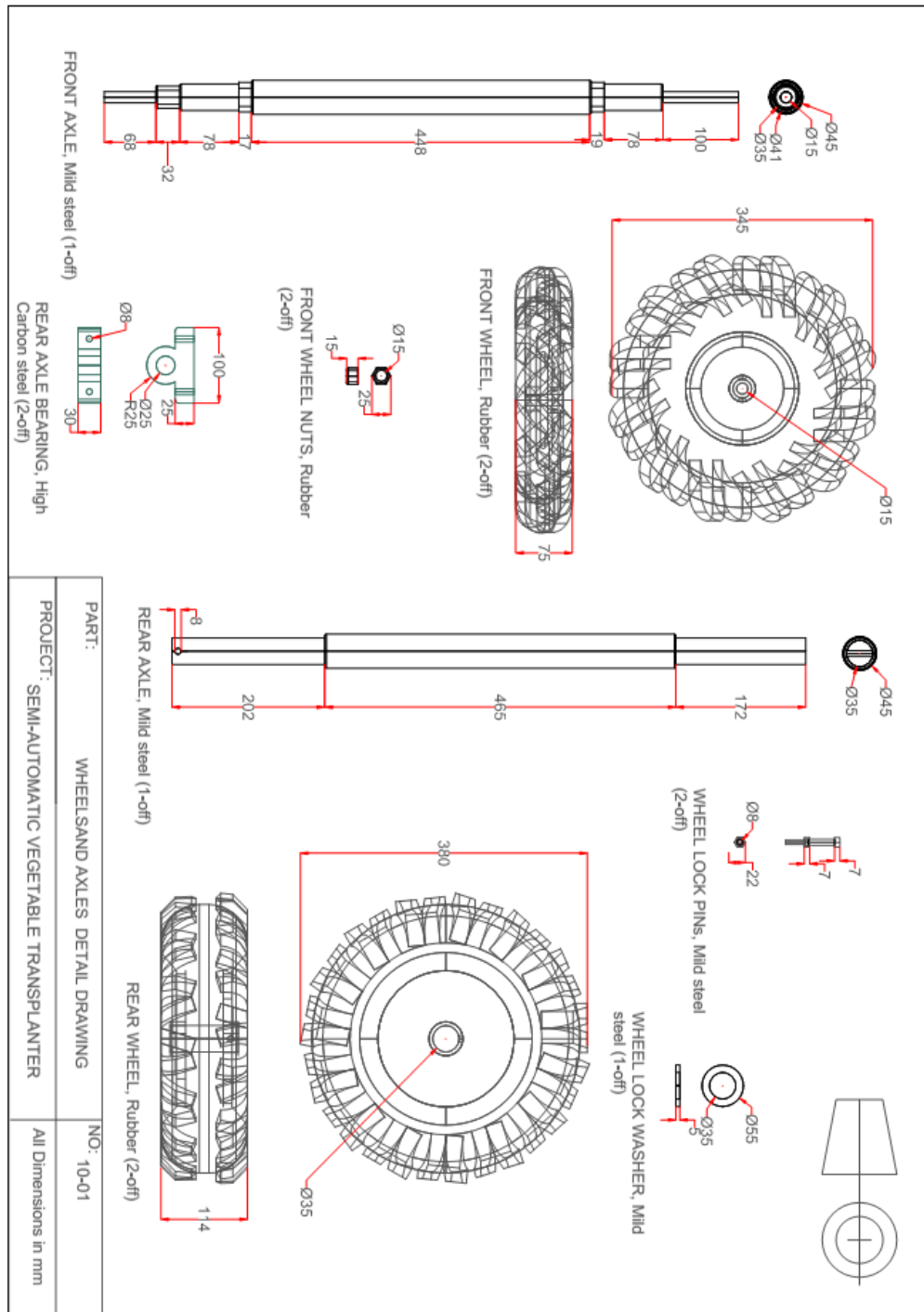
Appendix B9: Detail drawing of the actuator sub-assembly



Appendix B10: Detail drawing of the chain drive sub-assembly



Appendix B11: Detail drawing of the wheels sub-assembly



Appendix C: Design Calculations and Bill of Quantities

Appendix C1: Design of the Crank-Rocker Mechanism

Grashof's law

$$d + b \leq c + a$$

where $a = 250\text{mm}$, $b = 63\text{mm}$, $c = 320\text{mm}$ and $d = 190\text{mm}$

$$190 + 63 \leq 320 + 250$$

$$253 \leq 570.$$

Degree of Freedom

Gruebler's Equation: $F = 3(n - 1) - 2f_1$

where $n = 4$ and $f_1 = 4$.

$$F = 3(4 - 1) - 2 \times 4 = 1$$

Rotary speed of crank shaft (high speed shaft)

$$\begin{aligned} \text{Rotary Speed of the ground wheels} &= \frac{\text{speed of transplanter}}{\text{circumference of ground wheel}} \\ &= \frac{16.67}{\pi \times 0.38} = 14.0\text{rpm} \end{aligned}$$

$$\begin{aligned} \text{Speed of the crank shaft} &= \text{rotary speed of ground wheel} \times \text{speed ratio} \\ &= 14.0 \times 2.5 = 35\text{rpm} \end{aligned}$$

Appendix C2: Chain length for the mechanism

Pitch circle radius of the small sprocket (Pr)

The dimension AB = Pr

And Pr = 1/2 x pitch circle diameter of the small sprocket (Pd)

$$\text{However, } Pd = \frac{P}{\sin\left[\frac{180^\circ}{n}\right]}$$

$$AB = PR = \frac{1}{2} \times \frac{P}{\sin\left[\frac{180^\circ}{n}\right]}$$

$$= \frac{1}{2} \times \frac{12.7}{\sin\left[\frac{180^\circ}{15}\right]} = \frac{1}{2} \times \frac{12.7}{0.208} = 30.5\text{mm}$$

Pitch circle radius for the large sprocket (PR)

$$DE = \frac{1}{2} \times \frac{P}{\sin\left[\frac{180^\circ}{N}\right]}$$

$$= \frac{1}{2} \times \frac{12.7}{\sin\left[\frac{180^\circ}{37}\right]} = \frac{1}{2} \times \frac{12.7}{0.085} = 74.7\text{mm}$$

The length of side DF

$$DF = DE - AB$$

$$= 74.7 - 30.5 = 44.2\text{mm}$$

Value for angle a

$$\sin a = \frac{DF}{AD}$$

$$\sin a = \frac{44.2}{380} = 0.12$$

$$a = \sin^{-1}0.12 = 6.9^\circ$$

length of the chain between the pitch circle tangent points, BE

$$BE = AF = AD \times \cos a$$

$$= 380 \cos 6.9^\circ = 377.2\text{mm} = \frac{377.2}{12.7} = 30 \text{ pitch units}$$

Lengths of chain wrapped around each of the sprockets

Half the chain wrapped around the large sprocket is represented by arc ME

$$ME = MH + HE = \frac{N}{4} + N \frac{a}{360}$$

$$= \frac{37}{4} + 37 \times \frac{6.9}{360} = 10 \text{ pitch units}$$

$$KB = KG - BG = \frac{n}{4} - n \frac{a}{360}$$

$$\frac{15}{4} - 15 \times \frac{6.9}{360} = 3.5 \text{ pitch units}$$

The chain length (In pitch units) for the crank –rocker mechanism is

$$L_1 = 2 [BE + ME + KB]$$

$$= 2 [30 + 10 + 3.5] = 87 \text{ pitch units}$$



Appendix C3: Chain and Sprocket for the Actuator.

Known Parameters:

Desired speed ratio between the crank shaft and the actuator shaft = 1: 1

Number of sprocket teeth $n_1 = n_2 = 15T$

Distance between the crank shaft and the actuator shaft Centers (C_d) = 580mm

Pitch (P) = $\frac{1}{2}$ " = 12.7mm

Length of the actuator chain

$$L_2 = 2C_d/p + n \text{ (in pitch units)}$$

$$= 2 \times 580/12.7 + 15 = 106 \text{ pitch units}$$

Appendix C4: Design of the Crank Shaft in the transplanter

Shaft design

Torque in the shaft

The Maximum power(P) of the power tiller is 13Hp@2400rpm

$$= 9.561 \text{ kW @ 2400 rpm}$$

$$p = \frac{2\pi N \times T}{60 \times 10^3}$$

$$T = \frac{P \times 60 \times 10^3}{2\pi N} = \frac{9.561 \times 60 \times 10^3}{2 \times \pi \times 2400} = 38 \text{ Nm} = 0.038 \text{ kNm}$$

Weight of the crank at point A

The vertical weight of the crank F_{AY} is

$$F_{AY} = mg$$

$$m = \rho V$$

$$V = l \times b \times h$$

$$= 4.5 \times 0.5 \times 8 = 18 \text{ cm}^3$$

$$\rho = \text{density of the crank material (AISI 1020)} = 7.87 \text{ g/cm}^3$$

$$m = 7.87 \times 18 = 141.66 \text{ g} = 0.142 \text{ kg}$$

$$\text{Therefore, } F_{AY} = 0.142 \times 9.81 = 1.393 \text{ kN}$$

$$F_{AX} = F_{AY} \tan 30 = 1.39 \tan 30 = 0.804 \text{ kN}$$

Forces due to Chain and Sprocket

The Mechanism chain drive

$$F_E = \frac{2T}{D}$$

Where T = Torque = 0.038 kNm

D = Pitch circle diameter of sprocket on the shaft = 0.061 m = 0.1 m

$$F_E = \frac{2 \times 0.038}{0.1} = 0.76 \text{ kN}$$

The horizontal component of the force F_E is calculated as

$$F_{EX} = F_E \sin a$$

Where a = wrap angle of the mechanism chain = 6.9°

$$F_{EX} = 0.76 \times \sin 6.9 = 0.091 \text{ kN}$$

The vertical component of the force F_E is calculated as

$$F_{EY} = F_E \cos a = 0.76 \times \cos 6.9 = 0.754 \text{ kN}$$

The actuator Chain drive

$$F_B = \frac{2T_B}{D}$$

D = Pitch circle diameter of sprocket on the shaft = 0.061 m = 0.1 m

T_B = Torque in the shaft = 0.038 kNm

$$F_B = \frac{2 \times 0.038}{0.1} = 0.76$$

The actuator chain drive inclination to the horizontal is the angle p

from Figure 26 which can be calculated as

$$\tan p = \frac{BQ}{QR} = \frac{380}{450} = 0.844$$

$$p = \tan^{-1} 0.844 = 40.2^\circ$$

The horizontal component of the force F_B is

$$F_{BX} = F_B \cos p = 0.76 \times \cos 40.2 = 0.580 \text{ kN}$$

The vertical component of the force F_B is

$$F_{BY} = F_B \sin p = 0.76 \times \sin 40.2 = 0.490 \text{ kN}$$

Clockwise moments = anticlockwise moments

$$(F_{AY} \times 0.08) + (R_{DY} \times 0.44) = (F_{EY} \times 0.49) + (F_{BY} \times 0.57)$$

$$(1.393 \times 0.08) + (R_{DY} \times 0.44) = (0.754 \times 0.49) + (0.490 \times 0.57)$$

$$0.111 + 0.44R_{DY} = 0.369 + 0.2793$$

$$R_{DY} = 1.221 \text{ kN}$$

For equilibrium,

Total upward forces = total downward forces

$$R_{CY} + R_{DY} = F_{AY} + F_{EY} + F_{BY}$$

$$R_{CY} + 1.21 = 1.39 + 0.75 + 0.49$$

$$R_{CY} = 1.416 \text{ kN}$$

Taking point A as the reference point, x as the shaft length, and applying singularity function in Microsoft excel, the shearing forces (V) and bending moments (M) were calculated as follows:

$$V = -1.393*(x>0)+R_{cy}*(x>0.08)+R_{dy}*(x>0.52)-0.754*(x>0.57)-0.49*(x>0.65) \text{ and}$$

$$M = -1.393*x*(x>0)+R_{cy}*(x-0.08)*(x>0.08)+R_{dy}*(x-0.52)*(x>0.52)-0.754*(x-0.57)*(x>0.57)-0.49*(x-0.65)*(x>0.65).$$

Shaft length, x (m)	Shear Force, V (kN)	Bending moment, M (kNm)
0	0.000	0.000
0.00001	-1.393	0.000
0.05	-1.393	-0.070
0.08	-1.393	-0.111
0.08001	0.023	-0.111
0.1	0.023	-0.111
0.15	0.023	-0.110
0.2	0.023	-0.109
0.25	0.023	-0.108
0.3	0.023	-0.106
0.35	0.023	-0.105
0.4	0.023	-0.104
0.45	0.023	-0.103
0.5	0.023	-0.102
0.52	0.023	-0.102
0.52001	1.244	-0.102
0.55	1.244	-0.064
0.57	1.244	-0.039
0.57001	0.490	-0.039
0.6	0.490	-0.025
0.65	0.490	0.000
0.6500001	0.000	0.000

Source: Field survey Karimu (2019)

Reactions at the Bearings Due to Horizontal Loading:

Taking moments about point C in fig 3.12,

Clockwise moments = anticlockwise moments

$$(F_{EX} \times 0.495) + (F_{BX} \times 0.575) = (F_{AX} \times 0.08) + (R_{DX} \times 0.445)$$

$$(0.15 \times 0.495) + (0.954 \times 0.575) = (0.804 \times 0.08) + (R_{DX} \times 0.445)$$

$$0.6228 = 0.06432 + 0.445R_{DX}$$

$$0.558 = 0.445R_{DX}$$

$$R_{DX} = 1.254kN$$

For equilibrium,

Total upward forces = total downward forces

$$R_{CX} + F_{DX} = F_{AX} + F_{EX} + F_{BX}$$

$$R_{CX} + 1.254 = 0.111 + 0.15 + 0.954$$

$$R_{CX} = 0.130kN$$

Taking A as the reference point, s as the shaft length, and applying singularity function in Microsoft excel, the shearing forces (V) and bending moments (M) were calculated as follows:

$$V = -0.804*(s > 0) + R_{cx}*(s > 0.08) + R_{dx}*(s > 0.52) - 0.091*(s > 0.57) -$$

$$0.58*(s > 0.65) \text{ and}$$

$$M = -0.804*s*(s > 0) + R_{cx}*(s - 0.08)*(s > 0.08) + R_{dx}*(s - 0.52)*(s > 0.52) -$$

$$0.091*(s - 0.57)*(s > 0.57) - 0.58*(s - 0.65)*(s > 0.65).$$

Shaft length, S (m)	Shear force, V (kN)	Bending moment, M (kNm)
0	0.000	0.000
0.00001	-0.804	0.000
0.05	-0.804	-0.040
0.08	-0.804	-0.064
0.08001	-0.036	-0.064
0.1	-0.036	-0.065
0.15	-0.036	-0.067
0.2	-0.036	-0.069
0.25	-0.036	-0.070
0.3	-0.036	-0.072
0.35	-0.036	-0.074
0.4	-0.036	-0.076
0.45	-0.036	-0.078
0.5	-0.036	-0.079
0.52	-0.036	-0.080
0.52001	0.671	-0.080
0.55	0.671	-0.060
0.57	0.671	-0.047
0.57001	0.580	-0.047
0.6	0.580	-0.029
0.65	0.580	0.000
0.6500001	0.000	0.000

Source: Field survey Karimu (2019)

Sizing the shaft

According to maximum shear stress theory or Guest's theory, maximum shear

(τ_{max}) stress is given by:

$$\tau_{max} = \frac{1}{2} \sqrt{[(\delta_b)^2 + 4\tau^2]}$$

Where δ_b = stress due to bending moment, and τ = stress due to twisting moment

But

$$M = \frac{\pi}{32} \times \delta_b \times d^3 \text{ and}$$

$$T = \frac{\pi}{16} \times \tau \times d^3$$

Making δ_b and τ the subjects from the above equations and substituting them into equation (3.14) results in

$$T_e = \sqrt{(M^2 + T^2)} = \frac{\pi}{16} \times \tau \times d^3$$

Given

$$T = 0.038 \text{ kNm} = 38 \text{ Nm} = 38 \times 10^3 \text{ Nmm}$$

$$M = -0.111 \text{ kNm} = -111 \text{ Nm} = -111 \times 10^3 \text{ Nmm}$$

$$\tau = 42 \text{ MPa} = 42 \text{ N/mm}^2$$

substituting the values into equation (3.15) gives

$$\sqrt{[(111 \times 10^3)^2 + (38 \times 10^3)^2]} = \frac{\pi}{16} \times 42 \times d^3$$

$$117324.3368 = 8.24668d^3$$

$$d = \sqrt[3]{\left[\frac{117324.3368}{8.247}\right]}$$

$$d = 24.23 \text{ mm}$$

Appendix C5: Deflection of the shaft

The angle of twist was computed from the relation;

$$\phi = \frac{TL}{JG}$$

Where:

T- is the torque subjected on the shaft = 0.038kN

L = Length of the shaft = 655mm

$$J\text{- polar moment of inertia} = \frac{\pi D^4}{32}$$

$$J = \pi \times \frac{0.025^4}{32} = 3.835 \times 10^{-8} m^4$$

$$G\text{- Modulus of rigidity} = \frac{E}{2(1+\nu)}$$

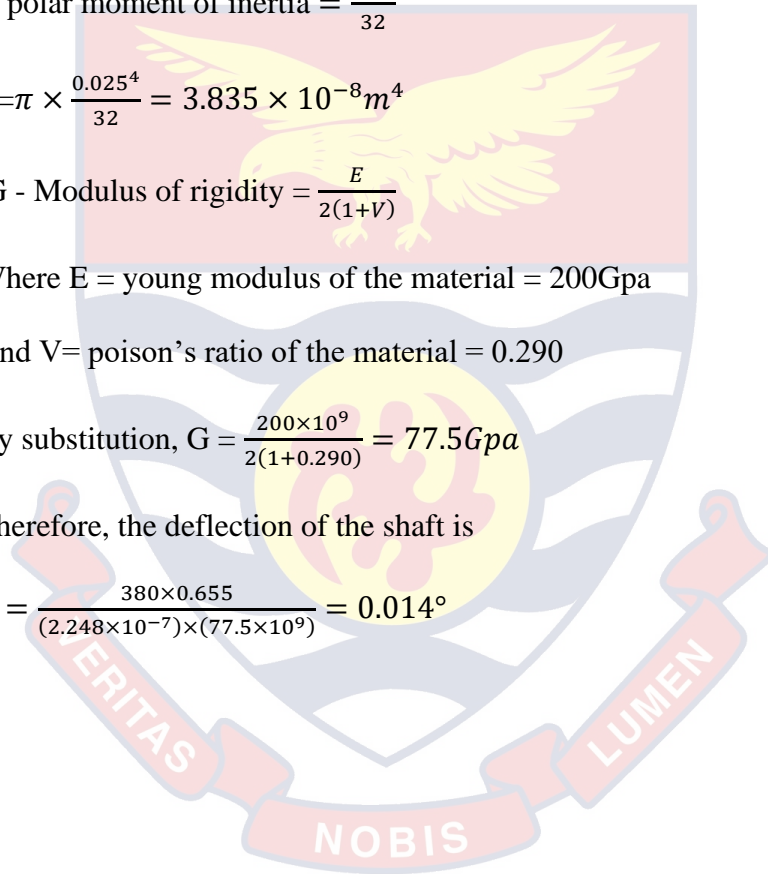
Where E = young modulus of the material = 200Gpa

And ν = poison's ratio of the material = 0.290

$$\text{By substitution, } G = \frac{200 \times 10^9}{2(1+0.290)} = 77.5 Gpa$$

Therefore, the deflection of the shaft is

$$\phi = \frac{380 \times 0.655}{(2.248 \times 10^{-7}) \times (77.5 \times 10^9)} = 0.014^\circ$$



Appendix C6: Bearing selection

Known Parameters

Single groove ball bearing, Bore diameter = 25mm, Outside diameter <100mm,

Radial Load, $F_r = 1.256 \text{ kN}$, Speed, $n = 35 \text{ rpm}$, Basic Rating life, $L_h \geq 10,000 \text{ hrs}$

Speed factor (f_n)

$$\text{This is calculated as } f_n = \left(\frac{10^6}{500 \times 60n} \right)^{\frac{1}{3}} = (0.03n)^{1/3}$$

Substituting in the the value of n gives

$$f_n = \left(\frac{10^6}{500 \times 60 \times 35} \right)^{\frac{1}{3}} = 1$$

Bearing Load (P)

This is given by

$$P = F_r \times F_w$$

Where F_r = Radial load = 1.256 kN,

F_w = load factor = 3

$$P = 1256 \times 3 = 3768 \text{ N}$$

The nominal life at 10% probability of failure for ball bearings is given as

$$L_{10} = \left(\frac{C}{P} \right)^3$$

Where C = basic load rating (N), P = bearing load or equivalent load (N)

Basic rating life in hours

$$L_h = \frac{10^6}{60n} \left(\frac{C}{P} \right)^3 = 500 F_h^3$$

Where f_h = fatigue life factor

$$f_h = F_n \frac{C}{P}$$

From tables, for $L_h \geq 10,000 \text{ hours}$, $F_h \geq 2.72$

$$2.72 = 1 \times \frac{C}{1630}$$

$$C = 10249 \text{ N}$$

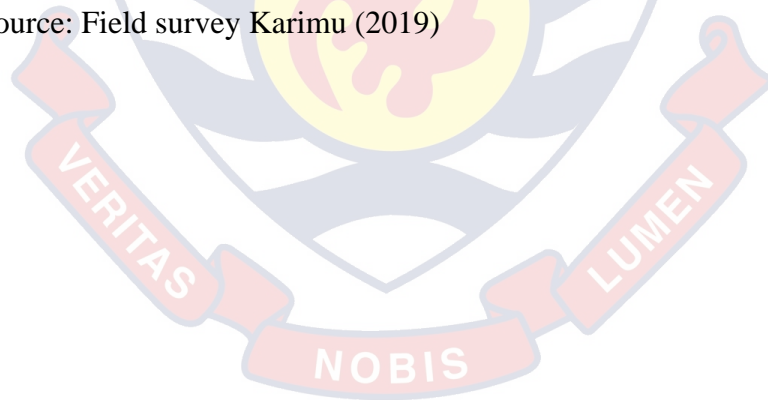
From the Bearing Selection Table for Bore Diameter 25-45mm in Appendix E, the bearing number that satisfies the above condition is 6205.

Appendix C7: Bill of Quantities

ITEM	UNITS	QTY	UNIT COST (GHC)	AMOUNT (GHC)
MATERIALS				
50mmx25mm M/S U-channel	pcs	1	150	150.00
50mmx50mm galvanized angle iron	pcs	1	100	100.00
40x40mm galvanized angle iron	pairs	1	90	90.00
30x30mm galvanized angle iron	pcs	1	80	80.00
40mmx20mm galvanized pipe	pcs	1	30	30.00
5x285x285mm galvanized plate	pcs	2	30	60.00
1.5mm galvanized plate	pcs	1	160	160.00
50x5mm mild steel flat bar	pcs	1	90	90.00
ø50mm x 500mm M/S pipe	pcs	2	50	100.00
ø40mm x 1200mm M/S shaft	pcs	1	100	100.00
cushion (470x470mm)	pcs	2	70	140.00
leather	yrds	2	30	60.00
207 pillow bearings	pcs	2	45	90.00
205 pillow bearings	pcs	2	35	70.00
6205 roller bearings	pcs	2	10	20.00
G10 Mild steel electrode	pkt	1	35	35.00
Cuting disc	pcs	5	17	85.00
Green oil paint	gal	1	65	65.00
Red oil paint	ltrs	1	15	15.00
Front tyre with rims (ø350mm Lugged tyres)	pairs	1	70	70.00
Rear tyres with rims (ø380mm Lugged tyres)	pairs	1	100	100.00
Chain (12.7mm pitch)	pcs	2	30	60.00

Large sprocket (37teeth, 12.7mm pitch, 74.7mm PCR)	pcs	1	30	30.00
Small sprockets (15teeth, 12.7mm pitch, 30.5mm PCR)	pcs	3	15	45.00
Steering Bolt (M24 Bolt and nut)	pcs	1	15	15.00
M20 Bolts and Nuts	pcs	2	10	20.00
M10 Bolts and nuts	pcs	17	1.5	25.50
M8 Bolts and nuts	pcs	13	0.7	9.10
Thinner	gal	1	30	30.00
Transportation		1	200	200.00
Subtotal (Material Cost)				2,144.60
Labour cost for the Manufacture (25% Material cost)				536.15
Miscellaneous (5% of material cost)				107.23
GRAND TOTAL				2787.98

Source: Field survey Karimu (2019)



Appendix C8: Evaluation calculations

The theoretical field capacity (C_{th}) of the transplanter

$$C_{th} = \frac{v \cdot W}{10}$$

$$C_{th} = \frac{0.9 \times 0.6}{10} = 0.054 \text{ ha/h}$$

Operating speed (V)

$$V = \frac{\pi D \times N}{t}$$

$$V = \frac{\pi \times 0.38 \times 7.44}{34.99} = 0.25 \text{ m/s} = 0.9 \text{ km/h}$$

Field efficiency

$$e = \frac{T_a}{T_a + T_l} \times 100 \%$$

$$e = \frac{315}{315 + 124} \times 100 \% = 71.75\%$$

The effective field capacity

$$C_e = \frac{V \cdot W \cdot e}{10}$$

$$C_e = \frac{0.9 \times 0.6 \times 71.75}{10} = 0.04 \text{ ha/h}$$

Field capacity of the manual transplanting

$$C_{em} = \frac{A}{T_p - T_n} \times 100$$

$$A = \text{area transplanted} = 93.6 \text{ m}^2 = 0.00936 \text{ ha}$$

$$C_{em} = \frac{0.00936}{0.85 - 0.17} \times 100 = 0.014 \text{ ha/h}$$

Appendix D: Simulation report for the transplanting arm



Report date

Nov 6, 2019 5:57:27 AM

Global Definitions

Global settings

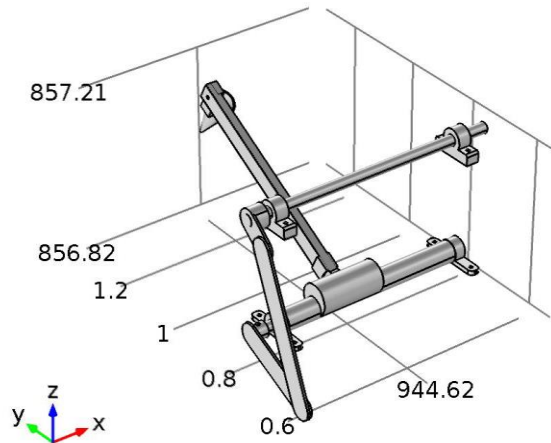
Name V Transp ff Simu oct 22 m.mph
Path C:\Users\Karimu Abdulai\OneDrive\Vegetable
transplanter\Simulation\V Transp ff Simu oct 22 m.mph
COMSOL version COMSOL 5.2 (Build: 166)
Source: Field survey Karimu (2019)

Used products

COMSOL Multiphysics
CAD Import Module
Multibody Dynamics Module
Structural Mechanics Module

Appendix D1: Component

Geometry



Units

Length unit m

Angular unit deg

Appendix D2: Material

Structural steel

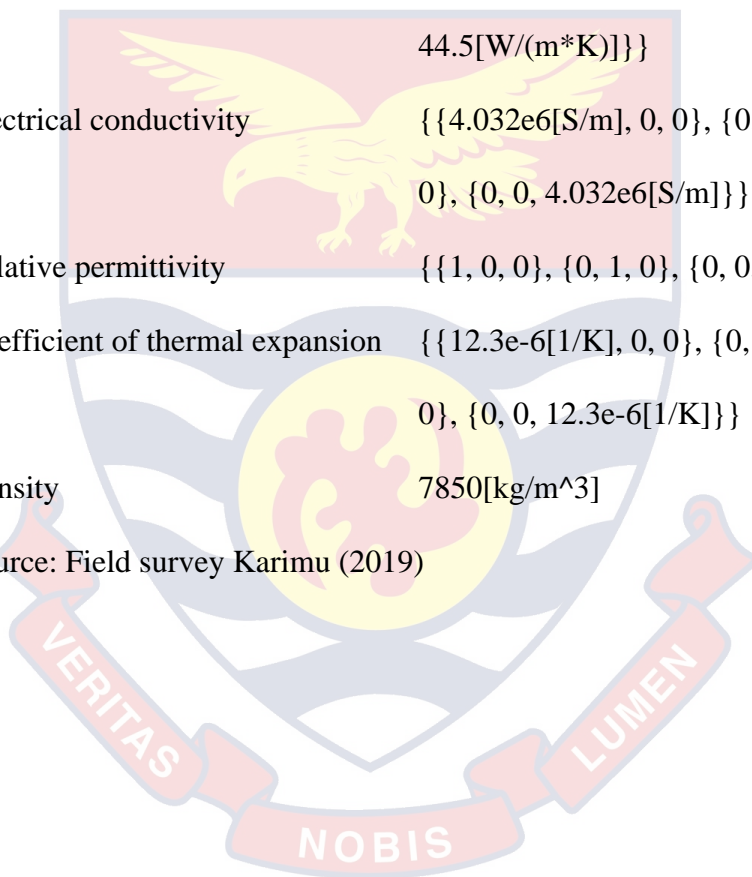
Material parameters

Name	Value	Unit
Density	7850[kg/m ³]	kg/m ³
Young's modulus	200e9[Pa]	Pa
Poisson's ratio	0.33	1

Source: Field survey Karimu (2019)

Appendix D3: Basic settings

Description	Value
Relative permeability	$\{\{1, 0, 0\}, \{0, 1, 0\}, \{0, 0, 1\}\}$
Heat capacity at constant pressure	475[J/(kg*K)]
Thermal conductivity	$\{\{44.5[\text{W}/(\text{m}^*\text{K})], 0, 0\}, \{0, 44.5[\text{W}/(\text{m}^*\text{K})], 0\}, \{0, 0, 44.5[\text{W}/(\text{m}^*\text{K})]\}\}$
Electrical conductivity	$\{\{4.032\text{e}6[\text{S}/\text{m}], 0, 0\}, \{0, 4.032\text{e}6[\text{S}/\text{m}], 0\}, \{0, 0, 4.032\text{e}6[\text{S}/\text{m}]\}\}$
Relative permittivity	$\{\{1, 0, 0\}, \{0, 1, 0\}, \{0, 0, 1\}\}$
Coefficient of thermal expansion	$\{\{12.3\text{e}-6[1/\text{K}], 0, 0\}, \{0, 12.3\text{e}-6[1/\text{K}], 0\}, \{0, 0, 12.3\text{e}-6[1/\text{K}]\}\}$
Density	7850[kg/m ³]
Source: Field survey Karimu (2019)	



Appendix D4: Equations

$$0 = \nabla \cdot \mathbf{s} + \mathbf{F}_v$$

Study

Computation information

Computation time 35 min 1 s

CPU Intel(R) Core(TM)2 Duo CPU E8400 @ 3.00GHz,
2 cores

Operating system Windows 10

Source: Field survey Karimu (2019)

Study settings

Description	Value
-------------	-------

Include geometric nonlinearity	On
--------------------------------	----

Times	Unit
-------	------

range(0,0.025,3)	s
------------------	---

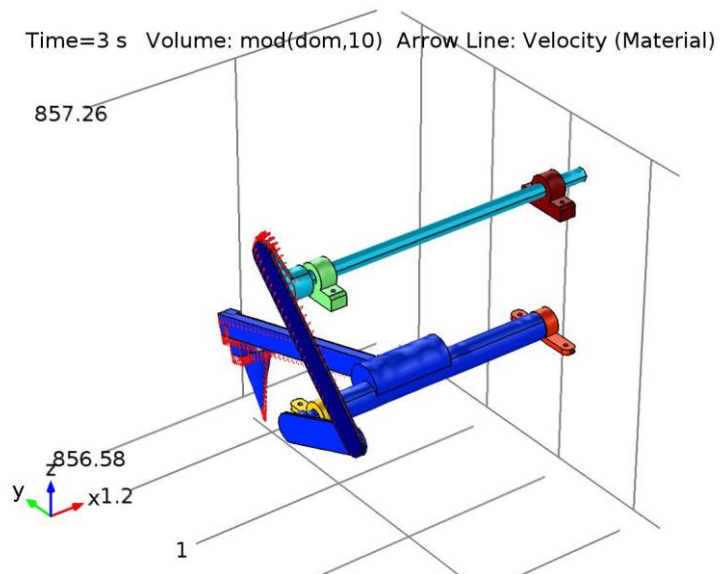
Physics and variables selection

Physics interface	Discretization
-------------------	----------------

Multibody Dynamics (mbd)	physics
--------------------------	---------

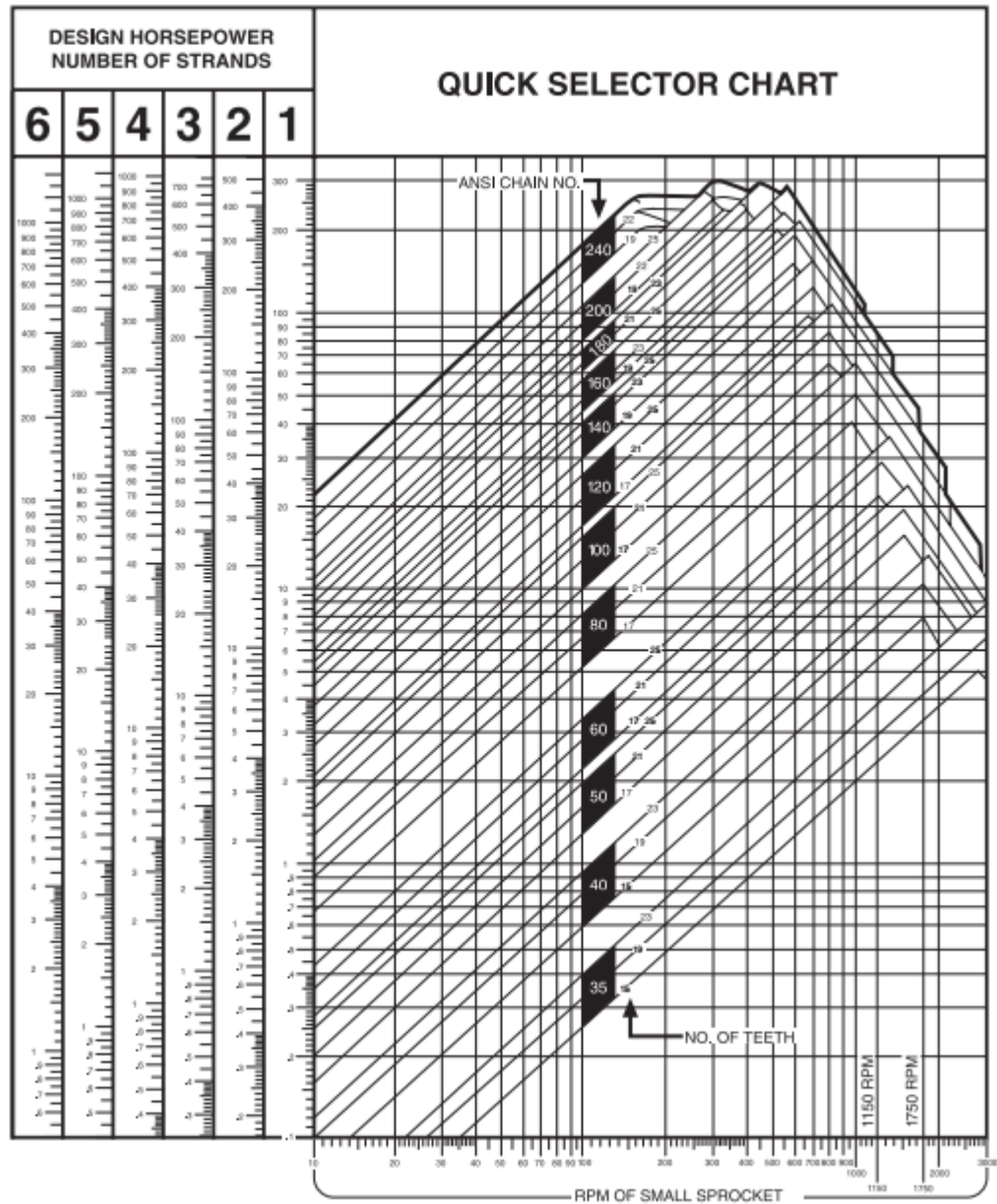
Appendix D5: Results

Velocity (mbd)



Appendix E: Design Calculation Tables and Charts

Appendix E1: Chain and sprocket selection guide table



Source: (Martin, 2016)

Appendix E2: Properties of AISI 1020 low carbon steel

Physical Properties	Metric	Imperial
Density	7.87 g/cc	0.284 lb/in ³

Mechanical Properties

The mechanical properties of AISI 1020 steel are:

Mechanical Properties	Metric	Imperial
Hardness, Brinell	111	111
Hardness, Knoop (Converted from Brinell hardness)	129	129
Hardness, Rockwell B(Converted from Brinell hardness)	64	64
Hardness, Vickers (Converted from Brinell hardness)	115	115
Tensile Strength, Ultimate	394.72 MPa	57249 psi
Tensile Strength, Yield	294.74 MPa	42748 psi
Elongation at Break (in 50 mm)	36.5 %	36.5 %
Reduction of Area	66.0 %	66.0 %
Modulus of Elasticity (Typical for steel)	200 GPa	29000 ksi
Bulk Modulus (Typical for steel)	140 GPa	20300 ksi
Poissons Ratio	0.290	0.290
Charpy Impact		
@Temperature -30.0 °C/-22.0 °F	16.9 J	12.5 ft-lb
@Temperature -18.0 °C/-0.400 °F	18.0 J	13.3 ft-lb
@Temperature -3.00 °C/26.6 °F	20.0 J	14.8 ft-lb
@Temperature 10.0 °C/50.0 °F	24.0 J	17.7 ft-lb
@Temperature 38.0 °C/100 °F	41.0 J	30.2 ft-lb
@Temperature 65.0 °C/149 °F	54.0 J	39.8 ft-lb
@Temperature 95.0 °C/203 °F	61.0 J	45.0 ft-lb
@Temperature 150 °C/302 °F	68.0 J	50.2 ft-lb
Izod Impact	125 J	92.2 ft-lb
Shear Modulus (Typical for steel)	80.0 GPa	11600 ksi

Source: (Azo Materials, 2015)

Appendix E3: Application coefficient (service factor) table

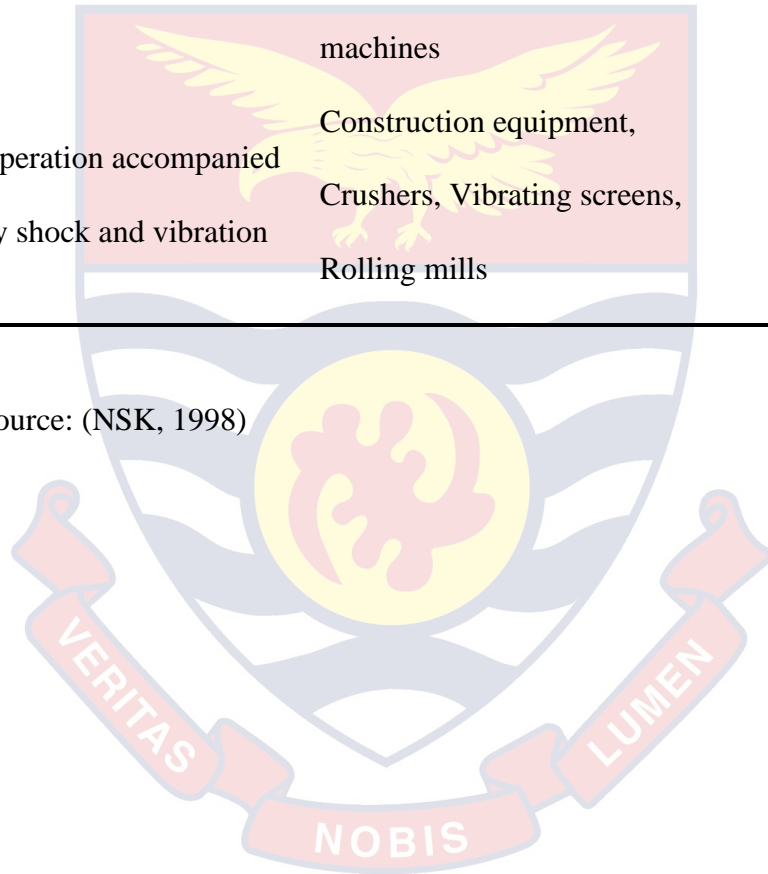
Impact type	Prime Motor Type/ Typical	Turbine motor	Internal combustion engine	
			With fluidic mechanism	Without fluidic mechanism
Smooth transmission	Belt conveyor with small load variation, chain conveyor, centrifugal pump centrifugal blower, general textile machinery, general machinery with small load variation.	X 1.0	X 1.0	X 1.2
	Centrifugal compressor, Marine propeller, Conveyor with moderate load variation, Automatic furnace, Drier, Pulveriser, General machine tools, Compressor, General Earth-moving machinery, General paper manufacturing machinery	X 1.3	X 1.2	X 1.4
Transmission with moderate impact	Press, Crusher, Construction and mining machinery, Vibrator, oil well digger, Rubber mixer, roll, Rollgang, General machinery with reverse or impact load.	X 1.5	X 1.4	X 1.7
Transmission with large impact				

Source: (Misumi, 2009)

Appendix E4: Bearing load factor values table

Operating condition	Typical application	f_w
Smooth operation free from shocks	Electric motors, Machine tools, Air conditioners, Air blowers, Compressors,	1 to 1.2
Normal operation	Elevators, Cranes, Paper making machines	1.2 to 1.5
Operation accompanied by shock and vibration	Construction equipment, Crushers, Vibrating screens, Rolling mills	1.5 to 3

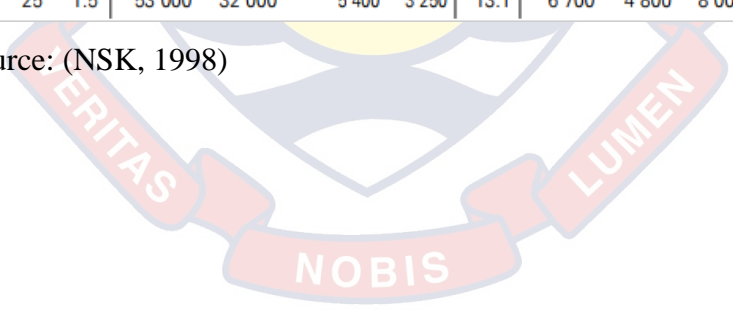
Source: (NSK, 1998)



Appendix E5: Bearing selection table for bore diameter 25-45mm

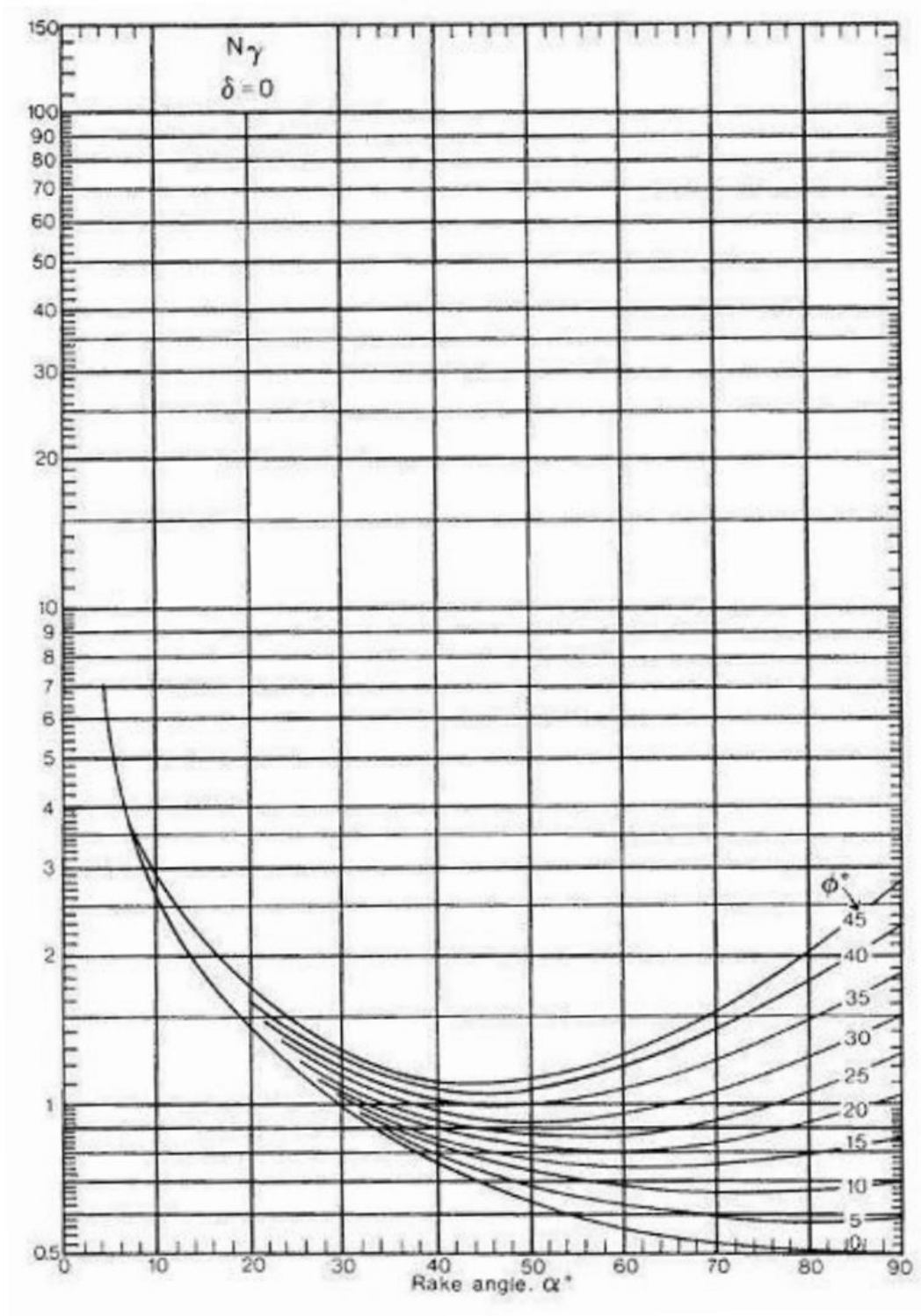
Boundary Dimensions (mm)				Basic Load Ratings (N)				Factor f_0	Limiting Speeds (rpm)			Bearing Numbers			
d	D	B	r min	C_r	C_{0r}	(kgf)			Grease		Oil	Open	Shielded	Sealed	
25	37	7	0.3	4 500	3 150	455	320	16.1	18 000	10 000	22 000	6805	ZZ	VV	DD
	42	9	0.3	7 050	4 550	715	460	15.4	16 000	10 000	19 000	6905	ZZ	VV	DDU
	47	8	0.3	8 850	5 600	905	570	15.1	15 000	—	18 000	16005	—	—	—
	47	12	0.6	10 100	5 850	1 030	595	14.5	15 000	9 500	18 000	6005	ZZ	VV	DDU
	52	15	1	14 000	7 850	1 430	800	13.9	13 000	9 000	15 000	6205	ZZ	VV	DDU
	62	17	1.1	20 600	11 200	2 100	1 150	13.2	11 000	8 000	13 000	6305	ZZ	VV	DDU
28	52	12	0.6	12 500	7 400	1 270	755	14.5	14 000	8 500	16 000	60/28	ZZ	VV	DDU
	58	16	1	16 600	9 500	1 700	970	13.9	12 000	8 000	14 000	62/28	ZZ	VV	DDU
	68	18	1.1	26 700	14 000	2 730	1 430	12.4	10 000	7 500	13 000	63/28	ZZ	VV	DDU
30	42	7	0.3	4 700	3 650	480	370	16.4	15 000	9 000	18 000	6806	ZZ	VV	DD
	47	9	0.3	7 250	5 000	740	510	15.8	14 000	8 500	17 000	6906	ZZ	VV	DDU
	55	9	0.3	11 200	7 350	1 150	750	15.2	13 000	—	15 000	16006	—	—	—
32	55	13	1	13 200	8 300	1 350	845	14.7	13 000	8 000	15 000	6006	ZZ	VV	DDU
	62	16	1	19 500	11 300	1 980	1 150	13.8	11 000	7 500	13 000	6206	ZZ	VV	DDU
	72	19	1.1	26 700	15 000	2 720	1 530	13.3	9 500	6 700	12 000	6306	ZZ	VV	DDU
35	58	13	1	15 100	9 150	1 530	935	14.5	12 000	7 500	14 000	60/32	ZZ	VV	DDU
	65	17	1	20 700	11 600	2 120	1 190	13.6	10 000	7 100	12 000	62/32	ZZ	VV	DDU
	75	20	1.1	29 900	17 000	3 050	1 730	13.2	9 000	6 300	11 000	63/32	ZZ	VV	DDU
40	47	7	0.3	4 900	4 100	500	420	16.7	14 000	7 500	16 000	6807	ZZ	VV	DD
	55	10	0.6	10 600	7 250	1 080	740	15.5	12 000	7 500	15 000	6907	ZZ	VV	DDU
	62	9	0.3	11 700	8 200	1 190	835	15.6	11 000	—	13 000	16007	—	—	—
	62	14	1	16 000	10 300	1 630	1 050	14.8	11 000	6 700	13 000	6007	ZZ	VV	DDU
45	72	17	1.1	25 700	15 300	2 620	1 560	13.8	9 500	6 300	11 000	6207	ZZ	VV	DDU
	80	21	1.5	33 500	19 200	3 400	1 960	13.2	8 500	6 000	10 000	6307	ZZ	VV	DDU
	52	7	0.3	6 350	5 550	650	565	17.0	12 000	6 700	14 000	6808	ZZ	VV	DD
	62	12	0.6	13 700	10 000	1 390	1 020	15.7	11 000	6 300	13 000	6908	ZZ	VV	DDU
	68	9	0.3	12 600	9 650	1 290	985	16.0	10 000	—	12 000	16008	—	—	—
45	68	15	1	16 800	11 500	1 710	1 180	15.3	10 000	6 000	12 000	6008	ZZ	VV	DDU
	80	18	1.1	29 100	17 900	2 970	1 820	14.0	8 500	5 600	10 000	6208	ZZ	VV	DDU
	90	23	1.5	40 500	24 000	4 150	2 450	13.2	7 500	5 300	9 000	6308	ZZ	VV	DDU
45	58	7	0.3	6 600	6 150	670	625	17.2	11 000	6 000	13 000	6809	ZZ	VV	DD
	68	12	0.6	14 100	10 900	1 440	1 110	15.9	9 500	5 600	12 000	6909	ZZ	VV	DDU
	75	10	0.6	14 900	11 400	1 520	1 160	15.9	9 000	—	11 000	16009	—	—	—
	75	16	1	20 900	15 200	2 140	1 550	15.3	9 000	5 300	11 000	6009	ZZ	VV	DDU
	85	19	1.1	31 500	20 400	3 200	2 080	14.4	7 500	5 300	9 000	6209	ZZ	VV	DDU
100	25	1.5	53 000	32 000	5 400	3 250	13.1	6 700	4 800	8 000	6309	ZZ	VV	DDU	

Source: (NSK, 1998)



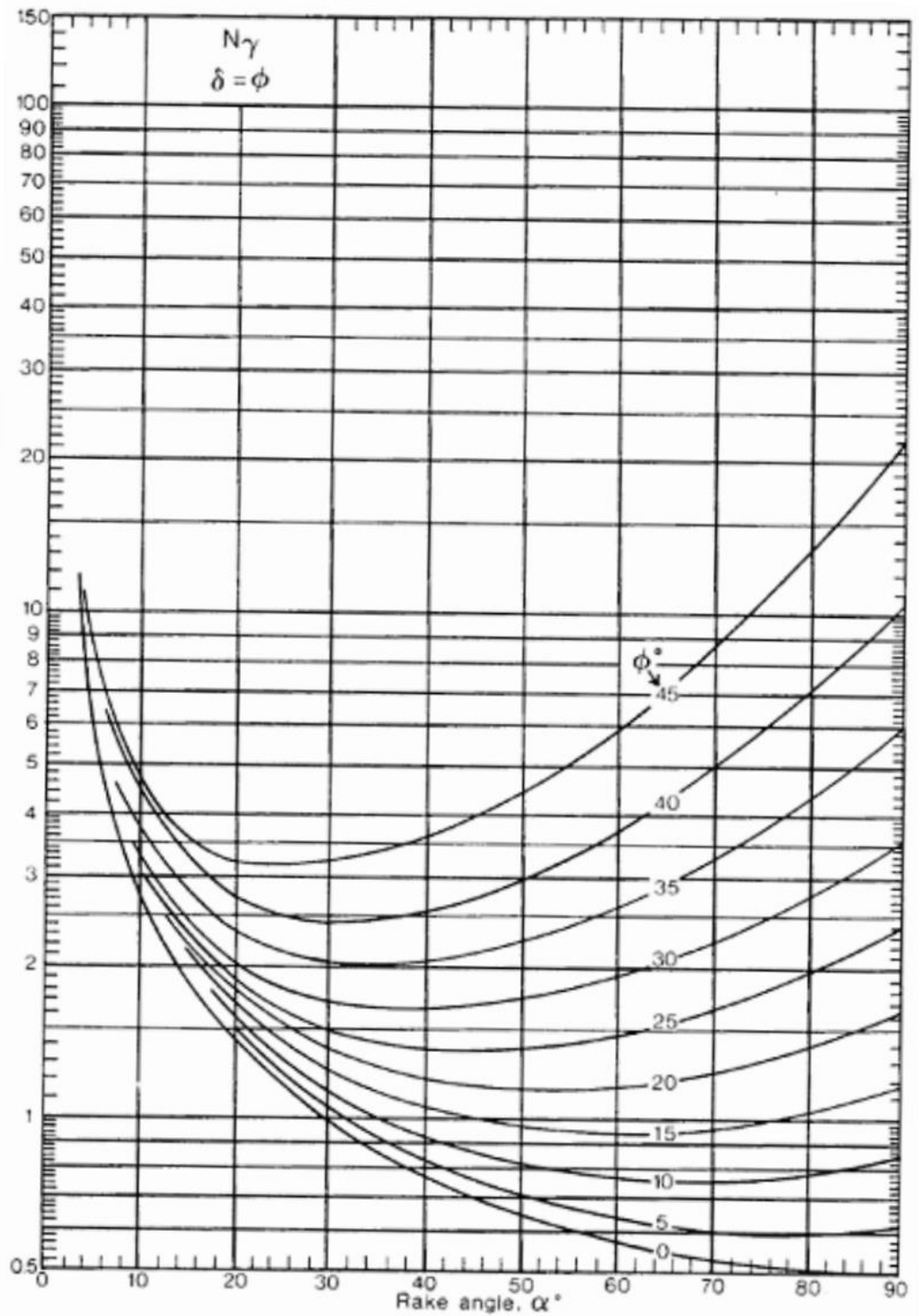
Appendix F: N-factor Charts

Appendix F1: Chart of N_γ for $\delta=0$ (Gravitational: Smooth)



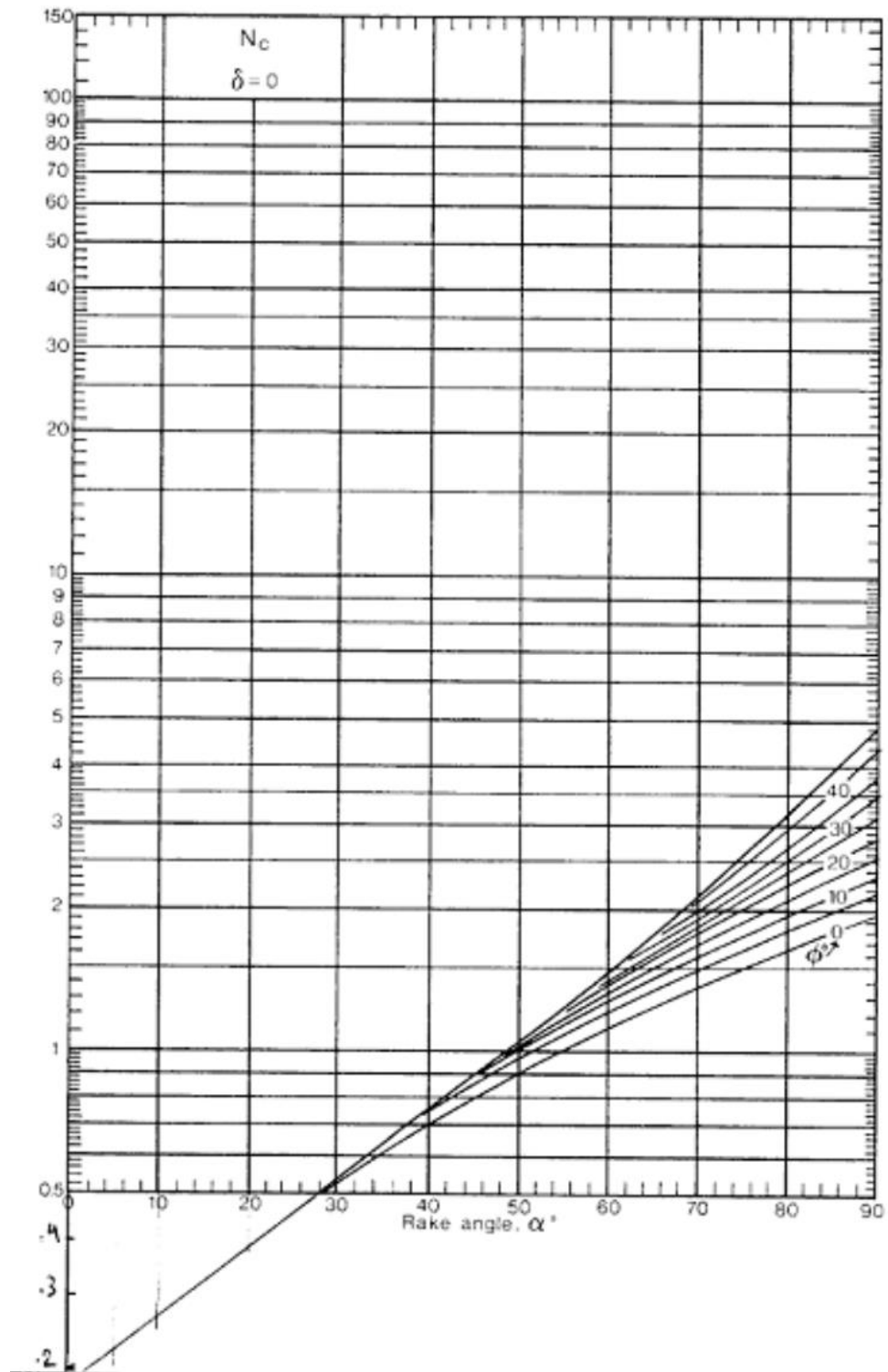
Source: (Demirel & Gölbası, 2011)

Appendix F2: Chart of N_γ for $\delta=\phi$ (Gravitational: Rough)



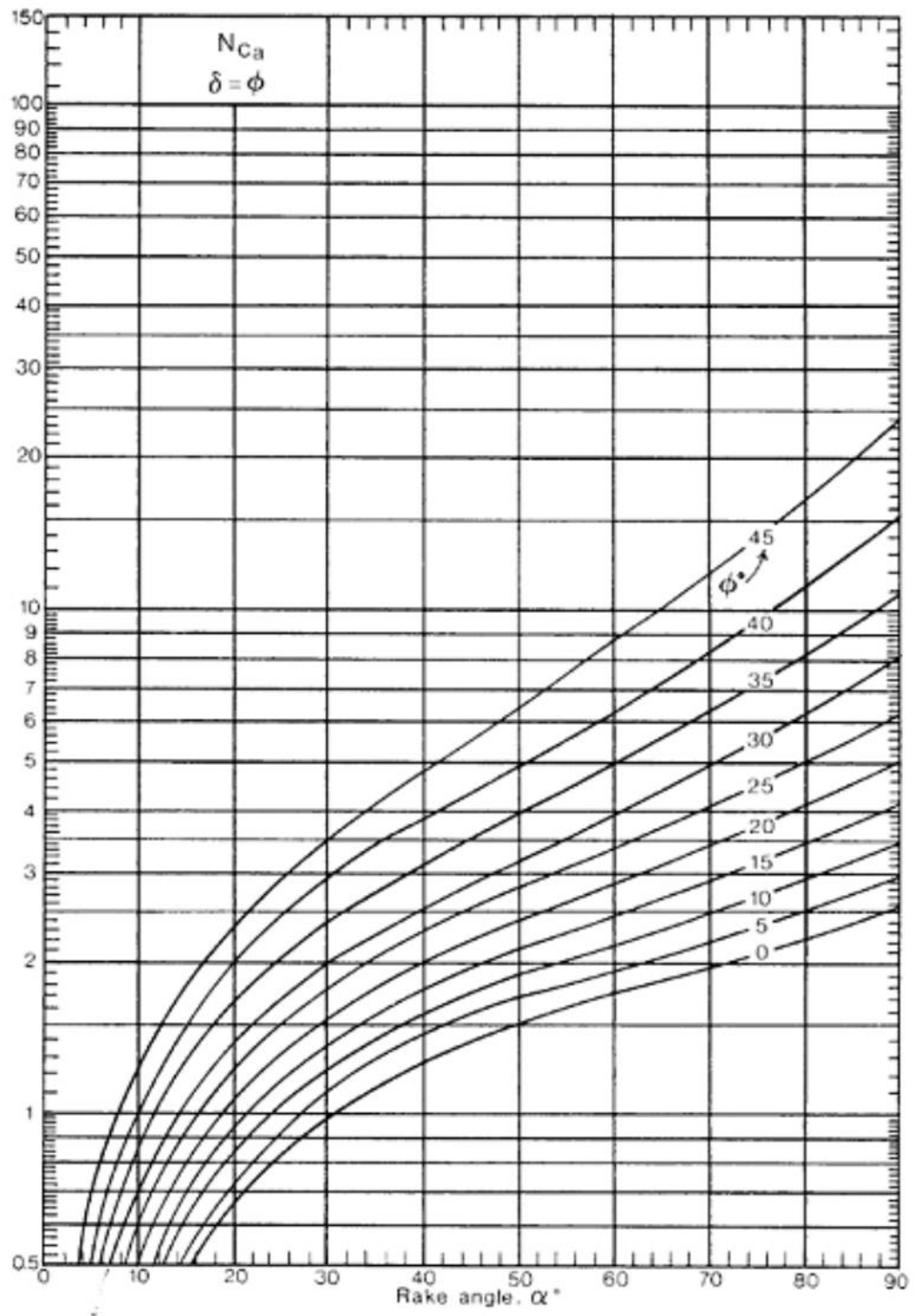
Source: (Demirel & Gölbası, 2011)

Appendix F3: Chart of N_c for $\delta=0$ (Cohesive: Smooth)



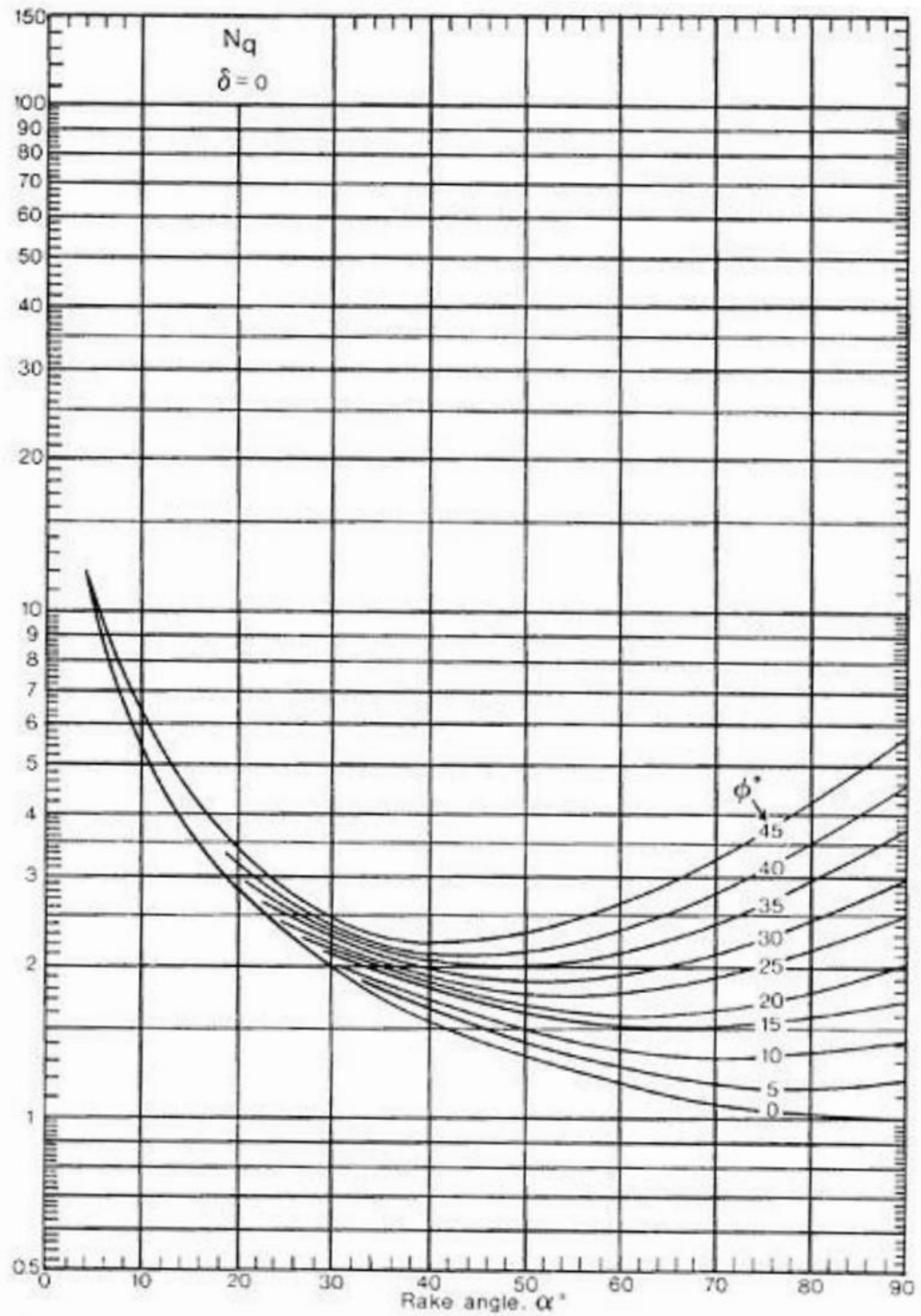
Source: (Demirel & Gölbası, 2011)

Appendix F4: Chart of N_c for $\delta=\phi$ (Cohesive: Rough)



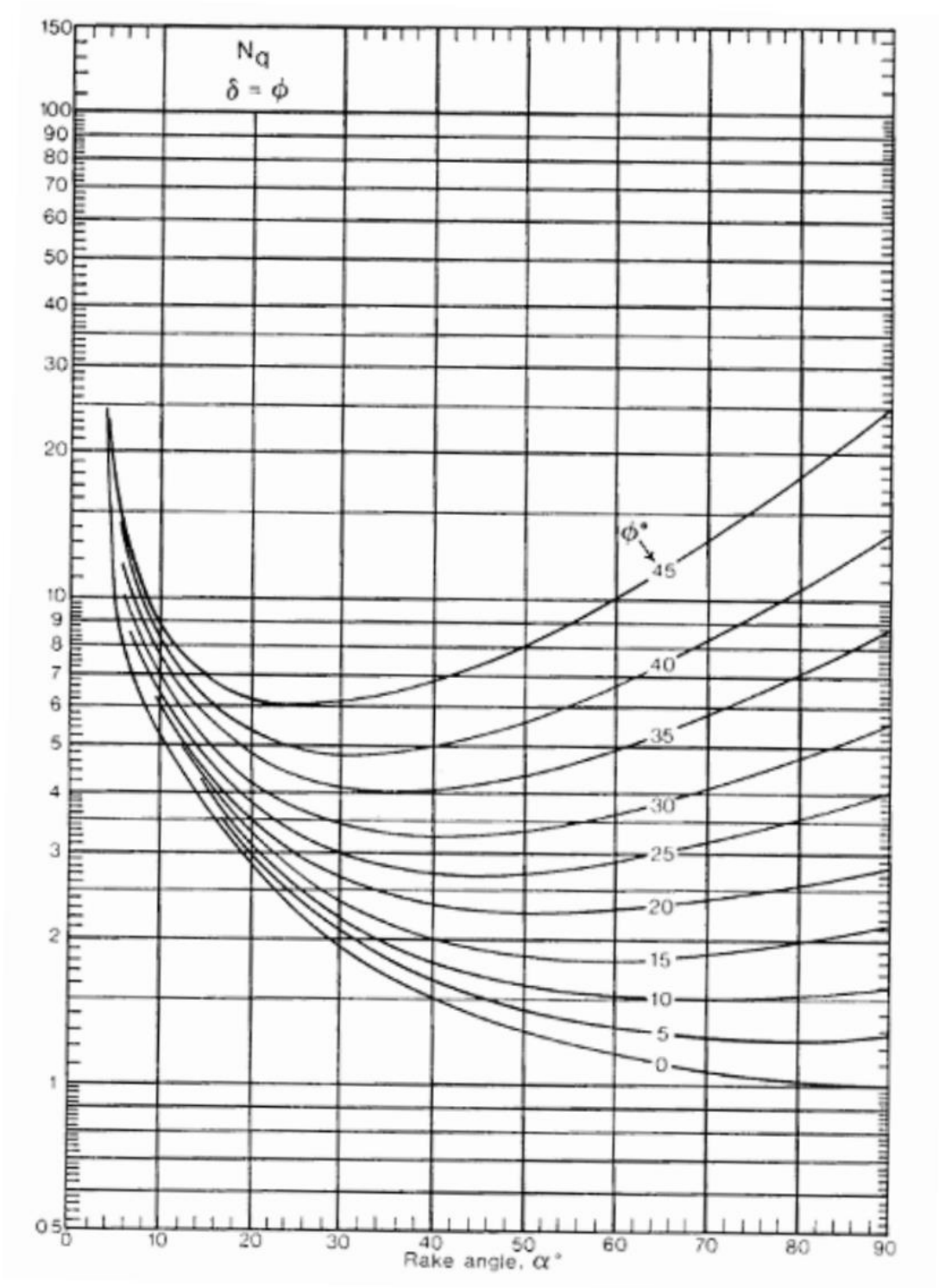
Source: (Demirel & Gölbası, 2011)

Appendix F5: Chart of N_q for $\delta=0$ (Surcharge: Smooth)



Source: (Demirel & Gölbası, 2011)

Appendix F6: Chart of N_q for $\delta=0$ (Surcharge: Smooth)



Source: (Demirel & Gölbası, 2011)